TECHNISCHE UNIVERSITÄT MÜNCHEN

Lehrstuhl für Radiochemie

Production of non carrier added (n.c.a.) ^{177}Lu for radiopharmaceutical applications

Christoph Barkhausen

Vollständiger Abdruck der von der Fakultät für Chemie der Technischen Universität München zur Erlangung des akademischen Grades eines

Doktors der Naturwissenschaften (Dr. rer. nat.)

genehmigten Dissertation.

Vorsitzender:	Univ.- Prof. Dr. Ulrich K. Heiz
Prüfer der Dissertation:	1. Univ.-Prof. Dr. Andreas Türler 2. apl. Prof. Dr. Ulrich Boesl – von Grafenstein

Die Dissertation wurde am 13.07.2011 bei der Technischen Universität München eingereicht und durch die Fakultät für Chemie am 06.09. 2011 angenommen.

Quand tu veux construire un bateau, ne commence pas par rassembler du bois, couper des planches et distribuer du travail, mais réveille au sein des hommes le désir de la mer grande et large.

Antoine de Saint-Exupery

If you want to build a ship, don't drum up the men to gather wood, divide the work and give orders. Instead, teach them to yearn for the vast and endless sea.

Antoine de Saint-Exupery

Wenn Du ein Schiff bauen willst, dann trommle nicht Männer zusammen um Holz zu beschaffen, Aufgaben zu vergeben und die Arbeit einzuteilen, sondern erwecke in ihnen die Sehnsucht nach dem weiten, endlosen Meer.

Antoine de Saint-Exupery

But the sun doesn't give the light to the moon - assuming the moon owes him one.

Die vorliegende Arbeit wurde am Lehrstuhl der Technischen Universität München in Garching unter Anleitung von Herrn Dr. Konstantin Zhernosekov in der Zeit von März 2007 bis Juli 2011 durchgeführt.

Abstract

The low-energy β^--emitter ^{177}Lu has been already successfully used in targeted radionuclide therapy and is due to its physical and radiochemical properties ideal for the treatment of metastatic cancers. Through successful applications in endoradiotherapy and brachytherapy the demand for ^{177}Lu is growing worldwide. However, very high requirements concerning the quality of the nuclide complicate the production process and thus the accessibility.

^{177}Lu was produced via the indirect production route ^{176}Yb(n,γ)^{177}Yb $\xrightarrow{\beta^-}$ ^{177}Lu by irradiation of massive, highly enriched ^{176}Yb targets at the research reactor FRM II in Garching. In that way, ^{177}Lu was obtained in its non carrier added form. A semi-automated separation system was developed on the basis of cation exchange chromatography. Yb target masses up to 150 mg were processed and up to 120 GBq of n.c.a.^{177}Lu could be produced. The outstanding quality of the final product was verified by labelling experiments and a comparison between n.c.a.^{177}Lu and carrier added (c.a.)^{177}Lu. N.c.a.^{177}Lu proved stable over a period over 15 days, displaying labelling results from > 98 % using a 1:4 molar ratio n.c.a.^{177}Lu : DOTATATE.
The results show that ^{177}Lu can be produced at a multi-Curie level achieving the required high quality standards for therapeutical applications.

Additionally, three ways were evaluated to recycle the irradiated target material, which can be re-used for further irradiations due to the low burn-up. The precipitation as oxalate salt turned out to be the most feasible technique to recover Yb quantitatively.

The project was funded by the Bayerische Forschungsstiftung (BfS) and was conducted in cooperation with Isotopes Technologies Garching (ITG) GmbH, where it developed to a commercially available product.

Zusammenfassung

Der niederenergetische β^--Strahler ^{177}Lu wurde bereits erfolgreich in der gezielten Radionuklidtherapie eingesetzt. Aufgrund seiner physikalischen und radiochemischen Eigenschaften ist ^{177}Lu ideal für die Behandlung von Krebsmetastasen. Durch erfolgreiche klinische Ansätze in der Endoradiotherapie und Brachytherapie wächst die Nachfrage nach dem Reaktornuklid ^{177}Lu weltweit. Sehr hohe Anforderungen an die Qualität des Nuklids erschweren allerdings den Herstellungsprozess und dadurch die Zugänglichkeit.

^{177}Lu wurde durch die Bestrahlung von massiven, hochangereicherten ^{176}Yb-Proben am Forschungsreaktor FRM II in Garching hergestellt. Hierbei wurde die indirekte Produktionsroute ^{176}Yb(n,γ)^{177}Yb $\xrightarrow{\beta^-}$ ^{177}Lu gewählt, um auf diese Weise ^{177}Lu in seiner non carrier added Form zu erhalten. Massen des hoch angereicherten Yb bis zu 150 mg wurden gehandhabt womit bis zu 120 GBq n.c.a.^{177}Lu konnten hergestellt wurden. Die herausragende Qualität des finalen Produkts wurde durch Labelling-Experimente und einem Vergleich zwischen n.c.a.^{177}Lu und carrier added (c.a.)^{177}Lu untersucht und bestätigt. N.c.a.^{177}Lu erwies sich über einen Zeitraum von 15 Tagen als stabil. Labelling Ergebnisse von > 98 % wurden bei einem Verhältnis der molaren Massen von 1:4 n.c.a.^{177}Lu : DOTATATE erzielt.
Die erhaltenen Ergebnisse zeigen, dass es möglich ist ^{177}Lu auf multi-Curie Niveau zu produzieren und die erforderlichen hohen Qualitätsanforderungen für therapeutische Anwendungen zu erfüllen.

Des Weiteren wurden drei Wege evaluiert das bestrahlte Target-Material zu recyceln. Dies kann auf Grund des vernachlässigbaren Burn-ups für weitere Bestrahlungen wieder verwendet werden. Die Ausfällung als Oxalat-Salz erwies sich als praktikabelste Methode Yb quantitativ wiederzugewinnen.

Das Projekt wurde von der Bayerischen Forschungsstiftung (BfS) finanziert und in Kooperation mit Isotopes Technologies Garching (ITG) GmbH durchgeführt. Bei letzterer ist n.c.a.^{177}Lu zu einem kommerziellen Produkt gereift.

Acknowledgments

This thesis was conducted in the frame of research at the Institute of Radiochemistry at the Technical University Munich from March 2007 until June 2011 under the excellent guidance of Prof. Dr. Andreas Türler and Dr. Konstantin Zhernosekov.

In the first place, I want to express my deepest gratitude to the best guide one can wish for on through the jungle of radiochemistry, Dr. Konstantin Zhernosekov. His devotion to (t)his field of research and his seemingly endless knowledge about it and all kind of topics connected to it inspired me a lot. Throughout his work here at RCM this and his always ready to help attitude made a great impression on me and made me proud that I was under his guidance. I owe him very much!

I would very much like to thank Prof. Dr. Andreas Türler for giving me the opportunity to get access to this field of research. His cordially welcome here at the institute and his introduction to what my thesis will be about, aroused my curiosity and encouraged me to take on the interesting task.

I deeply appreciate the help I gratefully received from my boss Dr. Christoph Lierse von Gostomski. Not only did he always answer all of my questions, sometimes rudimentary ones, sometimes non-professional ones, with enormous patience but also gave me all the time I needed to finish my thesis.

Many thanks go to the extraordinary people I had the great opportunity to work with and to those of them with whom I'm still working. Nothing can compensate for and release more creativity and energy than a caring and sometimes positively demanding working environment. And those people created it for me. I benefited from endless discussions, professional and non-professional, with my closest colleagues Annett Klaschwitz, Dr. Silvia Lehenberger and Dr. Reimar Graeger. I cannot express how grateful I am to have met these people. Some of them became my best friends and some of them even changed my life! Special thanks to Dr. Gerhard Jörg who helped me a lot of times with his profound knowledge about radiochemistry and chemistry itself.

I enjoyed many discussions with my other co-workers here at RCM from other working groups who gave me many interesting glimpses of their professional work and opened my mind for different uses of radiochemistry beside my own field of research. I would like to thank our workshop very much for quick and reliable help with any task we came up with for them. Special thanks for all my colleagues at radiation safety who protected me from any immediate harm radiation could have imposed on me. Working with these people made me wonder where all those prejudices about radiation protection works against scientists and vice versa come from! Big thanks to Hansi Zott, the master of all computers, for helping me out every time I crushed any PC. I thank Irmgard Kaul for giving me a hand with the much beloved bureaucracy tasks.

Many thanks to the people from ITM/ITG I had the great pleasure to work with. Leena Nikula, Paula Perkins, Dr. Richard Henkelmann, Dr. Tuomo Nikula, Dr. Mark Harfensteller, Sebastian Marx and Dr. Thorsten August. Special thanks to Dr. Josue Moreno for his help with the recycling topic and for his ever helpful, sacrificially caring and warm-hearted personality.

Last but not least I would like to thank very much girlfriend Anita Frank and my family for their uncompromising help and support no matter which mood of mine they were confronted with!

Christoph Barkhausen

1

CONTENT

1 Content

1 Content 14

2 Motivation 17

3 Introduction 20

3.1 Targeted Radionuclide Therapy (TRT) 20

3.2 Metalloradiopharmaceuticals 21

3.2.1 Radionuclides 23

3.2.2 Targeting molecules - Peptides & Antibodies 26

3.2.3 Chelator and Linker 29

3.3 ^{177}Lu for medical applications 34

3.4 The research reactor FRM II as neutron source for the production of ^{177}Lu 37

4 Radiochemical aspects of n.c.a.^{177}Lu production and working hypothesis 45

4.1 Irradiation Yield 45

4.2 Achievable Specific Activity 47

4.3 Radionuclidic & chemical purity 51

4.4 Chemical Approach 54

4.5 Working Hypothesis 56

5 Experimental 58

5.1 Reagents 58

5.2 Sample preparation & irradiation 60

5.3 Column preparation & resin preconditioning 61

5.4 Radiometric measurements 62

5.5 Experimental set-ups 63

5.5.1 Set-up 1 63

5.5.2 Set-up 2 65

5.6 Separations 66

5.6.1 Separations with set-up 1 66

5.6.2 Separations with set-up 2 67

5.6.3 High activity sample processing/ Proof of concept 67

5.7 Target recovery 71

5.7.1 Recovery set-up 1 71

5.7.2 Recovery set-up 2 73

5.7.3 Recovery set-up 3 73

5.8 Preparation of ^{177}Lu-labelled compounds 73

6 Results and Discussion 76

6.1 Yb(macro) / ^{177}Lu(micro) Separations 76

6.1.1 Separations 77

6.1.2 Routine production model / proof of concept 84

6.1.3 Cl-conversion 86

6.2 Target recovery 86

6.2.1 Cation exchange chromatography method 86

6.2.2 Extraction chromatography method 87

6.2.3 Oxalate method 87

6.3 Labelling experiments - Utilisation of n.c.a. ^{177}Lu in radiolabelling reactions 88

6.3.1 n.c.a. ^{177}Lu 88

6.3.2 c.a. ^{177}Lu 91

7 Conclusion and Outlook 96

8 Referecenes 101

9 Annex 112

9.1 Cross section 112

9.2 List of figures 116

9.3 List of tables 118

9.4 Abbreviations 119

2

MOTIVATION

2 Motivation

Targeted radionuclide therapy (TRT) is a rapidly expanding scientific field that applies radioactive nuclides bound to carriers, if not intrinsically tumour seeking, to transfer a cytotoxic level of ionizing radiation to a disease site. In contrast to external beam radiation or brachytherapy, the knowledge of the exact location and geometrical shape of the tumour is not necessary in order to maximise the damage done to the cancer cells. Multi-focal tumours and metastasis cancer sites are not treatable with those therapies and so a huge effort has been dedicated to improving endoradiotherapy as a method of choice for treatments based on radiation.
As a requirement for successful application to avoid pharmacological side effects or suboptimal tumour uptake caused by bioactive substances or limited amount of binding sites, respectively, the radioisotope must be applied with a high quality. Especially important is the specific activity, A_s, expressed as [GBq/g] or [GBq/mol], which represents the ratio of the activity of the given radionuclide to the overall mass of all its stable and unstable isotopes. Because most therapeutic radionuclides are neutron rich and decay by β^--emission, they are produced in nuclear reactors. For reactor-produced isotopes, the A_s value is of course amongst other criteria, determined by the way of production. Taking as production route the direct activation via the (n,γ) nuclear reaction, obviously results in the carrier added (c.a.) form of the nuclide, which provides only limited achievable specific activity because of the presence of cold target isotopes.

The low-energy β^--emitter ^{177}Lu has been already successfully used in TRT and is ideal for the treatment of metastatic cancers where the above mentioned alternative therapies would, to a large extend, expose the normal tissue surrounding the tumour to radiation. The common production route via irradiation of highly enriched ^{176}Lu provides the isotope ^{177}Lu as c.a. ^{177}Lu. It contains up to 0.01% of the relatively long-lived metastable by-product ^{177m}Lu which has a half-life of 160.1 d. Despite those drawbacks, today's demand for this nuclide is mainly saturated by taking the direct route using highly enriched target material and powerful nuclear reactors ($\Phi_{th} \geq 4 \cdot 10^{14}$ n/cm^2/s) in order to obtain reasonable specific activities. To avoid these disadvantages, efforts have to be devoted to develop a production system for n.c.a.^{177}Lu.

In the present work a route was evaluated to produce ^{177}Lu in its n.c.a. form at a multi-Curie level (> 0.1 TBq) using the nuclear reaction $^{176}Yb(n,\gamma)^{177}Yb \xrightarrow{\beta^-} {}^{177}Lu$. In detail, the particular goals included the characterisation of the desired, highly enriched target material ^{176}Yb, the development of target handling procedures, the build-up of a (semi-) automated production to handle activities reaching TBq-levels, and especially, the development of a separation method by means of cation exchange chromatography to find an effective method to isolate the micro amounts of ^{177}Lu from the macro amounts of Ytterbium (Yb).

3

INTRODUCTION

3 Introduction

3.1 Targeted Radionuclide Therapy (TRT)

Endoradiotherapy (targeted radionuclide therapy) is a systemic approach, involving a radiolabeled targeting vector with a well-characterised biochemical strategy to selectively deliver a cytotoxic level of ionizing radiation to a disease site on a cellular/molecular level. It is a rapidly expanding field since it allows treating serious illnesses, e.g. cancer, with a higher efficiency and less side effects than conventional methods, e.g. chemotherapy. The radioisotopes, that are brought into the human body (e.g. via infusion into the bloodstream), are finally placed directly on to or are even internalised into the malignant cells and thus destroying them by release of ionizing radiation during radioactive decay (Roesch, 2007; Roesch, et al., 2004).

The therapeutic effects of radiation have long been known and have now been used clinically for over 100 years. Therefore, not only the approach mentioned above has been evaluated but a variety of procedures under different pathological conditions. For example, an external beam of particles or photon radiation, focused on malignancies (external beam radiation therapy) or the implantation of activated solids like a wire or a pellet in close proximity to the tumour (brachytherapy) (Volkert, et al., 1999). It is quite obvious regarding this kind of therapy, that it is less effective if not absolutely unsuitable for multifocal or disseminated tumours. Targeted radionuclide therapy instead uses vehicles like peptides or antibodies to target cancer cells on whose surface the specific receptors are over-expressed. This key-lock-principle ensures to a very high degree that the destructive force behind the ionizing radiation focuses mainly on the diseased cells and leaves healthy tissue mainly unharmed.
The best known example, if already an exemption from what was mentioned above, is ^{131}I. An exception as such, that Iodine is specifically accumulated in the thyroid cells without needing a specific carrier. On the other hand, Iodine can also be directly (covalently) attached to Tyr residues on proteins or peptides (Volkert, et al., 1999; Becker, et al., 1996).

The first therapeutic use of ^{131}I was reported as early as 1941 (Becker, et al., 1996). It is effective for treatment of hyperthyroidism[1] and differentiated thyroid carcinoma due to the specific uptake to provide selective irradiation (primarily from β^--particle emissions) to the thyroid gland or thyroid cancer tumours.
This simple radioactive anion ($^{131}I^-$) serves as the most prominent example demonstrating that widely disseminated tumours can be systematically targeted by a therapeutic radiopharmaceutical with sufficient specificity to totally eradicate the metastatic disease in humans (Coakley, 1998).

3.2 Metalloradiopharmaceuticals

Radioactive nuclides, besides Iodine, are not tumour-seeking and need to be bound to a biomolecule that is selectively targeting tumour cells. In general, the design of such an agent can be divided into three different parts (Fig. 1)

1. a biofunctional chelator (BFC),
2. a linker between the biomolecule and
3. a biomolecule e.g. peptides or antibodies which play the role of the counterpart (key) for the receptors (lock, 4), expressed on the surface of the cells.

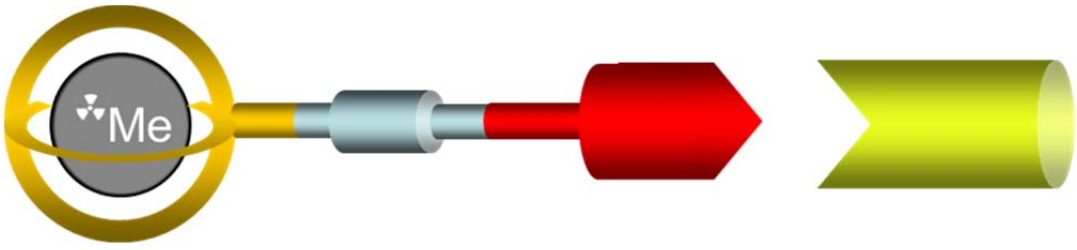

Fig. 1: Design of a receptor mediated radiopharmaceutical; 1: BFC; 2: linker; 3: biomolecule; 4: receptor

[1] overactive tissue within the thyroid gland, resulting in overproduction and thus excess an of circulating free thyroid hormones

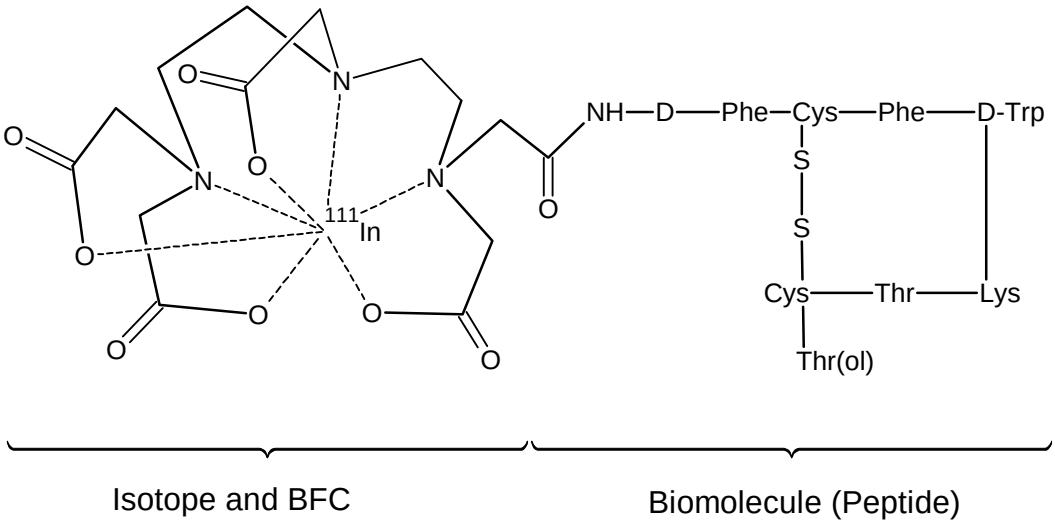

Fig. 2: Example for a receptor mediated radiopharmaceutical: [^{111}In]DTPA-octreotide (OctreoScan)

Fig. 2 shows the design of a metalloradiopharmaceutical, [^{111}In]DTPA-octreotide (OctreoScan), that was the first peptide-based tumour imaging agent approved for clinical use in 1991. A modified somatostatin-analogon in contrast to somatostatin shows more stability towards metabolism, labelled with ^{111}In an electron capture nuclide for diagnosis.

Some targeting vehicles utilized for radionuclide therapy are listed in table 1 (Zalutsky, 2003). Small inorganic complexes, peptides, Abs, and vitamins are used as carrier molecules. As bifunctional chelators, molecules such as 1,4,7,10-tetraazacyclododecane-1,4,7,10-tetraacetic acid (DOTA) are implemented, which form strong complexes with the metal ion while being covalently bound to the targeting biomolecule.

Table 1: Targeting vehicles

Carrier	Example
Colloid	^{165}Dy-labeled ferric hydroxide macroaggregates
Organic molecule	Meta-[^{131}I]iodobenzylguanidine
Inorganic complex	[^{153}Sm]EDTMP
Peptide	^{90}Y-labeled DOTA-octreotide
Protein	^{131}I-labeled anti-tenascin antibody 81 C6
Drug	^{211}At-labeled Syncovit
Steroid	^{125}I-labeled estradiol analogues
Nucleoside	5-[^{125}I]iodo-2'-deoxyuridine

3.2.1 Radionuclides

In endoradiotherapy the used radiolabeled compounds selectively deliver a high therapeutical dose to the targeted tissue. Radionuclides in question are particle emitters that convey via a high linear energy transfer (LET) of the projectile the deposition of a high amount of energy within a small volume. In use are α-, β- and also in some cases Auger electron emitters (Kwekkeboom, et al., 2005; Buchegger, et al., 2006; Zalutsky, 2003).

Table 2: relevant therapeutic radiometals (Maecke, et al., 2003)

Isotope	Half-life	Mode of decay	$\bar{E}_{\beta-/\alpha}$ [MeV] (%)	E_γ [keV] (%)
^{90}Y	2.67 d	β^-	0.93 (100)	No γ
^{188}Re	16.98 h	β^-	0.766 (100)	155 (15)
^{67}Cu	2.58 d	β^-	0.19 (20), 0.12 (57)	93 (16), 185 (49)
^{213}Bi	46 min	A	5.87 (2), 0.49 (65), 0.32 (32)	440 (27)
^{225}Ac	10 d	A	5.83 (51)	100 (3.5)
Lanthanides				
^{177}Lu	6.71 d	β^-	0.15 (79)	208 (10.36)
^{161}Tb	6.9 d	β^-	0.155 (100)	75 (9.8)
^{166}Ho	26.8 h	β^-	0.69 (51), 0.65 (48)	80.6 (6.2)
^{153}Sm	1.95 d	β^-	0.23 (43), 0.2 (35)	103 (28)
^{149}Pm	53.1 h	β^-	0.37 (97)	286 (2.9)
^{175}Yb	4.2 d	β^-	0.48 (100)	396 (13.2), 283 (3.1)

Due to the development of effective radiochemical labelling procedures more and more radioisotopes of the heavy metals are introduced in therapeutical applications (Liu, et al., 2001; Maecke, et al., 2003) (Table 2). Therapeutic radiolanthanides including ^{90}Y, which emit β^--particles are of special interest (Maecke, et al., 2003; Roesch, 2007; Roesch, et al., 2004). A strategic advantage of those elements is their chemical alikeness what allows usage of the same radiolabelling chemistry. By choosing different radioisotopes of this series, it is therefore possible to compare their decay characteristics such as decay mode, energy of the particle, and half-life to optimize the therapeutic effect.

The high-energy β^--emitter ^{90}Y with no γ-component suits very well for therapeutic applications. ^{177}Lu is a low-energy β^--emitter that emits a γ-component of 208 keV with 11% intensity.

Those photons allow visualisation of the nuclide *in-vivo* by means of szintigraphy. Both nuclides provide the so-called 'Cross-Fire-Effect', which make them especially useful for treatment of tumour-masses. Since the lower energy of the β^--particles results in a shorter range in tissue, ^{177}Lu is preferably used in the therapy of smaller tumours and metastasis.

Fig. 3 shows a theoretical evaluation of the nuclides ^{90}Y and ^{177}Lu, done by a group from Göteborg university (Bernhardt, et al., 2001; Uusijärvi, et al., 2006). They developed a mathematical model to evaluate the relation between the tumour-to-normal-tissue mean absorbed dose-rate ratio (TND) and the electron energy, photon-to-electron energy ratio (p/e) and the tumour size. Normal tissue and tumours were simulated as ellipsoid and spheres, respectively (Uusijärvi, et al., 2006).

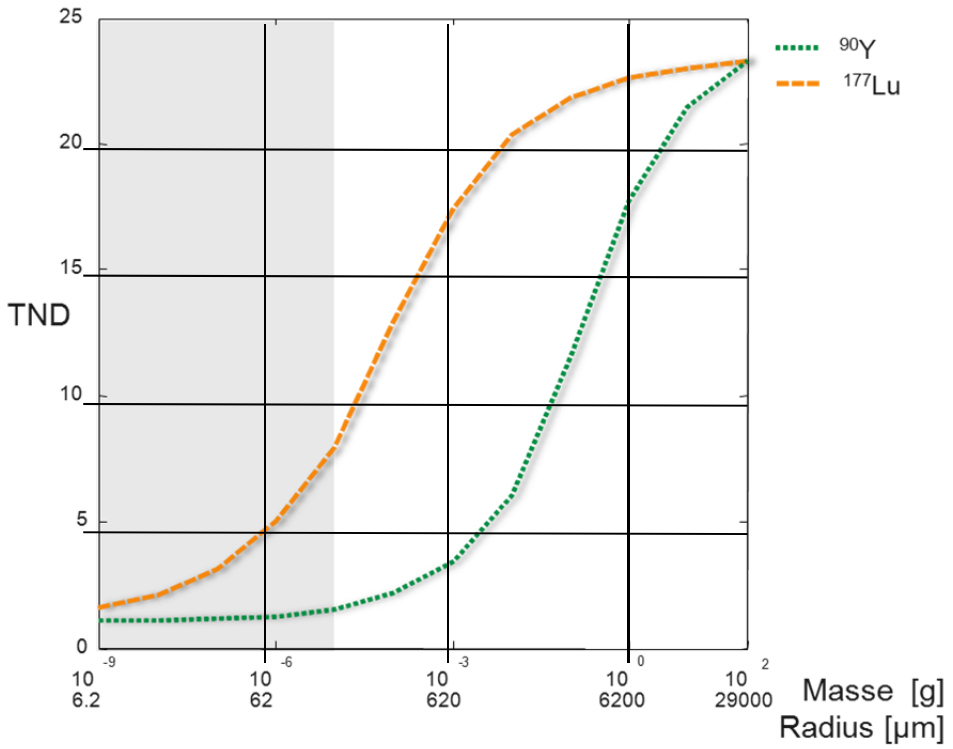

Fig. 3: Tumour to normal tissue mean adsorbed dose rate (TND) as a function of tumour mass and radius; comparison of ^{90}Y and ^{177}Lu (Uusijärvi, et al., 2006)

In this evaluation, only ^{177}Lu reaches high TND levels regarding small tumours ($< 10^{-5}$ g, < 310 µm), which means, the dose rate absorbed by normal tissue is very low in contrast to the other investigated nuclides. ^{90}Y for example is only effective with bigger tumours ($> 10^{-3}$ g, > 620 µm) owing to its high mean β^--energy (2.3 MeV) which allows a longer range of the particles and therefore a rather inefficient energy transfer to small malign cells or cell clusters. Due to the relatively short range of the ^{177}Lu β^--particle in the tissue and consequently high local damage, it provides high cytotoxicity (Buchegger, et al., 2006; Behr, et al., 2000).

There is already a wide experience in therapeutic applications of ^{90}Y- and ^{177}Lu-labeled compounds. Particularly in the treatment of neuroendocrine tumours, these radionuclides are involved in routine clinical use. Those tumours over-express the somatostatin receptor that can be addressed and thus treated with ^{90}Y-/^{177}Lu-labelled somatostatin analogues such as DOTATOC (1,4,7,10-Tetraazacyclododecane-1,4,7,10-tetraacetic acid-Phe(1)-Tyr(3))octreotide), DOTATATE (1,4,7,10-Tetraazacyclododecane-1,4,7,10-tetraacetic acid-(Tyr(3))octreotate) (Stahl, et al., 2006; Waldherr, et al., 2002; Kwekkeboom, et al., 2003; Stahl, et al., 2006). A response rate of up to 30 – 35 % can be achieved with ^{90}Y-DOTATOC and ^{177}Lu-DOTATATE, depending on the type of the tumour and the therapy scheme (Kwekkeboom, et al., 2005).

3.2.2 Targeting molecules - Peptides & Antibodies

3.2.2.1 Peptides

Peptides are small macromolecules that consist of up to 50 amino acids (Zalutsky, 2003). Two important differences between antibodies (see below) and peptides result. Peptides have a much faster blood clearance and as a consequence of their lower weight a faster uptake into tissues. The relatively fast blood clearance and their less immunogenic potency reduce the exposure of healthy tissue to radiation on the one hand and allow multiple dose administration strategies on the other hand.

The most commonly used and investigated peptide for peptide-mediated radionuclide therapy is the Somatostatin peptide (SST) and its analogues.

Somatostatin is a regulatory peptide that is produced by neuroendocrine, inflammatory, and immune cells in response to ions, nutrients, neuropeptides, neurotransmitters, thyroid and steroid hormones, growth factors, and cytokines. The peptide is released in large amounts from storage pools of secretory cells, or in small amounts from activated immune and inflammatory cells. It acts as an endogenous inhibitory regulator of the secretory and proliferative responses of target cells that are widely distributed in the brain and periphery. A family of receptors that comprise five distinct subtypes, termed SSTR 1…5 according to their chronological discovery, mediates these actions (Patel, 1999). Receptor subtype 1 is frequently found in gastrinomas[2] and insulinomas[3], while its expression is reduced in carcinoid tumours and functionally inactive tumours. SSTR 2 is present in almost all gastronomas and insulinomas and in most carcinoid tumours and functionally inactive neoplasms. SSTR 3 and 4 are rarely expressed. Subtype 5 is frequently present in gastrinomas and insulinomas and to a lesser extend in carcinoid tumours[4] and functionally inactive neoplasms (Patel, 1999).

Derivatisation of the naturally occurring Somatostatin peptides, namely Somatostatin-14[4] (Fig. 4), Cortistatin-14[4] and Somatostatin-28[5], is mandatory because of their relatively fast degradation in blood. The most common substitutes are Octreotid (Sandostatin®, Fig. 5), Lanreotid (Somatuline®, Fig. 5) and Vapreotid (Octastin®, Fig. 6) (Jurkin, 2009).

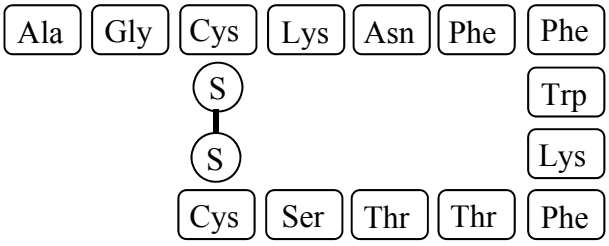

Fig. 4: Somatostatin-14

[2] Gastrinomas are tumours characterized by secretions of large amounts of gastrin, a hormone that increases the amount of acid released by the stomach.
[3] Insulinomas are tumours in the pancreas that produce too much insulin.
[4] Carcinoid tumours are rare, slow-growing cancers that usually start in the lining of the digestive tract or in the lungs.
[5] The number referring to the quantity of amino acids

Fig. 5: left: Octreotide; right: Lanerotide

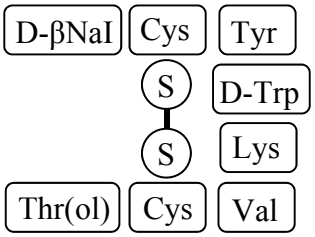

Fig. 6: Vapreotide

The range of cancers susceptible to octreotide and related somatostatin analogues includes mammary, pancreatic, gastric, colorectal, prostate, thyroid, and lung carcinomas.

All five receptors bind somatostatin-14 with same affinity, while somatostatin-28 is preferably recognized by SSTR 5 (protein containing 363 amino acids). From a therapeutic point of view, SSTR 2 (protein containing 369 amino acids) and SSTR 5 are the most important receptor subtypes since the routinely used somatostatin analogues octreotide and lantreotide are recognized by these receptors.

3.2.2.2 Antibodies

Antibodies are specialized immune proteins, produced in an automatic response to an introduction of an antigen into the body, and which possesses the remarkable ability to combine with the very antigen that triggered its production. It is possible to produce antibodies that react with antigenic structures that are present on cancerous cells and with the ever-growing knowledge about the nature of tumour cells the ability to describe those structures and to design antibodies with higher affinity to these cells is improving steadily.

The problem with antibodies that scientists had to face before the invention of a methodology to produce monoclonal antibodies (mAbs) by Köhler and Milstein was their polyclonal nature (Köhler, et al., 1975).

That means these animal-derived polyclonal antibodies consist of a range of specificity and affinity for an antigenic target whereas mAbs have a defined antigen specificity and affinity.

In contrast to the other radiopharmaceutical carriers, antibodies or immunoglobulins (Ig) are macromolecules with a weight of about 150 kDa [6].
There are five different classes of immunogloblins, IgG, IgE, IgD, IgA and IgM, of which IgG is the predominant class found in human blood and therefore the vast majority of mAb-type used in radioimmunotherapy (RIT)[7] (Zalutsky, 2003).

3.2.3 Chelator and Linker

As already mentioned above, a bifunctional chelator (BFC) has to be introduced into the targeting biomolecule to provide a connection between the latter and the radioisotope. The choice of BFC is largely dependent upon the nature and oxidation state of the metal ion and requires a good understanding of the coordination chemistry of the given radiometal (Volkert, et al., 1999; Liu, et al., 2001; Zalutsky, 2003).

A BFC usually contains three parts:

1. a bonding unit,
2. a ligand framework (arrangement of bonding units),
3. a conjugation group (Volkert, et al., 1999).

That means, that one end of the BFC strongly coordinates to the metallic radionuclide while the other is covalently attached to the biomolecule either directly or through a linker. The nature of the linker depends on the pharmacokinetic requirements of the pharmaceutical i.e., it may influence the hydrophilicity of the conjugate and thus improve the pharmacokinetics.

[6] In biochemistry and molecular biology, when talking about mass of molecules, the term 'Dalton' is used, with the symbol Da. 1 Da = $1{,}6605402*10^{-24}$ g
[7] Therapy, that uses radiolabeled antibodies as targeting agents

The linker can also act as a separator between the BFC and the biomolecule to prevent steric influence of the chelator on the binding affinity of the receptor targeting part of the pharmaceutical (Liu, et al., 2001).

The BFC must be able to form a metal complex with high thermodynamic stability and kinetic inertness (which reflects the rate of dissociation of the metal ion from BFC)

to prevent the release of the radionuclide. As a rule, acyclic chelators (Fig. 7) or chelators with non-optimal denticity provide fast dissociation kinetics of the complex. One reason for that is the loss of entropy, which results from the decrease of degrees of freedom during chelation. Pre-organisation of the chelating framework helps to reduce this effect. Complexes for example formed with trans-cyclohexanediaminetetraacetic acid (CyEDTA) (Fig. 7, structure 3) proved more stable in comparison with ethylenediaminetetraacetic acid (EDTA). That means, if the spatial arrangement of the bonding units is already determined, no big loss in entropy can occur.

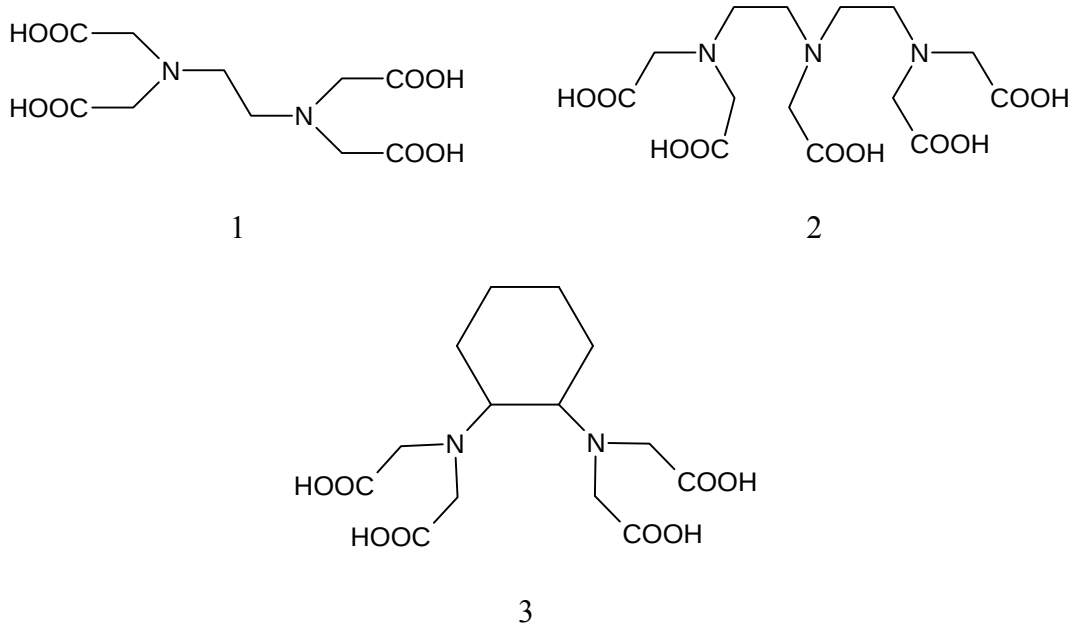

Fig. 7: acyclic chelators, 1: EDTA, 2: DTPA, 3: CyEDTA

In that respect, higher denticity provides enhanced thermodynamic stability and kinetic inertness for BFCs in radiopharmaceuticals.

The lanthanides and Yttrium for example are large metal ions and able to form stable complexes with poly amino carboxylates. The complexes can accept eight to nine donor atoms to saturate their coordination spheres. Macrocyclic chelators such as DOTA (1,4,7,10-tetraazacyclododecane-1,4,7,10-tetraacetic acid) or derivates thereof like

TETA (1,4,8,11-tetraazacyclotetradecane-1,4,8,11-tetraacetic acid), DOTMP (1,4,7,10-tetraazacyclododecane-1,4,7,10-tetramethylenphosphonic acid) (Fig. 8), etc.

are used to satisfy the different size and coordination geometry preferences of the different radiometals (Liu, et al., 2001).

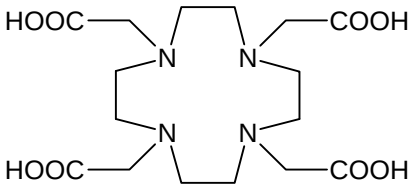

1

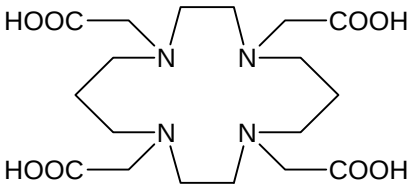

2

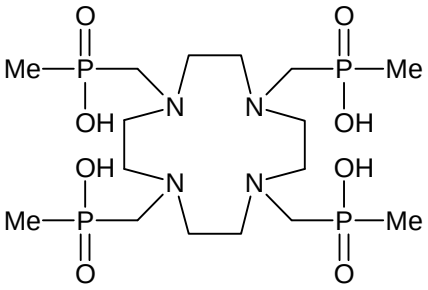

3

Fig. 8: macrocyclic chelators, 1: DOTA, 2: TETA, 3: DOTMP

Through a study conducted by Kodama (Kodama, et al., 1991), it was found, that increasing the size of the cycle obviously results in higher flexibility of the chelator framework and hence complexes formed with e.g. PEPA (1,4,7,10,13-pentaazacyclododecane-1,4,7,10,13-pentaacetic acid) or HEHA (1,4,7,10,13,16-hexaazacyclododecane-1,4,7,10,13,16-hexaacetic acid) (Fig. 9) show a decrease in kinetic inertness and thermodynamic stability. As follows from this, the preferential framework in comparison to the DOTA-derived chelators is the Cyclen (1,4,7,10-Tetraazacyclododecan) skeleton.

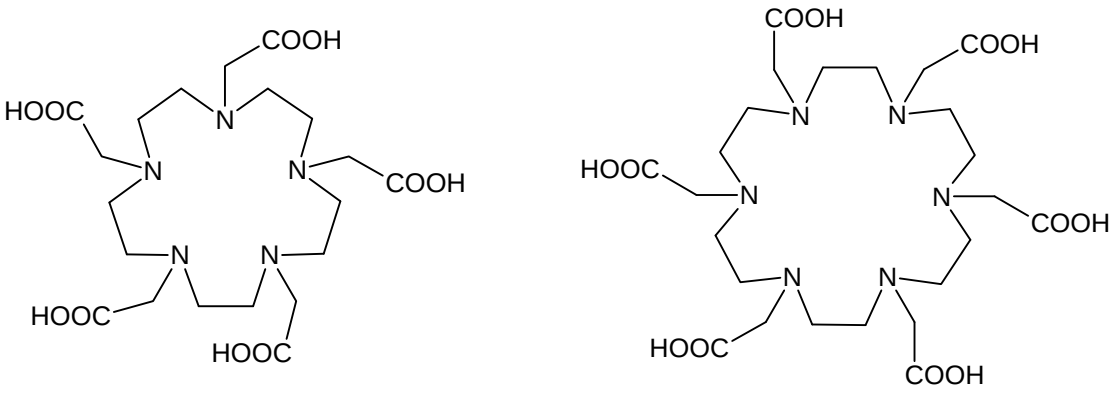

Fig. 9: macrocyclic chelators left: PEPA and right: HEHA

Advantages that come with improved stability and inertness often require harsh labelling condition, i.e. high temperatures, to achieve high labelling yields (Maecke, et al., 2003; Liu, et al., 2001). This might not be too much of a problem with peptides, but with antibodies, it certainly is. A too high temperature may result in the loss or at least a degradation of the affinity of the antibody towards the receptors on the tumour cells and can cause the unfolding of the protein.

The Linker is often used for modifying the pharmacokinetic properties of the radiopharmaceutical. A linker can be for example a simple hydrocarbon chain to increase lipophilicity, or a peptide sequence to improve the hydrophilicity and renal clearance (e.g. polyglycine, polyserine, polyasparatic). Fig. 10 shows several types of linkers that are common in the design of targeting biomolecules.

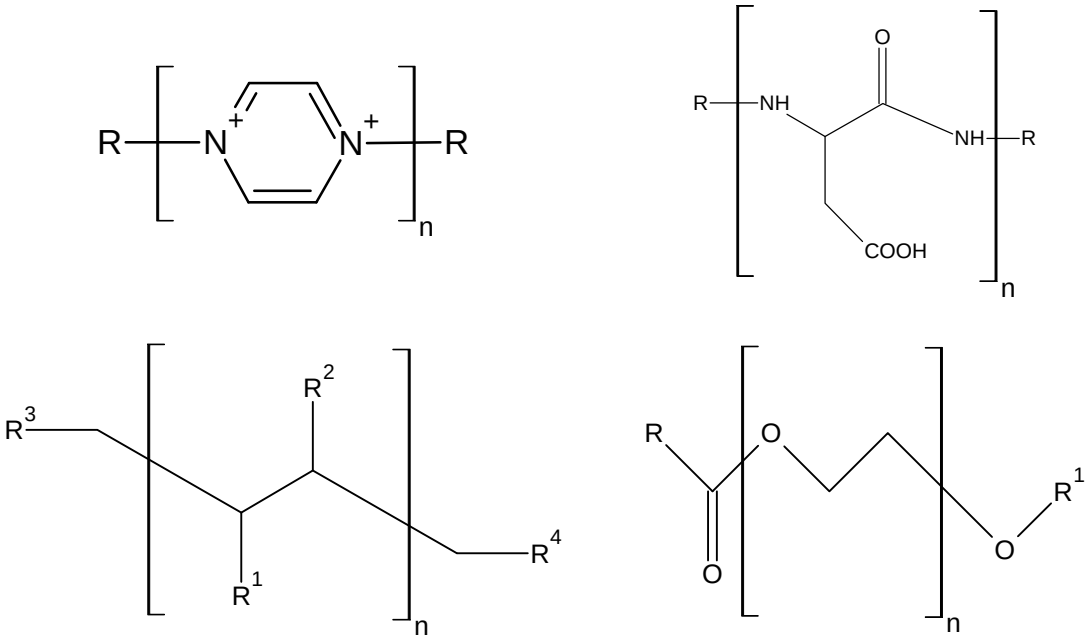

Fig. 10: Types of linker for radiopharmaceuticals; clockwise from above, left: cationic, anionic, cleavable, neutral linker

Depending upon the radionuclide and the bifunctional chelator, linker groups capable of rapid metabolism can increase the clearance of the radiopharmaceutical from the blood via the renal system. The choice of a linker depends foremost on the pharmacokinetic requirements for the radiopharmaceutical.

The last step obviously comprises the conjugation between the BFC and the biomolecule, either directly or via a linker. In principle there are two approaches (Fig. 11): the pre-labelling and post-labelling approach. In the latter the conjugation of the BFC with the biomolecule occurs before the radiolabelling with the respective radionuclide. In the first one the radiolabelling step comes first. The post-labelling approach seems suitable for biomolecules that are more resistant the harsh chemical environment during the chelation step such as for peptides. More sensitive biomolecules are labelled via the pre-labelling approach (Liu, et al., 2001).

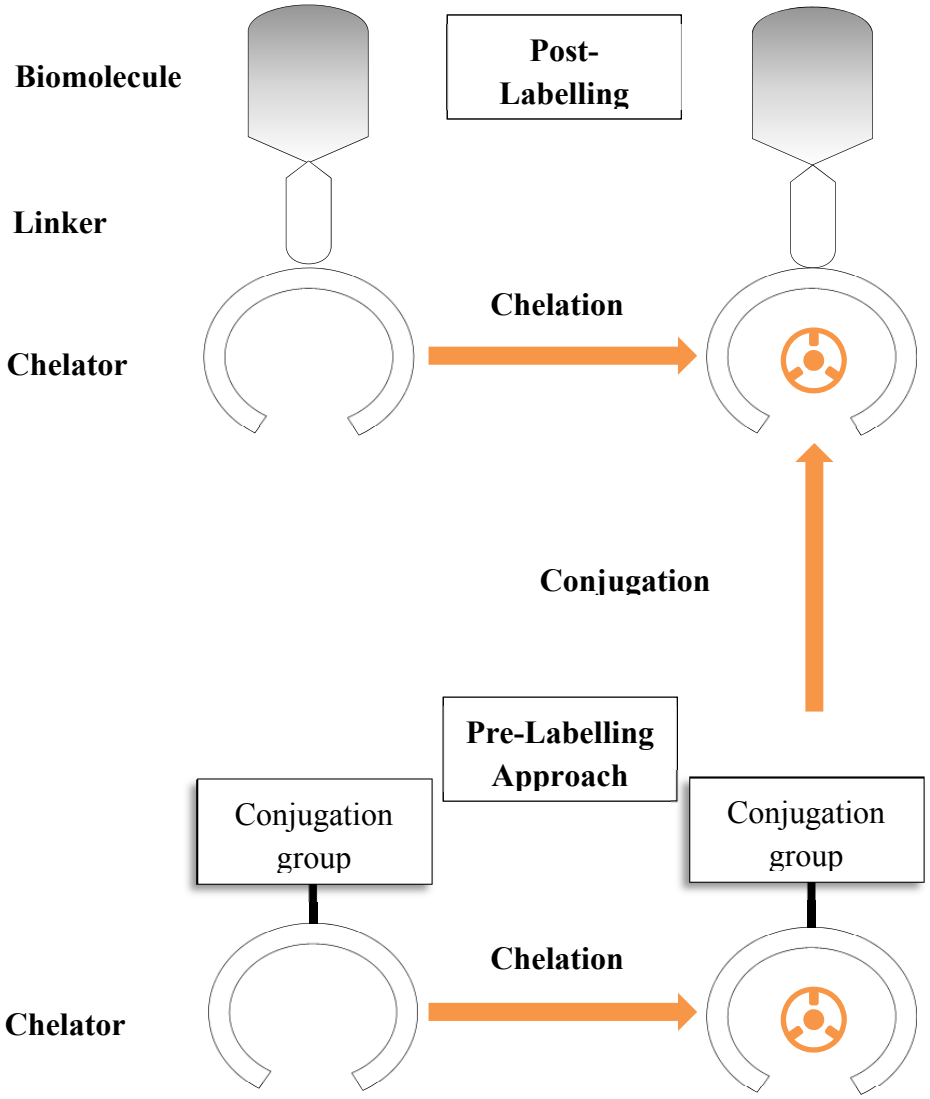

Fig. 11: Radiolabelling approaches (Liu, et al., 2001)

3.3 ^{177}Lu for medical applications

The successful application of ^{177}Lu is determined by the technically achievable specific activity (SA) [GBq/g] or [GBq/mol] and its chemical purity. A high SA of the radionuclide is essential for an efficient radiolabelling reaction.

^{177}Lu can be obtained via two alternative routes (Fig. 12):

(1) ^{176}Lu(n,γ)^{177}Lu

(2) ^{176}Yb(n,γ)^{177}Yb $\xrightarrow{\beta^-}$ ^{177}Lu

Route (1) represents a neutron capture reaction on the isotope ^{176}Lu which is activated to ^{177}Lu. This production way provides only a reduced specific activity since target material cannot be separated from ^{177}Lu chemically. Besides, by irradiation of ^{176}Lu the long-lived radionuclidic impurity ^{177m}Lu is co-produced (Fig. 12). With a half-life of 160.1 days it might cause radiation protection and waste disposal problems.

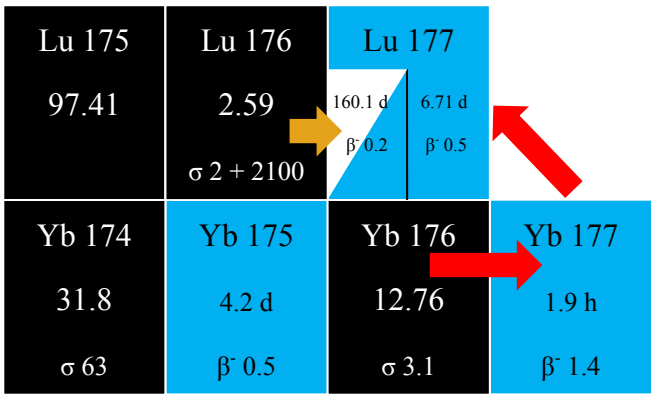

Fig. 12: Cut-out form chart of the nuclides: red arrows indicate route (1), orange arrow indicates route (2)

The ^{177m}Lu content is mainly depending on two factors: irradiation time and cooling period. The amount of ^{177m}Lu can rise up to 0.01% of the ^{177}Lu activity (Dvorakova, 2007). Typically, carrier added (c.a.) ^{177}Lu is produced at nuclear reactors with intermediate neutron flux of 1 - 3·10^{14} cm^{-2} s^{-1} and irradiation times of up to 14 days. Under the above mentioned conditions reported values for the ^{177m}Lu/^{177}Lu ratio from several reactors vary between 0.01% - 0.02% at EOB (Knapp, Jr., et al., 1995; Dvorakova, 2007; Pawlak, et al., 2004). Hospitals are using their ^{177}Lu up to one week after EOB when the ^{177m}Lu/^{177}Lu ratio has doubled (Fig. 23). A usual therapeutic dose of ^{177}Lu ranges between 7 and 9 GBq. When the ^{177m}Lu/^{177}Lu ratio is 0.02%, this means, that a dose includes approximately 1.4 – 1.8 MBq ^{177m}Lu.

^{177}Lu is already commercially available and can be obtained with a specific activity of 0.19 - 0.6 TBq/mg. Besides the relatively low SA all these products are produced via route (2) and therefore contain ^{177m}Lu.

An attractive alternative is the indirect nuclear reaction. Through irradiation of highly enriched ^{176}Yb (> 99%), the short-lived intermediate radioisotope ^{177}Yb is produced (T½ = 1.9 h), which subsequently decays into ^{177}Lu (Fig. 12). Here, the aspired nuclide ^{177}Lu represents an isotone of the target nuclide ^{176}Yb and thus can be chemically isolated in n.c.a. form. Since no ^{177m}Lu is formed (Fig. 12) by the decay of ^{177}Yb (Firestone, et al.), ^{177}Lu is produced with a very high radionuclidic purity.

A disadvantage of this method is the required chemical separation of micro amounts of ^{177}Lu from macro amounts of Yb. For large-scale production, massive ^{176}Yb targets must be irradiated. The chemical separation of ^{177}Lu (micro) from Yb (macro) has already been described elsewhere (Lebedev, et al., 2000; Horwitz, et al., 2005). For example, it was possible to precipitate macroscopic quantities of Yb (up to 200 mg) on a Na (Hg) amalgam electrode in a so-called cementation process (Lebedev, et al.). However, the use of mercury in this process is a critical point for preparation of pharmaceutical grade radionuclides. Another method implemented extraction chromatography and resulted in separable amounts of Yb of up to 50 mg (Horwitz, et al., 2005). Solely, the decontamination factors were very low and hence multiple repetitions in order to multiply these factors were necessary.

Another nuclide to mention is the Hafnium isotope, which is produced through the decay of ^{177}Lu, ^{177}Hf ($^{177}Lu \xrightarrow{\beta^-} {}^{177}Hf$). Fortunately, its ingrowth is negligible as Hf does not interfere with the labelling, although, the ^{177}Hf mass already surpasses that of ^{177}Lu after a little more than 14 days what Breeman could demonstrate in a study conducted with DOTA as chelator (Breeman, et al., 2003) (Fig. 13).

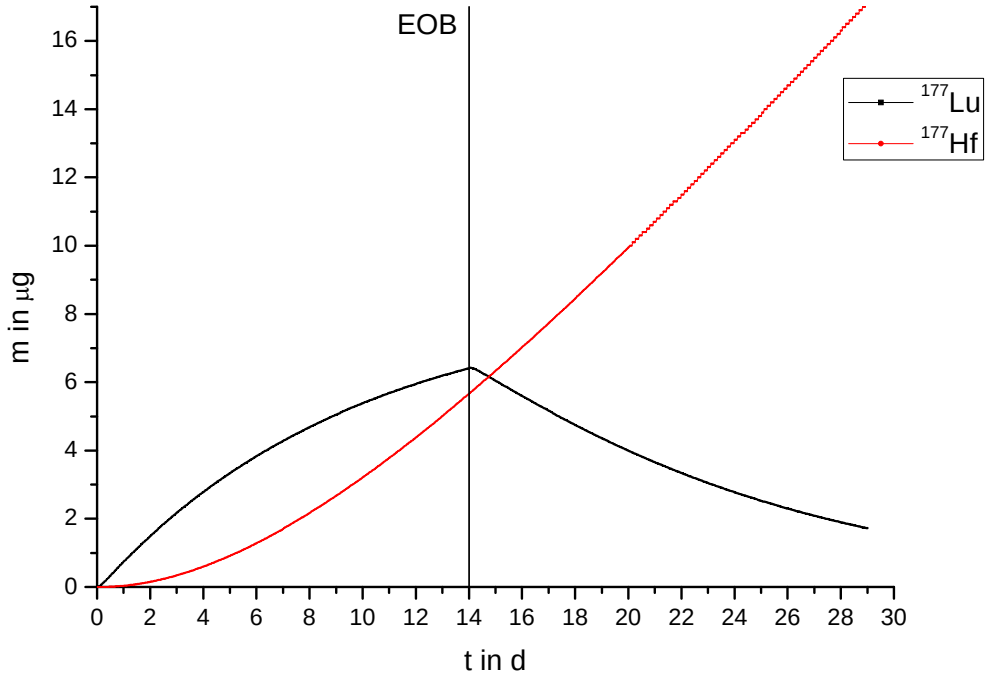

Fig. 13: Increase of the masses of ^{177}Hf and ^{177}Lu over irradiation (14 days) and decay time (15 days); Neutron flux = $1.29 \cdot 10^{14}$ n/cm^2/s; Target mass = 100 mg; EOB = End Of Bombardment

3.4 The research reactor FRM II as neutron source for the production of ^{177}Lu

Since its start of operation in 2004, the new neutron research reactor FRM II at the Forschungszentrum Garching has become an important source for radionuclide production. The concept of the reactor is based on ideas which were for the first time implemented in the build-up of the ILL (Institut Laue-Langevin) reactor in Grenoble/France.

The research reactor in Garching is a medium-flux reactor with a maximum flux of up to $1.3 \cdot 10^{14}$ n/cm^2/s. It comprises 11 irradiation positions, 1 channel reserved for an extra-fast irradiation system, 4 hydraulic capsule irradiation positions and 6 pneumatic rabbit irradiation positions.

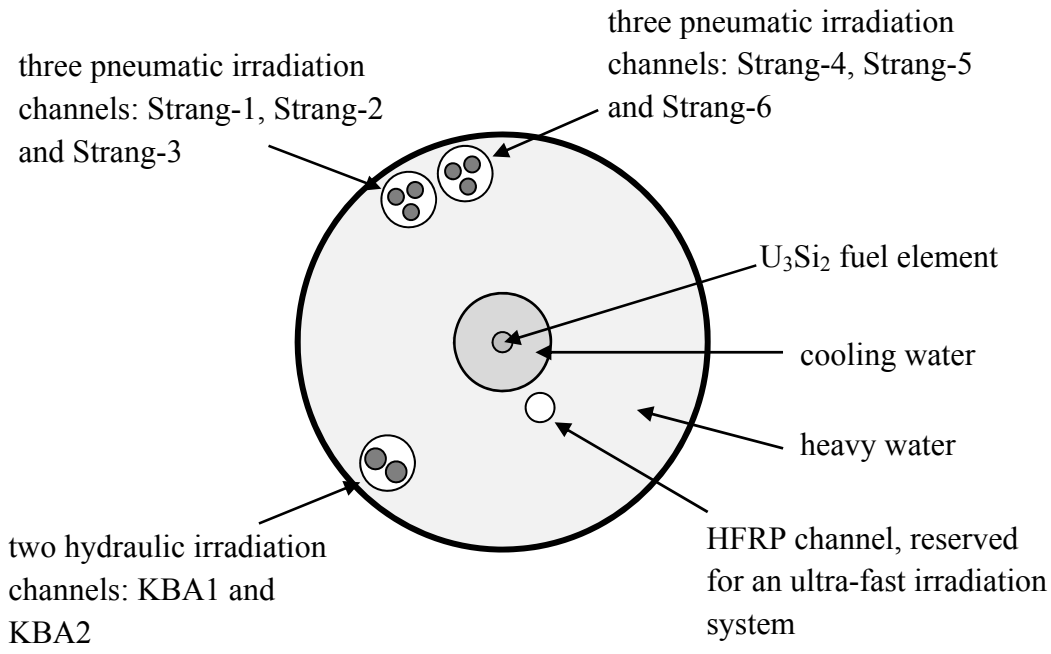

Fig. 14: Sketch of the irradiation positions at FRM II (Lin, et al., 2006)

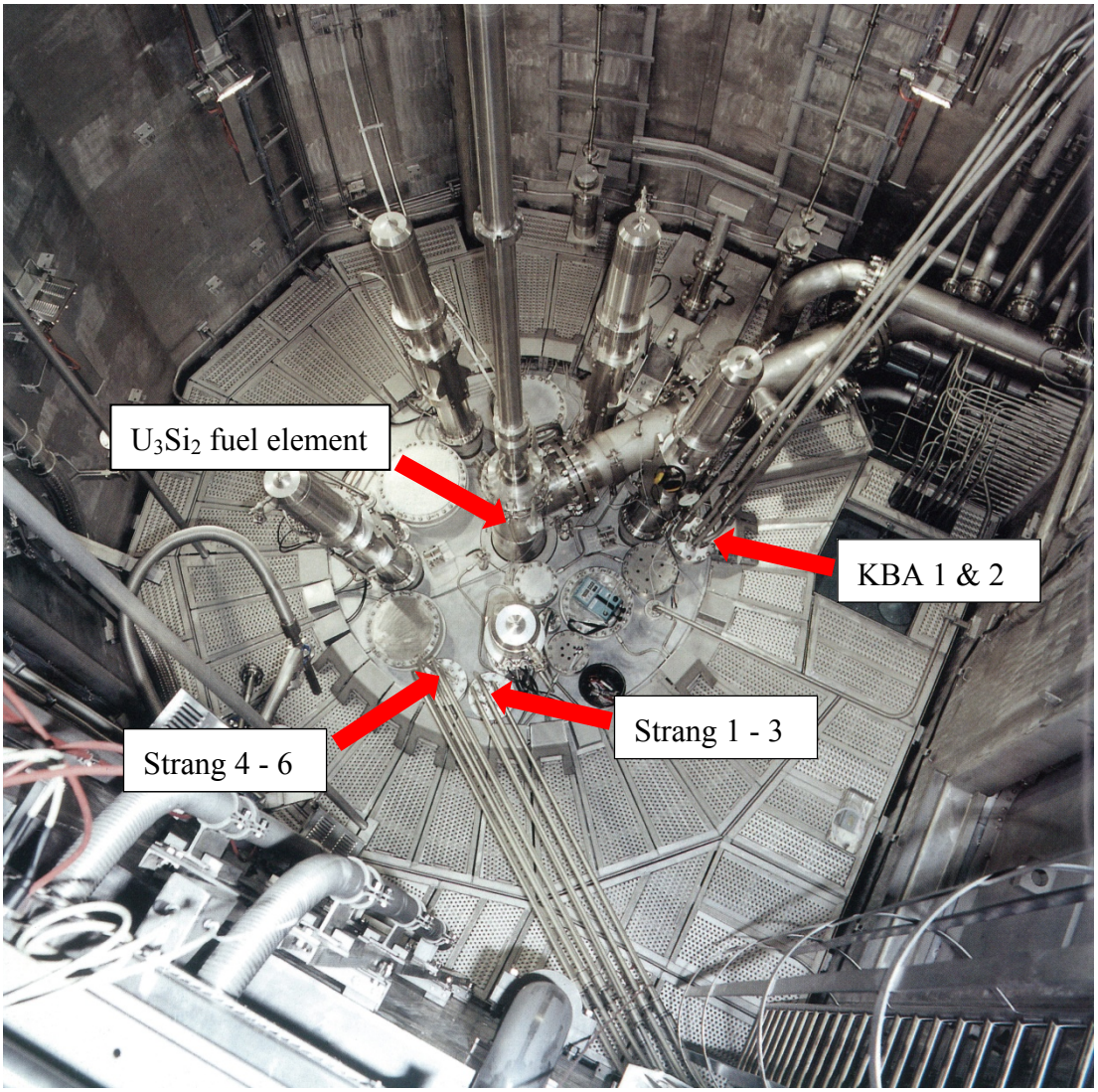

Fig. 15: View from above onto the reactor pool at FRM II (FRM-II)

Five cycles take place per year, which means, each cycle takes about 50 days. The fuel element itself, U_3Si_2, contains uranium enriched up to 93 % and is embedded in an aluminium matrix. The hollow cylinder core has an outer diameter of 24 cm, a rather small size, which results in a relatively small reactor power of 20 MW (compared to the old FRM reactor with 4 MW or to the international high-flux reactor ILL with a maximal power of 57 MW). For the cooling of the fuel cylinder, light water is passed through its core, which on its outer part is surrounded by heavy water (D_2O), the moderator for the neutrons.

Due to the compact architecture of the element, 70 % of the neutrons escape the uranium zone and build up the undisturbed maximum of the thermal neutron flux density (~ $8 \cdot 10^{14}$ $n/cm^{-2}/s^{-1}$) outside of the core, in a distance of approximately 12 cm. This area of maximum flux density is usable for experiments. Along its outline, a series of beam tubes and radiation channels are assembled.

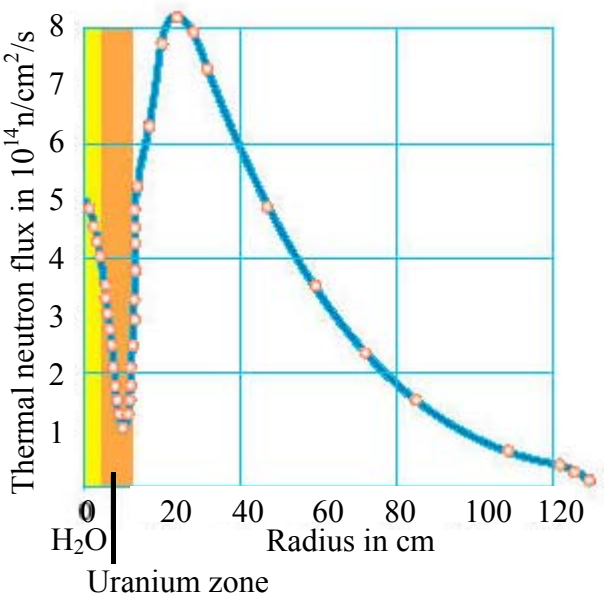

Fig. 16: Thermal neutron flux density in dependence of the distance to the fuel core at half height of the fuel element. The maximum lies approximately at a distance of 12 cm from the core. (FRM-II)

Fig. 16 shows the thermal neutron flux in dependence of the distance to the fuel core.

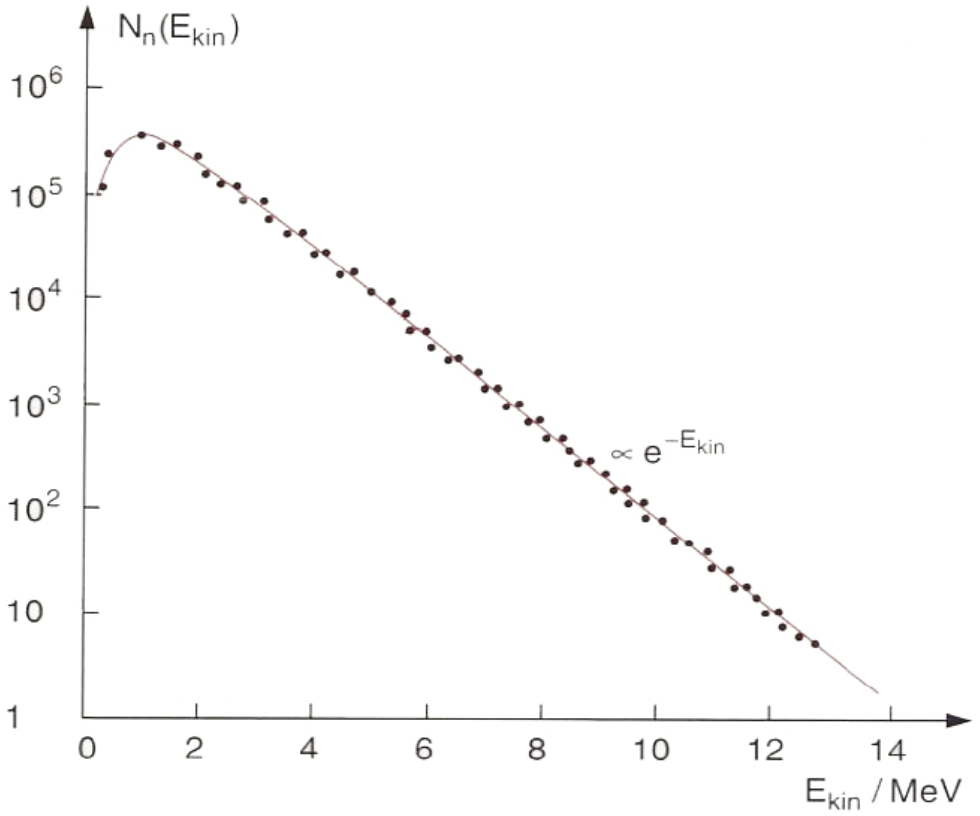

Fig. 17: Number of neutrons emitted during fission process plotted against their kinetic energy (FRM-II)

Fig. 17 shows the number of neutrons emitted during a fission process plotted against their kinetic energy. It becomes evident through this figure, that most neutrons have energies in the MeV-region and therefore must be moderated in order to be used in n,γ-reactions.

The probability of a neutron capture depends on the kinetic energy of the neutron. The slower the neutron is, the higher is the probability of a capture because of the longer dwell time in the vicinity of the nuclear core. For the production of radioisotopes at nuclear research reactors, the interest lies on those neutron capture reactions, which produce neutron rich isotopes that decay preferentially via β^--decay. Generally speaking, there are three groups of neutrons with different energy levels that can be classified as follows:

1. Fast neutrons – neutrons with energies above 0.1 MeV; no significance for radioisotope production.
2. Epithermal neutrons – neutrons in the range between ~ 0.5 eV and 10 keV; their distribution can be described according to the 1/E-law.
3. Thermal neutrons – neutrons below the cadmium cut-off edge of 0.5 eV; those slow neutrons are, as already mentioned above, moderated to a velocity or an energy, respectively, where the cross sections for simple n,γ-reactions are high and therefore usable for radioisotope production.

Fig. 18 extends the 3 groups of neutrons and shows the wide range of neutrons and their application in modern science nowadays.

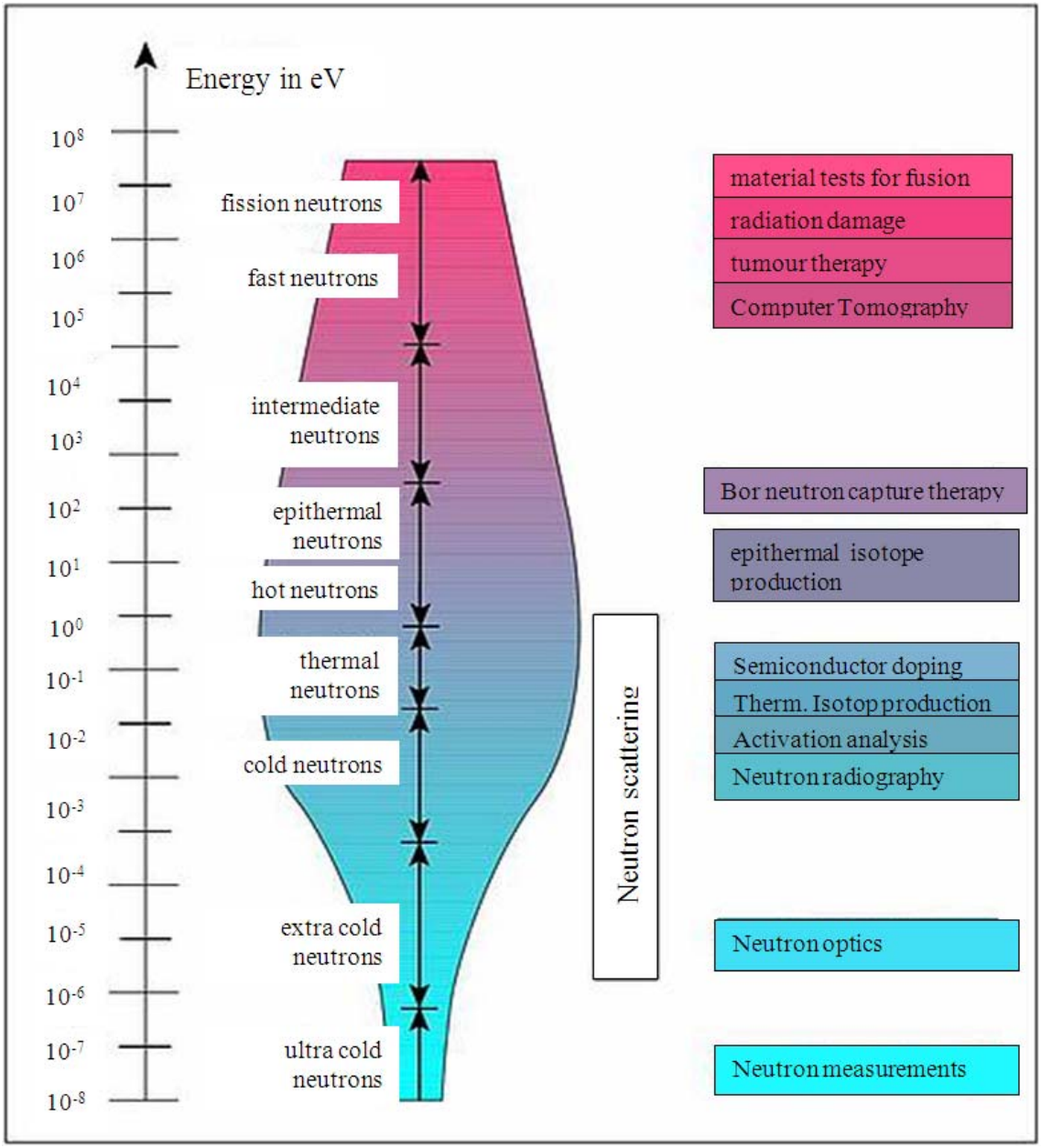

Fig. 18: Energy of different types of neutron and there specific application. The size of the coloured regions is proportional to the amount of neutrons available. (FRM-II)

4

RADIOCHEMICAL ASPECTS OF N.C.A. ^{177}LU PRODUCTION AND WORKING HYPOTHESIS

4 Radiochemical aspects of n.c.a.^{177}Lu production and working hypothesis

4.1 Irradiation Yield

As the production of ^{177}Lu is accomplished via the indirect production route the equation for a (n,γ) nuclear reaction cannot be applied. In that case, the subsequent decay of the intermediate ^{177}Yb to ^{177}Lu has to be considered (Eq. 3.1 & 3.2):

$$A_{177_{Lu}} = \sigma_{176_{Yb}} \cdot \Phi_{th} \cdot N_{176_{Yb}} . \lambda_{177_{Lu}} \left[\frac{1 - e^{-\lambda_{177_{Lu}} t}}{\lambda_{177_{Lu}}} + \frac{e^{-\lambda_{177_{Yb}} t} - e^{-\lambda_{177_{Lu}} t}}{\lambda_{177_{Yb}} - \lambda_{177_{Lu}}} \right] \tag{3.1}$$

$$A_{177_{Lu}} = \sigma_{176_{Yb}} \cdot \Phi_{th} \cdot N_{176_{Yb}} \cdot \lambda_{177_{Lu}} \left\{ \left[\frac{1 - e^{-\lambda_{177_{Lu}} t}}{\lambda_{177_{Lu}}} + \frac{e^{-\lambda_{177_{Yb}} t} - e^{-\lambda_{177_{Lu}} t}}{\lambda_{177_{Yb}} - \lambda_{177_{Lu}}} \right] \cdot e^{-\lambda_{177_{Lu}} t_d} + \frac{\left(1 - e^{-\lambda_{177_{Yb}} t}\right) \cdot \left(e^{-\lambda_{177_{Yb}} t_d} - e^{-\lambda_{177_{Lu}} t_d}\right)}{\lambda_{177_{Yb}} - \lambda_{177_{Lu}}} \right\} \tag{3.2}$$

Where $N_{176_{Yb}}$ is the initial number of ^{176}Yb atoms, $\sigma_{176_{Yb}}$ is the cross section of the ^{176}Yb(n,γ)^{177}Yb reaction, Φ_{th} is the neutron flux of the irradiation source, t is the irradiation time, t_d is the decay time after irradiation and $\lambda_{177_{Yb}}$ and $\lambda_{177_{Lu}}$ the decay constants of ^{177}Yb and ^{177}Lu, respectively (Fig. 19). In addition, equation 3.2 considers the time after the target is taken out of the reactor, i.e. the cooling time when no more ^{177}Yb is produced.

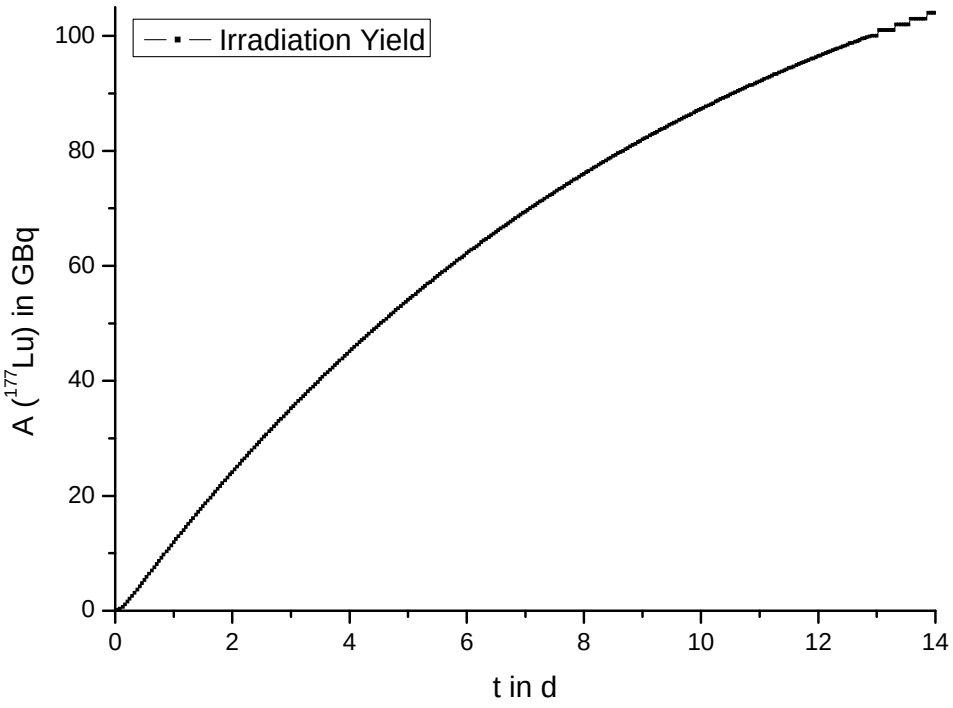

Fig. 19: Irradiation yield of ^{177}Lu; 100 mg Yb target (target 1) as a function of irradiation time; neutron flux: $1.29 \cdot 10^{14}$ n/cm^2/s; ^{176}Yb(n,γ)^{177}Yb → ^{177}Lu

Up to 12 GBq of ^{177}Lu can theoretically be produced after 14 days (about two half-lifes) irradiation of a 100 mg natural ^{176}Yb target at the KBA1-1 irradiation position ($1.29 \cdot 10^{14}$ n/cm^2/s) at the FRM II research reactor. There is no data available for the neutron capture cross section of the intermediate nuclide ^{177}Yb. However, it can be, assumed that ^{177}Yb quantitatively decays to ^{177}Lu due to the short half-live even at higher neutron flux and no significant losses through its neutron activation are to be expected. Concerning the other occurring stable nuclides of natural Yb (^{168}Yb, ^{170}Yb, ^{171}Yb, ^{172}Yb, ^{173}Yb, and ^{174}Yb), only ^{168}Yb has a rather high neutron capture cross section (2400 b). That means that no self-shielding effects might cause a decrease of the activation rate during irradiation.

In contrast, up to 94 GBq of ^{177}Lu can theoretically be produced implementing a highly enriched irradiation target (99.72% ^{176}Yb) assuming the same conditions as in the previous paragraph.

It is mandatory to use enriched Yb targets in order to get a high irradiation yield and highest specific activity, obligatory for a highly efficient use of ^{177}Lu. This point will be discussed in detail in the following chapter (4.2).

4.2 Achievable Specific Activity

As already described above, for targeted radionuclide therapy it is crucial to obtain the highest possible specific activity. Contaminations of the demanded radionuclide, here ^{177}Lu, with competitors for labelling positions on targeting vehicles like cold Lu, Yb, or any other lanthanide must therefore be excluded to the highest possible extent. On the one hand, this can be accomplished to a certain degree by the separation technique applied. On the other hand, a pre-selection of the target material is mandatory because similar atoms that only differ in their atomic mass numbers cannot be chemically separated by any means.

Two different target materials in respect to their grade of enrichment of the isotope ^{176}Yb were evaluated to show the effect of the enrichment of ^{176}Yb. Natural occurring Yb consists of seven stable isotopes (Fig. 20).

Yb 168	Yb 169	Yb 170	Yb 171	Yb 172	Yb 173	Yb 174	Yb 175	Yb 176
0.13		3.04	14.28	21.83	16.13	31.83		12.76
σ 2400		σ 12	σ 53	σ ~1.3	σ 16	σ 63		σ 3.1

Fig. 20: Cut-out form chart of the nuclides showing the stable isotopes of natural Yb with their natural abundance and their cross section

As can be seen clearly from Fig. 20, irradiation of natural Yb without further processing would not only yield ^{177}Yb but also the unstable isotope ^{175}Yb. The latter decays via β^--emission to ^{175}Lu, ($^{175}Yb \xrightarrow{\beta^-} {}^{175}Lu$), leading to an accumulation of stable lutetium in the system and decreasing the specific activity of the nuclide.

The following two different grades of enrichment are taken for the analysis: 99.72% (named afterwards target 1, Table 5) and 97.2% (named afterwards target 2, Table 7) ^{176}Yb, respectively. Special focus also has to be laid on the low content of ^{174}Yb because of the growth of ^{175}Lu through its activation. Its content in the two types of target material was as follows: 0.15% and 2.23%, respectively.

As mentioned above, the specific activity is defined as the activity of the nuclide divided by the total mass of all of its radioactive and stable isotopes. Thus, for the calculation of the specific activity, the activity of ^{177}Lu (eq. 3.2) is divided by all occurring masses present in the irradiated target that decrease the latter including ^{177}Lu itself. In this case the masses to consider are ^{177}Lu, ^{175}Lu, and cold Lu present in the target material (eq. 3.3).

$$A_{S\,177_{Lu}} = \frac{A_{177_{Lu}}}{m_{177_{Lu}} + m_{175_{Lu}} + m_{Lu}} \tag{3.3}$$

The calculation of the SA for the different target compositions is presented in Fig. 21 as a function of time of irradiation. An overall concentration of 5 ppm of Lu (Table 8) as general impurity was taken as a basis for the calculations which is the reason that the specific activity is not equivalent to the maximal theoretically achievable SA at the start. For all calculations (eq. 3.3), the following parameters of irradiation were chosen:

- cross section:
  - ^{176}Yb: $\sigma = 3.1 \cdot 10^{-24}$ cm^{-2}
  - ^{174}Yb: $\sigma = 63 \cdot 10^{-24}$ cm^{-2}
- irradiation position:
  - KBA 1-1: $\Phi_{th} = 1.29 \cdot 10^{14}$ n/cm^2/s (Fig. 21)
  - ILL (Grenoble)[8]: $\Phi_{th} = 1.5 \cdot 10^{15}$ n/cm^2/s (Fig. 22)
- content of cold Lu: 5 ppm

[8] The neutron source at the Institute Laue-Langevin (ILL) in Grenoble, France, serves only as an example of a high flux reactor in order to demonstrate the influence of a higher neutron flux. No real experiments with enriched target material were performed there in the scope of this work.

The maximum theoretically achievable specific activity for ^{177}Lu is ~ 4.07 TBq/mg. With target 2 and all above mentioned parameters a max. SA of about 3.89 TBq/mg (95.6% of theoretical value) is possible after an irradiation time of about 7.5 days, whereas with target 1 only 3.49 TBq/mg (after about 2 days, 85.7% of theoretical value) is achievable (Fig. 21). While it only takes about two days before target 1 reaches its highest possible SA under the given conditions and the decrease in quality already starts after 1/7 of the activation time, target 2 reaches the maximal SA (4.02 TBq/mg) not until 7.5 days of irradiation, i.e. after half of the irradiation time has passed. At end of bombardment (EOB) the specific activity of target 2 has only decreased to ~ 94.8% of the max. theoretical SA, that is 3.86 TBq/mg, so no significant decrease of the specific activity occurs. As the decline in SA for target 1 already starts after 2 days only about 64.1% of its highest achievable SA (3.86 TBq/mg) is obtained after 14 days. The decrease then accelerates further because the growth of ^{177}Lu subsides quickly after EOB ($t_{½}$ (^{177}Yb) = 1.9 h) while ^{175}Lu keeps steadily growing from decay of ^{175}Yb ($t_{½}$ = 4.2 d). After a cooling time of 15 days target 1 only yields a specific activity of about 806 GBq/mg, i.e. ~ 19.8% of max. theoretical value, while target 2 still shows a very high value of 3.01 TBq/mg (~ 74% of max. theoretical value).

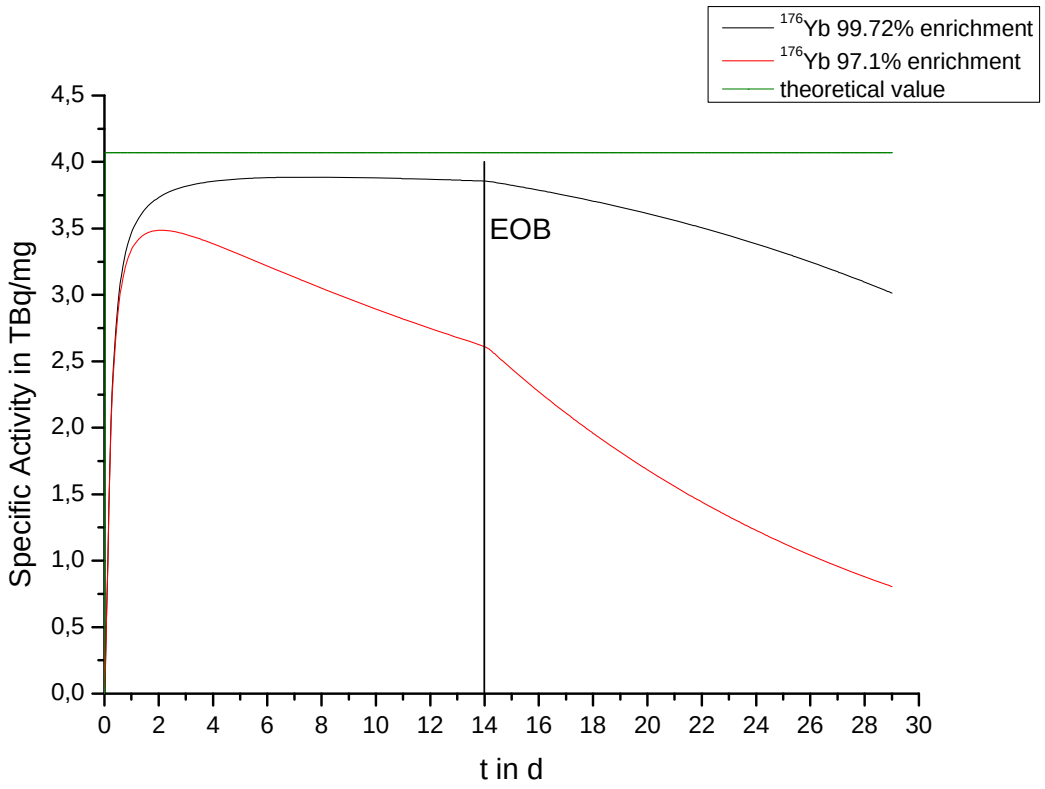

Fig. 21: Specific activity of ^{177}Lu of two different Yb-materials: black - grade of enrichment 99.72%; red 97.2%; irradiation time: 14 days; decay time: 15 days; cold Lu: 5 ppm;

A higher specific activity can be achieved by irradiations at a reactor with a higher neutron flux, like the reactor at the 'Institut Laue-Langevin' (ILL) in Grenoble, France. The maximal neutron flux there equals $1.5 \cdot 10^{15}$ n/cm^2/s. Fig. 22 shows the results for the SA again as a function of time of irradiation with the same parameters as above, but a higher neutron flux. For target 1 4.02 TBq/mg (98.8% of theoretical value) can be reached and even with target 2 the specific activity is extended to 3.86 TBq/mg (94.9% of theoretical value).

As these calculations show, it is essential to use a highly enriched ^{176}Yb as a target material with the lowest content of ^{174}Yb and cold lutetium in order to achieve the highest possible SA of ^{177}Lu.

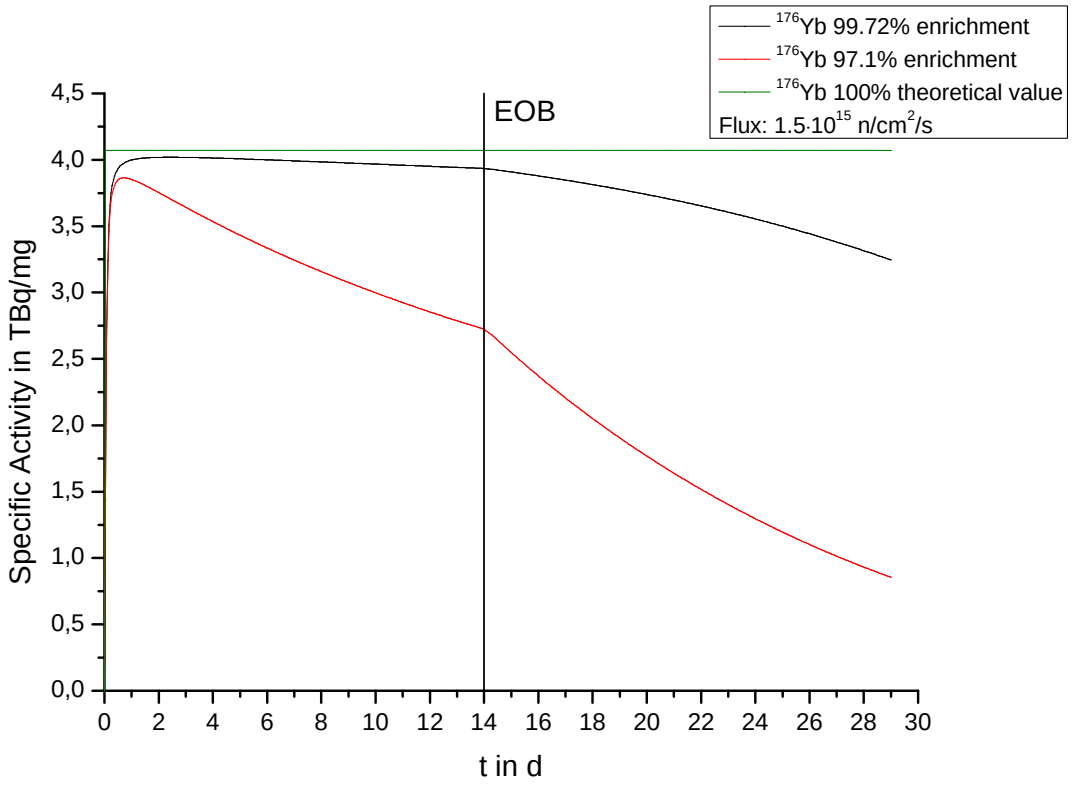

Fig. 22: Specific activity of ^{177}Lu two different Yb-materials: black - grade of enrichement 99.72%; red - 97.2%; irradiation time: 14 days; decay time: 15 days; Neutron flux = 1.5·10^{15} n/cm^2/s; Target mass = 100 mg; cold Lu: 5 ppm;

4.3 Radionuclidic & chemical purity

The content of ^{176}Lu(st) in the original target material (Table 7, Table 8) leads to accumulation of the relatively long-lived beta and photon emitter ^{177m}Lu ($T_{1/2}$ = 160.1 d) via the ^{176}Lu(n,γ)^{177m}Lu reaction. The relative content of ^{177m}Lu in the lutetium target increases with irradiation time and further grows after EOB due to the longer half-life of ^{177m}Lu in comparison to ^{177}Lu (Fig. 23).

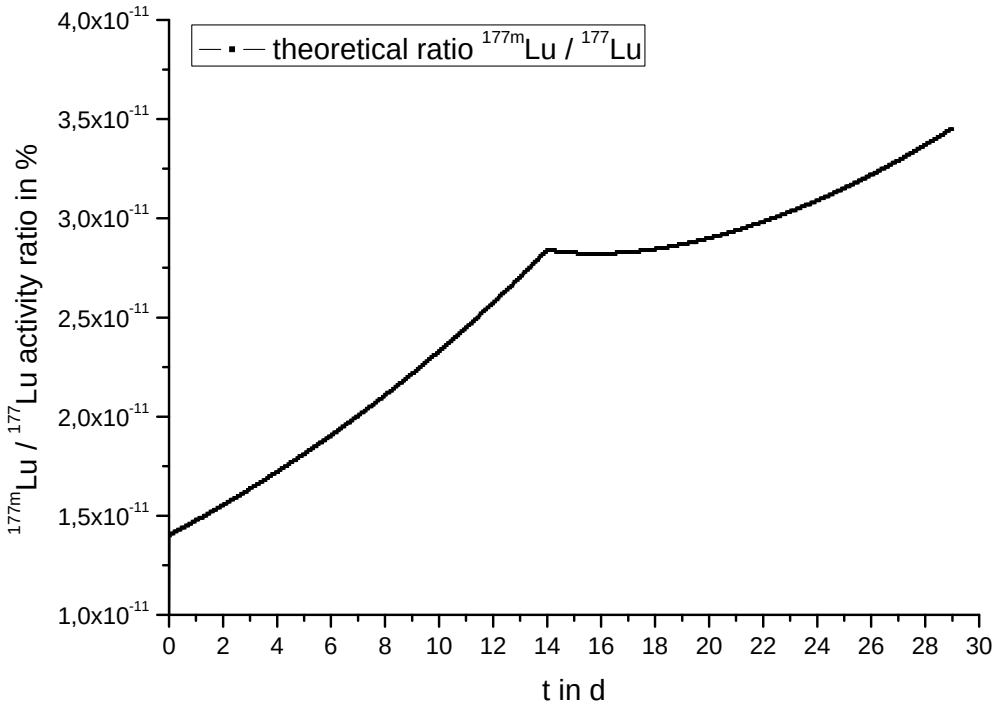

Fig. 23: Theoretical ratio of ^{177m}Lu and ^{177}Lu activities; of highly enriched ^{176}Yb target (Table 8, Table 6), 5 ppm Lu impurities, 14 d irradiation time

The same also applies to other metals that could decrease the labelling yield, for example other lanthanides. Table 3 shows the stability constants of DOTA with some metals in comparison to the Lu-DOTA complex. From this can be seen that not only cold Lu is a competitor for the available labelling positions but also a number of metals besides the lanthanides (Table 3). These metals display a similar or even higher (such as Fe(III)) stability constant and therefore will be strong competitors for radiolabelling reactions. It is crucial to exclude metal impurities in order to obtain excellent labelling results and in order to extend the shelf-life of n.c.a.^{177}Lu.

Table 3: Stability constants (logK) for metal-DOTA complexes; 1 - 14 (Tóth, et al., 1994); 15 (Chaves, et al., 1991); 16 – 18 (Delgado, et al., 1982)

	Element	logK
1	La(III)	20.7
2	Ce(III)	21.6
3	Pr(III)	22.4
4	Nd(III)	22.5
5	Sm(III)	23.3
6	Eu(III)	23.7
7	Gd(III)	23.6
8	Tb(III)	23.6
9	Dy(III)	23.5
10	Ho(III)	23.5
11	Er(III)	23.5
12	Tm(III)	23.7
13	Yb(III)	24.0
14	Lu(III)	23.5
15	Fe(III)	24.5
16	Ca(II)	17.2
17	Zn(II)	21.0

4.4 Chemical Approach

Production of adequate ^{177}Lu activities requires irradiation and processing of massive Yb targets (> 50 mg). 14 days irradiation of a highly enriched ^{176}Yb target at 10^{14} neutrons $cm^{-2}s^{-1}$ results in a Yb to ^{177}Lu ratio of about 10^3. Thus, Yb must be reduced by a factor > 10^4 in order to obtain a high quality of ^{177}Lu. For a 100 mg ^{176}Yb target with an enrichment of 99.72% (target 1) and 14 days irradiation at FRM II position KBA 1-1 ($\Phi = 1.29 \cdot 10^{14}$ n/cm^2/s), the ratio of Yb to ^{177}Lu is approximately $4 \cdot 10^3$. That means, to achieve the above-mentioned Yb to ^{177}Lu ratio of 1:10, a decontamination factor of about 10^4 is necessary.

The separation of two neighbouring lanthanides is challenging because of their chemical similarity. A chelator has to be introduced in order to modify the behaviour of the two atoms with respect to the stationary phase. I.e., the presence of a complex-forming agent leads to a decrease in the adsorption of cations on a cation exchanger. In this case, the stability constant of Lu is greater than that of Yb and therefore elutes first. It is noteworthy that the most efficient separating reagent for lanthanides, α-HIBA (Fig. 24), is a complexing agent identified 50 years ago. Despite a considerable amount of effort around the world, until present, no aqueous complexing agent has been identified that rivals α-HIBA in its sensitivity to lanthanide cation radii (Nash, et al., 2001).

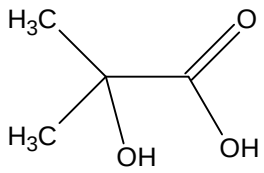

Fig. 24: Molecular structure of α-Hydroxisobutyric acid (α-HIBA)

The different stability constants of the respective Lu and Yb complexes make it possible that the Lu/α-HIBA complex elutes first. As Lu shows a higher stability constant, it interacts fewer with the resin and therefore elutes earlier. That means, the micro phase moves faster along the column and, therefore, any contamination of the system with the macro phase can be avoided. Even tubes and other technical parts of the system, which are in contact with the solution, stay clean of the macro phase that way.

However, increasing the target mass complicates the isolation of micro amounts of ^{177}Lu and specific optimization of the column process must be performed.

Table 4 shows the separation factors for the respective lanthanide pairs adjacent to each other on a cation-exchanger with α-HIBA as eluent. In contrast to other adjacent elements, only a separation factor of 1.54 for the Yb(III)/Lu(III) system can be achieved.

Table 4: Neighbouring lanthanides with separation factors on a Dowex 50 cation-exchanger resin; eluent: α-HIBA (Marhol 1982)

Element	α-HIBA (25°C)
Lu/Yb	1.54
Yb/Tm	1.70
Tm/Er	1.71
Er/Ho	1.73
Ho/Dy	1.80
Dy/Tb	2.30
Tb/Gd	2.40
Gd/Eu	1.65
Eu/Sm	1.88
Sm/Pm	2.13
Pm/Nd	1.54
Nd/Pr	1.68
Pr/Ce	1.85
Ce/La	1.97

The method of choice for the separation task in this work is ion exchange chromatography (IEC). IEC uses the different affinities of the ions in question or complexes thereof towards the selective, ionogenic groups of the stationary phase to separate them from each other. On the one hand, the resins used have to be very resistant to ionizing radiation because highly activated targets are loaded within a very small volume onto them in order to create optimal starting conditions in the following separation. On the other hand, a high specificity towards the nuclide in question must be ensured, as the separated isotope is only present in micro quantities compared to the stable elements.

4.5 Working Hypothesis

N.c.a. ^{177}Lu can be produced at a TBq level through irradiation of massive ^{176}Yb targets. High SA can be achieved by using on the one hand highly enriched ^{176}Yb target material, thus avoiding cold Lu and ^{177m}Lu and, on the other hand, ion exchange chromatography with a complexing agent as method of choice for the separation of the two adjacent elements.

5

EXPERIMENTAL

5 Experimental

5.1 Reagents

The solutions used in all processes within this work were prepared exclusively with water purified through a Millipore-System (Milli-Q plus 185, Millipore, Schwalbach; main resistance ≤ 18.2 MΩ·cm, TOC: 1-5 ppb).

α-Hydroxyisobutyric acid was purchased from Sigma-Aldrich Chemie GmbH (Taufkirchen) and used without any further purification. The stock solution thereof with a concentration of 1.2 M was adjusted to pH 4.75 with ammonia (32%) purchased from VWR International GmbH (Ismaning). The strong acidic resin for the columns used for most of the separations was a custom made cation exchanger. Purification of the resin was carried out with hydrochloric acid (37%) purchased from VWR International GmbH (Ismaning). The conversion into the NH_4^+-form was performed with NH_4Cl purchased from Sigma-Aldrich Chemie GmbH (Taufkirchen).

c.a.^{177}Lu for the labelling experiments was purchased from IDB-Holland B.V. with a claimed specific activity of 756.9 GBq/mg.

The natural Yb in its nitrate form ($Yb(NO_3)_3 \cdot 5\ H_2O$, 99,999%) used for the pre-experiments was purchased from Sigma-Aldrich Chemie GmbH (Taufkirchen) and used without further purification.

Enriched Yb target material was purchased from two different companies. From Trace Science International Corp. (Canada) with a grade of enrichment of ^{176}Yb of 97.1% (Table 5, Table 6) and from IsoFlex, with an enrichment of 99.72% (Table 7, Table 8).

Table 5: Isotopic distribution of Trace target material Yb_2O_3 (target 1)

Isotope	^{168}Yb	^{170}Yb	^{171}Yb	^{172}Yb	^{173}Yb	^{174}Yb	^{176}Yb
Content (%)	<0.01	<0.01	0.13	0.26	0.28	2.23	97.2 (± 0.1)

Table 6: Chemical impurities of Trace target material Yb_2O_3 (target 1)

Element	Na	K	Ca	Cu	Al	Fe	Ni	Si
Content (ppm)	20	< 30	40	< 10	40	< 20	< 10	20
Element	**Pb**	**Sn**	**Er**	**Tm**	**Lu**			
Content (ppm)	30	< 20	80	90	90			

Table 7: Isotopic distribution of IsoFlex target material Yb_2O_3 (target 2)

Isotope	^{168}Yb	^{170}Yb	^{171}Yb	^{172}Yb	^{173}Yb	^{174}Yb	^{176}Yb
Content (%)	<0.01	<0.01	0.03 (± 0.01)	0.05 (± 0.01)	0.04 (± 0.01)	0.15 (± 0.05)	99.72 (± 0.05)

Table 8: Chemical impurities of IsoFlex target material Yb_2O_3 (target 2)

Element	Fe	Cu	Pb	Tm	Ca	Zn	Lu	Ni	Cr
Content (ppm)	≤ 8	< 3	< 3	< 8	100	< 2	< 5	≤ 40	< 6

5.2 Sample preparation & irradiation

All irradiations of the Yb-targets were performed at the FRM II research reactor. The irradiation positions with a neutron flux of $3.57 \cdot 10^{13}$ n/cm^2/s and $3.88 \cdot 10^{13}$ n/cm^2/s were used for short irradiations of natural Yb-targets (up to 1 h). The activated samples were transported via a pneumatic delivery system directly to the laboratory.

For long-time irradiations up to 14 days the position with $1.29 \cdot 10^{14}$ cm^2/s neutron flux was used. Various masses of Yb-targets were prepared the following way: 10 mg, 25 mg, 50 mg, 90 mg, and 120 mg of natural Yb in its nitrate form were prepared. To assure accuracy, a stock solution (0.9 M) with Milli-Q water was prepared and the different masses pipetted into the ampoules (Heraeus Quarzglas HSQ300, Vogelsberger Quarzglastechnik, Munich, Germany). For the lower masses, (10 – 50 mg) thin-walled ampoules with a wall-thickness of 0.7 mm were used. For masses above 50 mg, a wall-thickness of 1 mm was used in order to ensure stability during irradiation. Both types of ampoules had an inner diameter of 6 mm. After pipetting the stock solutions into the ampoules, they were evaporated to dryness and thereafter sealed air tight. The ampoules were made of high purity quartz with a length after closing of about 4 cm. Fig. 25 shows a sealed ampoule.

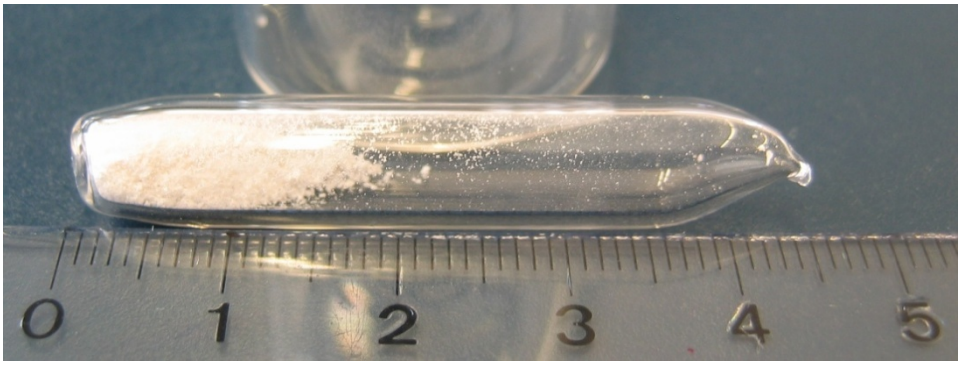

Fig. 25: $Yb(NO_3)_3$ target in sealed glass ampoule for irradiation

5.3 Column preparation & resin preconditioning

In the beginning, the columns used for the separations were assembled manually. Two different chromatographic columns with the dimensions 1 x 40 cm (32.5 cm bed height) and 1 x 55 cm (46.2 cm bed height) were prepared using the macroporous cation exchange resin (1.7 meq). At both ends, glass frits (Porosity 4, 10 - 16 µm) purchased from Sykam (Fuerstenfeldbruck, Germany) were installed between which the resin was arranged. On both sides, Peek column plungers closed the columns (Fig. 26).

A pre-column with the dimension of 1 x 5.6 cm (1.5 cm bed height) was prepared in the same way as described above.

A third chromatographic column with the dimension of 1.6 x 55 cm (49 cm bed height) was prepared using a commercially available system from G&E (Fig. 27). The column consists of high-precision borosilicate glass. The black/red end pieces, made of reinforced acetal plastic, holds the chromatographic tubes in position. Each end piece houses an O-ring, sealing ring, and locking ring. The end pieces also carry a tubing connector through which fluids enter or leave the column. The bottom and top pieces screw onto the column end piece.

Fig. 26: Manually assembled separation column

Fig. 27: Separation column from G&E Healthcare

To clear the resin from all impurities, it was first washed with 4M HCl until the elution solution showed a pH of about 2. Afterwards the column was flushed with a 0.5 M NH_4Cl solution to convert the resin to its NH_4^+ form. As a last step, approximately 1 ½ column volumes of pure H_2O were pushed through in order to generate homogeneous starting conditions.

5.4 Radiometric measurements

The qualitative and quantitative determination of the radioactivity of the samples in case of irradiated Yb targets was carried out by γ-ray spectrometry. γ-spectra were acquired using a high purity germanium detector coupled to a multichannel analyser (Canberra, Germany).

The energy calibration of the detector was performed regularly by a γ-ray standard covering the energy range from 59.5 keV (^{241}Am) to 1332.5 keV (^{60}Co). Samples were measured at a distance of 0, 15 cm and 25 cm from the detector. The obtained spectra were analysed on a VAX computer.

For qualitative analyses of the collected fractions of the separation and the performed thin layer chromatography during labelling (6.3) an Aktivimeter (ISOMED 1010) was purchased from Nuklear-Medizintechnik Dresden GmbH, Germany.

5.5 Experimental set-ups

5.5.1 Set-up 1

The first separation experiments were performed using with the following set-up (Fig. 28):

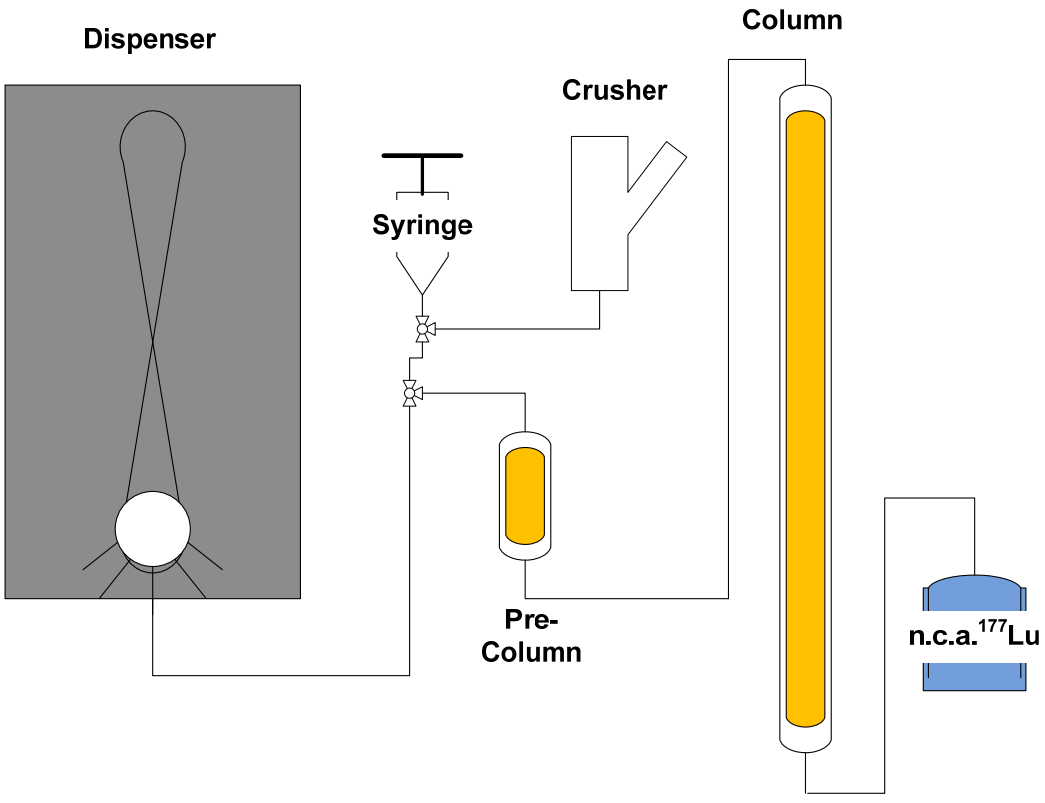

Fig. 28: Set-up 1

The dispenser (Variodisp[8], ScintOmics) was ordered from Sykam (Fuerstenfeldbruck, Germany). The dispenser is a syringe pump, which on the one hand delivered the dissolved target to the pre-column and on the other hand pumped the various solutions through the column during the separation with a speed of 0.5 mL/min. The pre-column was implemented to achieve a homogenous loading of the target onto the resin.

The crusher (Fig. 29) was used to break the irradiated ampoules and was connected to the syringe. The target material could be dissolved directly in the Teflon®-tube of the crusher with 3.0 mL loading solution (0.05 M NH_4Cl solution, pH = 3) solution. The crusher consisted of three parts:

1. A Teflon®-tube (length: 15 cm; inner diameter: 1 cm) to hold the ampoule of the irradiated target and to catch the broken glass
2. Two metal plates fixed together along one side with a joint
3. Peek column plunger with a glass frit on top

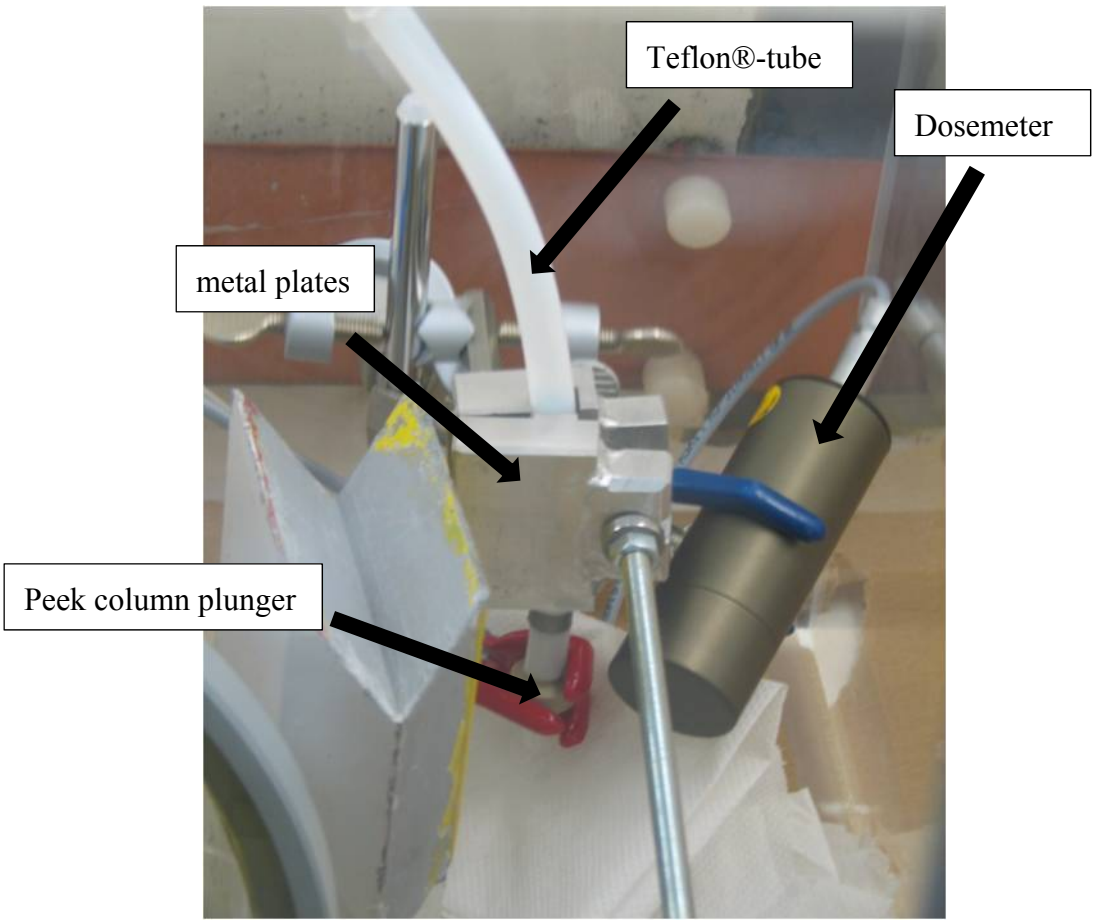

Fig. 29: Devise to crack the quartz-ampule containing the irradiation target material.

5.5.2 Set-up 2

To improve the quality of the elution (e.g. constant flow and pressure) set-up 2 (Fig. 30) a HPLC-pump (ISC 3000SP from Dionex, Idstein, Germany; flow rates 0.1 – 10 mL/min) was introduced into the system as a replacement for the dispenser as a solution pump. In this set-up of the separation system the dispenser is used for loading of the dissolved target onto the column. A glass frit (Porosity 4; pore size: 10 – 16 µm) was installed to hold back any impurities that might originate from crushing the ampoule and dissolving the contents afterwards.

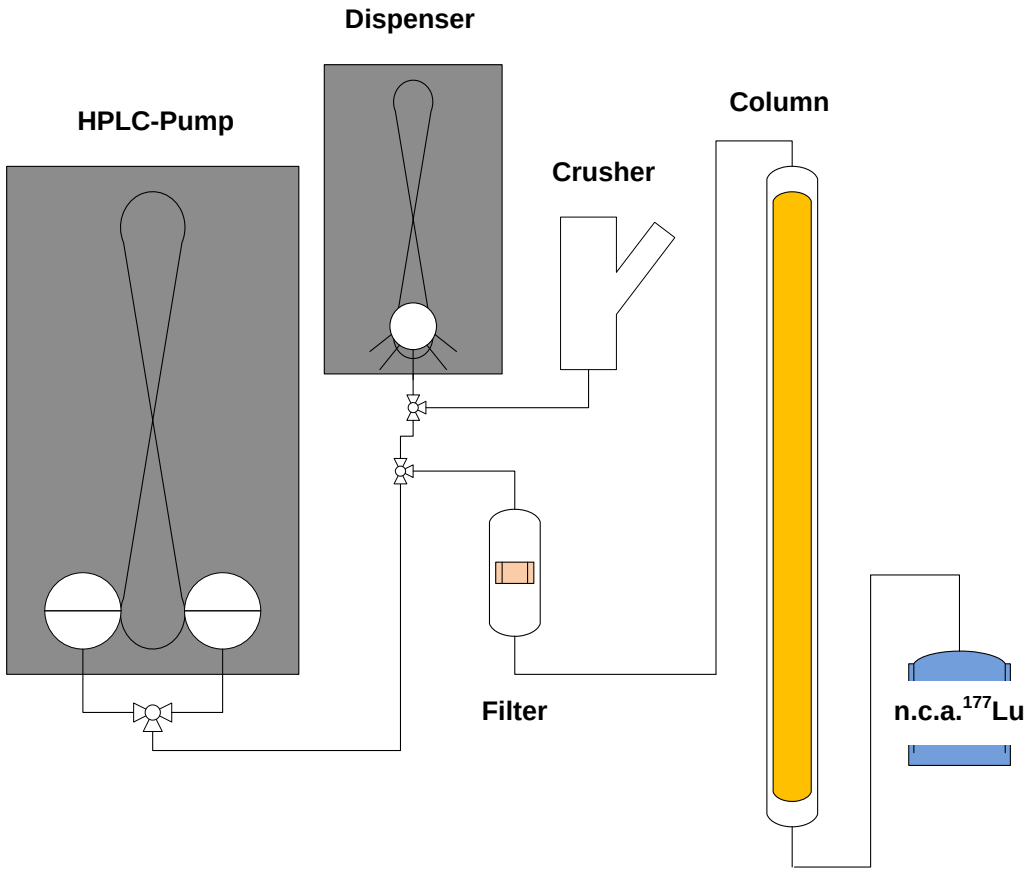

Fig. 30: Set-up 2

5.6 Separations

The model separation was performed with natural Yb targets comprising after irradiations up to 15 MBq ^{177}Lu and up to 550 MBq ^{175}Yb. The distribution of elements in the eluate were analysed by measuring aliquots by γ-ray spectrometry.

5.6.1 Separations with set-up 1

With the first set-up the solutions (e.g. 0.06 M α-HIBA) were delivered to the column by a dispensing system with a flow rate of 0.5 mL/min

The processing consisted of the following steps:

i) As a first step the ampoule with the activated target material was introduced into the teflon-tube. There it was washed with 5 mL Milli-Q water to clean it from external impurities on the quartz surface. Afterwards, the ampoule was broken by pushing the metal plates towards each other and thus squeezing the teflon-tube with the ampoule in between.

ii) The loading solution (HCl, H_2O, NH_4Cl) was pushed into the tubing to dissolve the solid target. The active solution was aspirated into the syringe of the dispenser and transferred onto the pre-column. The loading was performed with a flowrate of 0.25 mL/min. The separation was then started after the column was washed with about 1 column volume of MilliQ H_2O to remove air and to obtain reproducible starting conditions.

For the step gradient elution with set-up 1, twelve different solutions of α-HIBA were prepared, from 0.05 M to 0.16 M, and a 0.5 M solution. The solutions were adjusted to pH 4.75 with 32 % ammonia solution. In each case, 4 mL of every solution was passed through the columns aside from the highest concentration, which was only used afterwards to clean the column completely.

The fractions were collected and later measured by γ-ray spectrometry.

5.6.2 Separations with set-up 2

With set-up 2, a HPLC-pump (DIONEX, ICS-3000 SP) was used for the column elution. The HPLC-pump was equipped with a gradient mixer, so that single separation solutions did not have to be prepared beforehand. Merely Milli-Q water and a stock solution of 1.2 M α-HIBA (pH 4.75) had to be provided.

The opening and dissolution of the irradiated samples were performed as already described above (5.6.1). The activity was loaded with 0.5 mL/min. After the loading, the valve was switched and the HPLC-pump started. Before starting the separation, again water was flushed through the column for 10 min to remove air and to ensure stable and reproducible starting conditions for each separation. For the columns with an ID of 1 cm a flow rate of 0.7 mL/min was applied. The change to an ID of 1.5 cm required a change of the elution flow rate to 1.7 mL/min.

The gradient applied was as follows (Table 9):

Table 9: Gradient specifications, Flow: 1.7 mL/min

Reservoir	Eluent	Start	End	Time
1	Milli-Q water	95.8%	89%	680 min
2	α-HIBA	4.2%	11%	

5.6.3 High activity sample processing/ Proof of concept

5.6.3.1 Routine production model

The set-up 2 was selected to establish a semi-automated procedure for the production of n.c.a.^{177}Lu at high-activity levels, starting with irradiations of highly enriched ^{176}Yb. As column the G&E column with the dimensions of 1.6 x 55 cm (49 cm bed height) was implemented. For the separation, a gradient elution was used as given in Table 9. The whole set-up 2 (see Fig. 31) was installed in a shielded glove box which was placed in a fume-hood.

Target masses of up to 150 mg were irradiated at a neutron flux of $1.29 \cdot 10^{14}$ n/cm^2/s within 14 d resulting in up to 141 GBq ^{177}Lu at EOB. For detection of the activity a sensor was installed at the outlet of the column for on-line monitoring of the ^{177}Lu activity in the eluate in order to be able to cut the desired peak fraction.

The ^{177}Lu fraction, eluted at an α-HIBA concentration of about 0.08 M was accumulated in about 34 mL by controlling the dose rate on the column outlet. The fraction was collected until the dose rate decreased to 30 % of its maximum value. After cutting the peak and switching the valve, respectively, a remaining fraction containing ^{177}Lu in about 34 mL was collected in a waste bottle. This fraction was discarded afterwards. As soon as the dose rate started to increase rapidly again, the valve was switched back again and now the eluting ^{176}Yb was collected. After about 15 min (37.5 mL), the dose rate descreased again and the separation was stopped. After each separation, the column was conditioned with 1 M α-HIBA (~ 100 mL) to clean it from impurities brought into the system such as other lanthanides, iron etc.

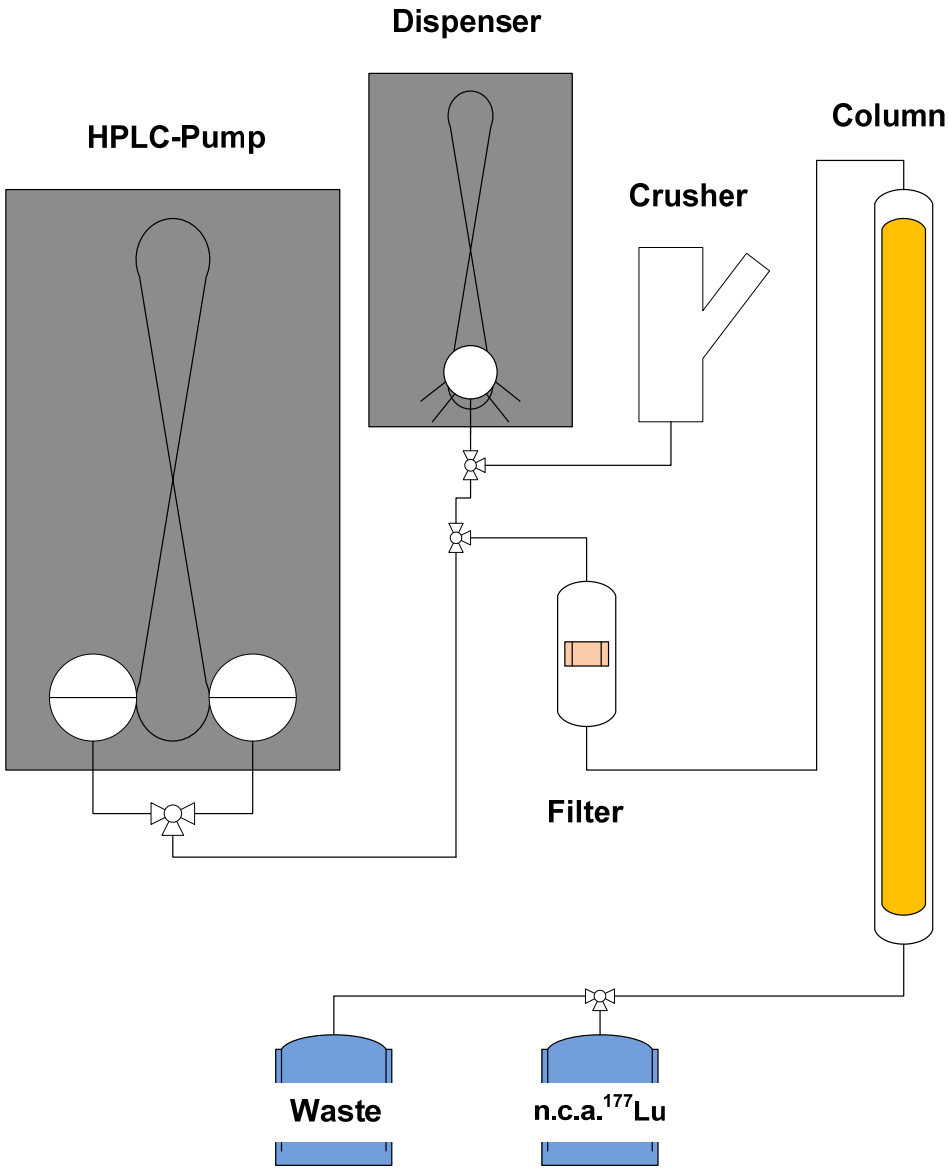

Fig. 31: Set-up for routine production model

5.6.3.2 ^{177}Lu conversion into chloride form

Finally, the produced ^{177}Lu needs to be transferred into a solution of small volume which is free of the complexing agent and useful for radiopharmaceutical applications. Fig. 32 shows the set-up used for the conversion of the radionuclide into the chloride form. Before processing the n.c.a.^{177}Lu solution, the pH was brought to about 1 in order to release the Lu from the α-HIBA. Via vacuum, the ^{177}Lu was sucked into a small tube, which only serves as an intermediate reservoir.

After switching the valve, the solution was loaded onto the column and washed for a few times (~ 10 mL) with 0.5 M HCl. Subsequently, ^{177}Lu was eluted with 4 M HCl and collected in a vial. After evaporation of the obtained acidic solution, the residue was re-dissolved with 200 µl of 0.04 M HCl.

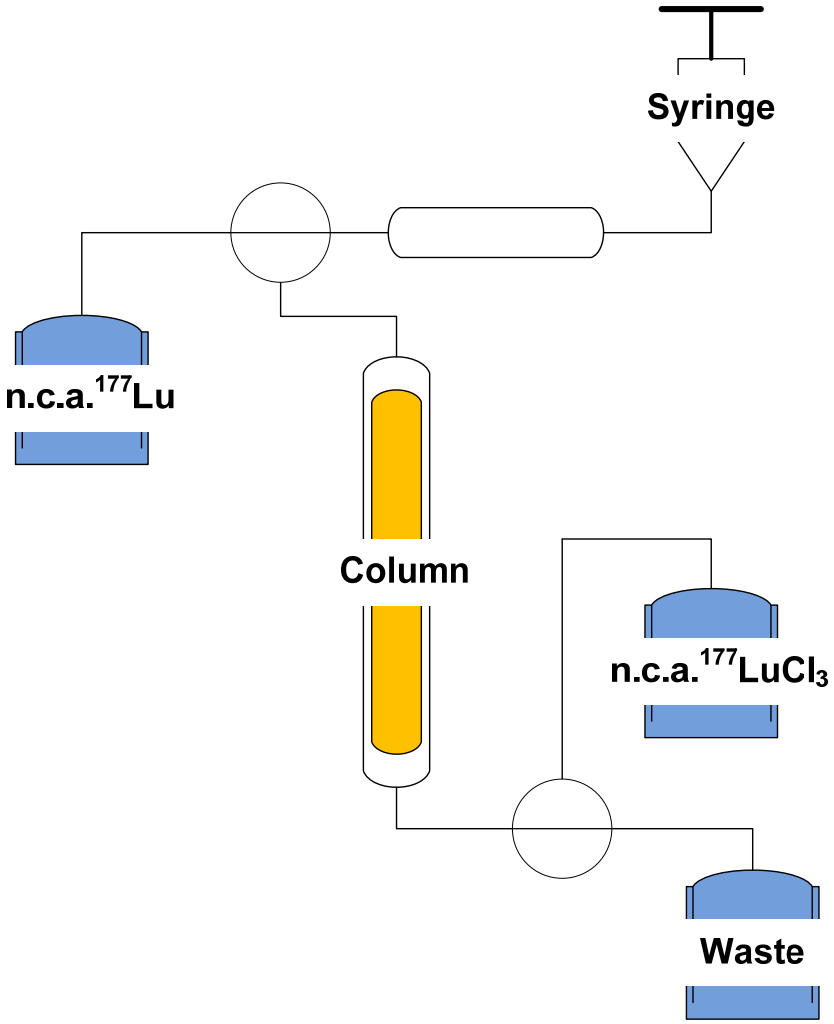

Fig. 32: System for conversion of produced n.c.a.^{177}Lu into n.c.a.^{177}LuCl$_3$

5.7 Target recovery

After isolation of the ^{177}Lu fraction, enriched target material was obtained in 250 mL of 0.5 M HIBA solution with an estimated content of 99% of the original Yb-target mass. After 3 – 4 separations, the accumulated Yb collected in waste bottles was about 400 – 600 mg. The arrangement of the set-up was adjusted in order to accommodate those masses.

Three different procedures were performed to recover the irradiated target material. The first method (5.7.1) used a column with a cation exchange resin to concentrate and to wash Yb. The second method (5.7.2) used extraction chromatography as recovery method (Moreno, 2009). The last way (5.7.3) precipitated Yb as $Yb_2(C_2O_4)_3$ to isolate it quantitatively from other impurities (Moreno, 2009).

5.7.1 Recovery set-up 1

Fig. 33 shows the set-up for the first recovery method. As resin AG 50W-X12 was used. Each time, a 500 mg target was processed which was diluted in approximately 130 mL α-HIBA solution. The column was dimensioned in that way, that the target occupied 50% of its total capacity at the most. For 500 mg targets 4 mL of the resin was used with a capacity of 2.1 mmol/mL. That means, about 35 % of the total resin capacity was occupied. Before the solution was passed through the column, the pH had to be adjusted with 65 % HNO_3 to about pH 1 in order to release the Yb from the Yb-α-HIBA complex. After its concentration on the column the resin was washed with 0.2 M HNO_3 for 45 min with a flow rate of 4 mL/min (~ 180 mL). Afterwards, the Yb was eluted with a 4 M HNO_3 solution for 15 min and flushed into a flask for evaporation under N_2. The attained solution of recycled Yb (~ 60 mL) was then evaporated to dryness.

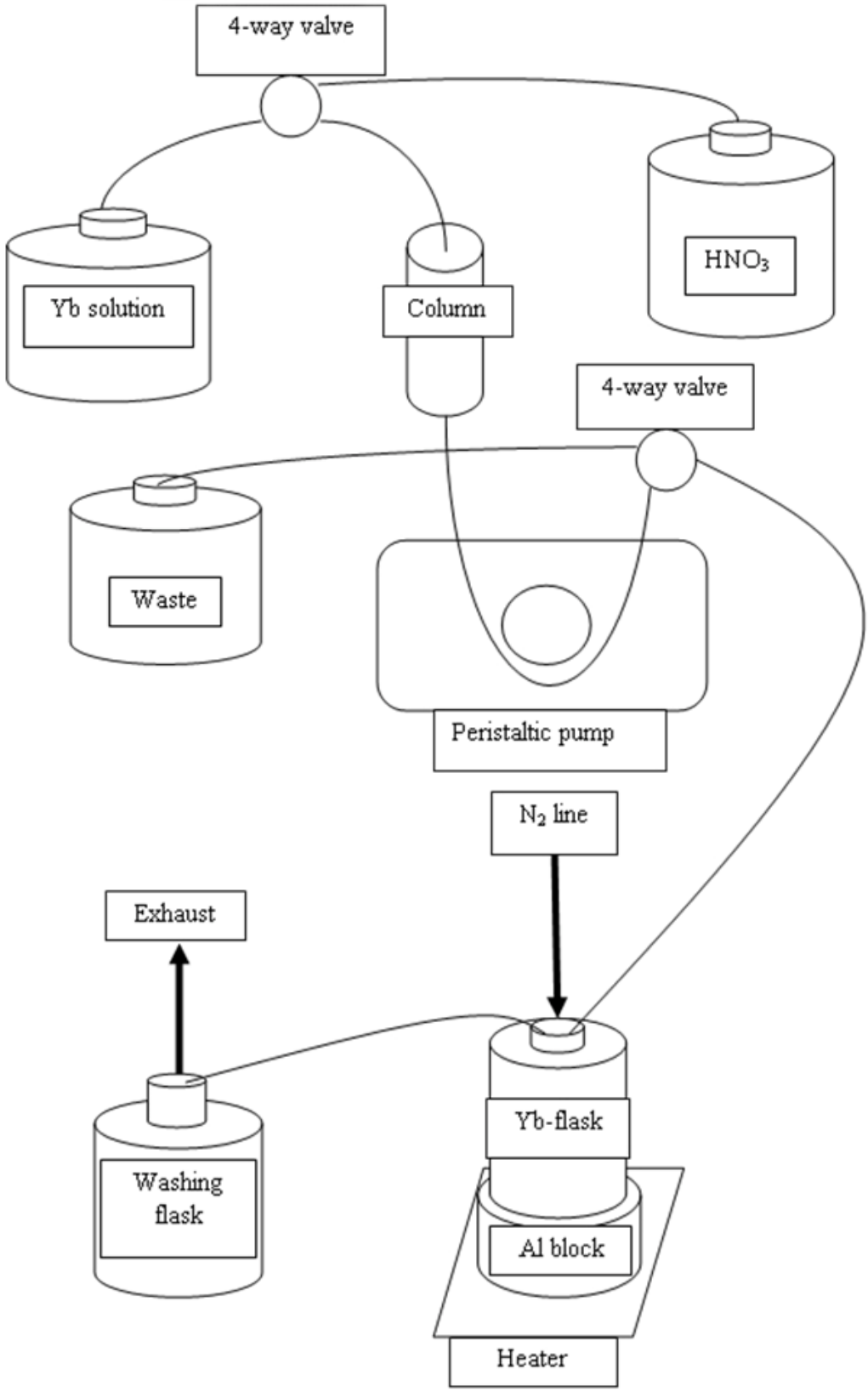

Fig. 33: System built-up for Yb-recovery via the cation exchange resin route

5.7.2 Recovery set-up 2

As with the latter set-up (5.7.1), in order to obtain free Yb, the Yb/α-HIBA solution had to be brought to a low pH-value (~ pH 1). Subsequently, the acidified solution was loaded onto a column that was filled with DGA resin from Eichrom. The capacity of the resin is indicated in dependence of the element Yb with 22 mg Yb per mL resin (Eichrom). A column with a 20 mL resin bed was used, which resulted in a total capacity of 440 mg. Again, the maximum loaded mass did not exceed 50% of the overall resin capacity. From this follows, that in this particular case 220 mg were processed each time. The retained Yb was washed with a 1 M HNO_3 solution (~ 5 free column volumes, ~ 50mL). After the washing of the Yb, it was eluted with 0.1 M HCl. The volume of the diluted HCl solution added up to about 200 mL. As a further step, the Yb was precipitated as described under 5.7.3.

5.7.3 Recovery set-up 3

300 mg of natural Yb was prepared in an α-HIBA solution simulating the separation conditions. Approximately 10 times the stoichiometric amount of oxalic acid ($C_2H_2O_4$) was added causing Yb-oxalate to precipitate quantitatively. After separating the precipitate from the supernatant solution, the solid was washed with a saturated solution of oxalic acid (~ 20 mL). In the next step, the precipitate was calcinated in a quartz vial with a heat gun (Steinel HL1910E) at 700 °C.

5.8 Preparation of ^{177}Lu-labelled compounds

DOTA-Tyr^3-octreotate (DOTATATE) was purchased from Bachem (Weil am Rhein, Germany). 500 MBq n.c.a. ^{177}Lu were added to a mixture of 0.03 M HCl (~ 25 µL) and 5 µL metal free Na-acetate buffer solution 0.5 M, resulting in a pH of about 4.5. 2.98 µg, 3.97 µg, 5.96 µg, and 9.93 µg DOTATATE, taken from a prepared 1 M DOTATATE solution with pure water, were added and incubated at 100 °C for 30 min. After letting cool down to room temperature 2 µL aliquots were taken out of the sample and put on a TLC aluminium sheet (silica gel 60, Merck).

The mobile phase used was a 0.1 M Na_3Citrate solution at pH 4.5. After the mobile phase reached the upper border, the aluminium sheet was cut in two halves and was measured with the Aktivimeter. The radiolabeled compound remains at the origin, whereas free ^{177}Lu(III) migrates with the mobile phase.

6

RESULTS & DISCUSSION

6 Results and Discussion

6.1 Yb(macro) / ^{177}Lu(micro) Separations

The ^{177}Lu activities obtained after irradiation at different neutron fluxes were in good agreement with the theoretically expected values. Following long-term irradiation, the estimated specific activity of ^{177}Lu, as related to the total Lutetium amount in the system produced at FRM II was about 3 TBq/mg and approaches the theoretical value of about 4 TBq/mg very closely. Even the higher masses showed no influence because of self-shielding effects. High stability of the samples during long-term irradiations at high neutron fluxes using Yb in its NO_3-form was provided, thus no broken ampoules due to overpressure produced by nitrogen oxides could be observed.

Table 10: Irradiation of different target masses of natural Yb; neutron flux: $3.57 \cdot 10^{13}$ n/cm^2/s;

Target mass in mg	Irradiation time in min	Decay time in d	Theoretical activities in MBq	Experimental activities in MBq
10	45	2	1.16	1.04 (10 %)
30	60	2	4.63	4.28 (7.5 %)
50	60	2	7.71	6.86 (11 %)
90	60	2	13.9	12.3 (11.3 %)
120	60	2	18.5	16.6 (10.3 %)
300	60	2	46.3	41.3 (10.8 %)

6.1.1 Separations

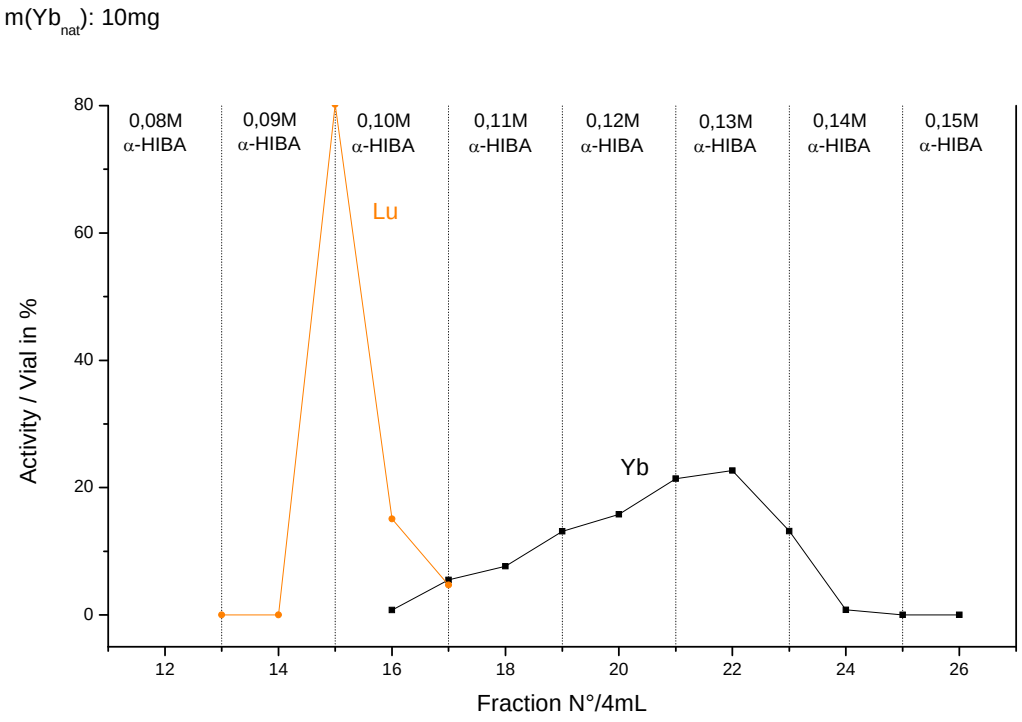

Fig. 34: Separation of ^{177}Lu from Yb, 10 mg target, 16.53 mL bed volume, 30 µm particle size, 32.5 cm bed height, 1 cm column diameter, flow rate 0.5 mL/min (0.64 mL/cm^2/min), gradient elution

Systematic investigations on separation conditions have been performed in order to optimize column processing of irradiated targets and to obtain ^{177}Lu with the Yb amount reduced by a factor of at least 10^4.

Fig. 34 shows an elution profile of a target processing with a mass of 10 mg of irradiated Yb. As mentioned above, this separation was performed with set-up 1. The irradiation time was 45 min, which yielded about 176 kBq ^{177}Lu and about 126 MBq ^{175}Yb at end of bombardment (EOB). The separation was performed 2 days after the target was removed from the reactor. ^{175}Yb yielded then ~ 81.5 MBq and ^{177}Lu had grown to about 1.04 MBq. The large activity of ^{175}Yb allowed a detection limit of Yb in the Lu-fraction of 10^{-4} % of its total.

Under the present separation conditions, it was possible to obtain not less than 80% of ^{177}Lu with a decontamination factor from Yb of $1.2 \cdot 10^2$. This experiment was carried out applying step gradient elution in order to evaluate the concentrations of α-HIBA at which n.c.a^{177}Lu and Yb elute.

Based on the obtained results, 0.08 M HIBA concentration was selected for isocratic elutions. The elution flow rate was 0.7 mL/min and set-up 2 was implemented. For this experiment, the irradiation time was extended to one hour, which yielded about 304 kBq ^{177}Lu and about 168 MBq ^{175}Yb at EOB.

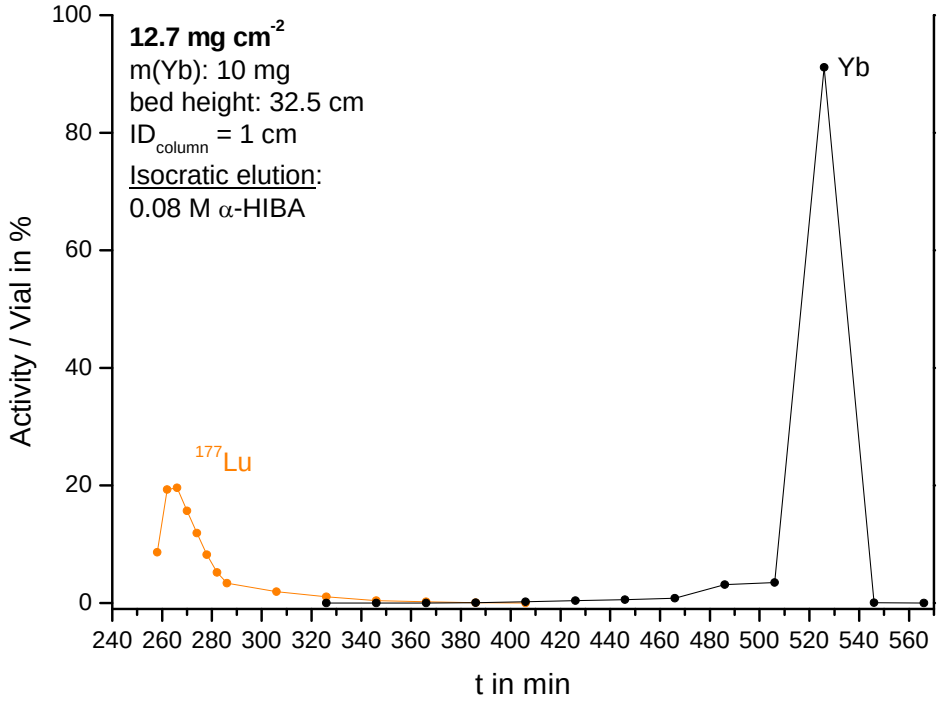

Fig. 35: Separation of ^{177}Lu from Yb, 10 mg target, 25.5 mL bed volume, 30 µm particle size, 32.5 cm bed height, 1 cm column diameter, flow rate 0.7 mL/min (0.89 mL/cm^2/min), isocratic elution

An excellent separation result could be obtained with this arrangement. With a decontamination factor from Yb of $5.8 \cdot 10^5$, 98.2% ^{177}Lu could be isolated in a 17 mL fraction (Fig. 35).

This result transferred to a highly enriched target irradiated at the high-flux position at FRM II (KBA1-1) for the same time span would yield a 1/10 ratio between Yb and ^{177}Lu, the claimed ratio set as condition for a high quality product (4.4). The mass per column cross-section in this experiment was 12.7 mg/cm^2 while the occupied resin sites were only about 0.17 % of the total resin capacity.

Systematic investigation of the Lu and Yb behaviour on the column was performed by increasing of the target masses to estimate the influence of the macro phase of Yb on the behaviour of micro amounts of ^{177}Lu.

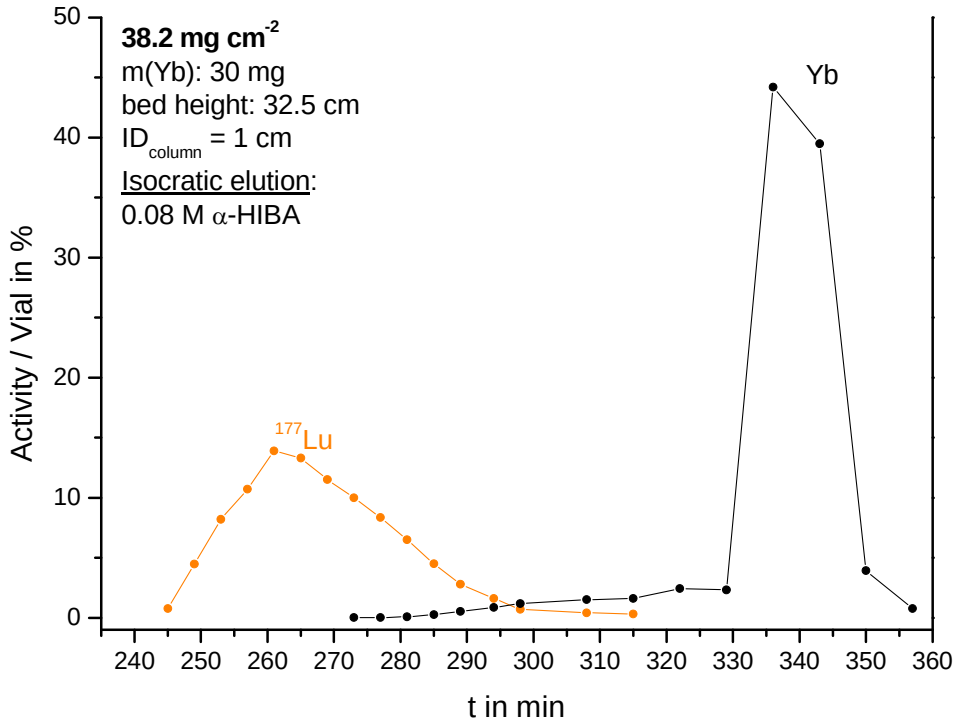

Fig. 36: Separation of ^{177}Lu from Yb, 30 mg target, 25.5 mL bed volume, 30 µm particle size, 32.5 cm bed height, 1 cm column diameter, flow rate 0.7 mL/min (0.89 mL/cm^2/min), isocratic elution

For the next experiment the target mass was augmented to 30 mg. The mass corresponds to 38.2 mg/cm^2 mass per column cross-section and 0.51 % of the total resin capacity.

An early elution of Yb could be observed and a tailing effect on the ^{177}Lu elution profile was exhibited. This led to the assumption, that with 38.2 mg/cm^2 the limit for this column was already exceeded in respect to its ability to process a successful separation of ^{177}Lu from the Yb target. As a consequence 57.6 % with a decontamination factor from Yb of $4.78 \cdot 10^3$ could be achieved.

The target mass was further increased to 50 mg and another separation under equal conditions was performed. The mass per column cross-section increased to 63.7 mg/cm^2. Only 55.1 % of ^{177}Lu could be isolated and the elution profile degraded drastically (Fig. 37). No reasonable ^{177}Lu peak form could be observed.

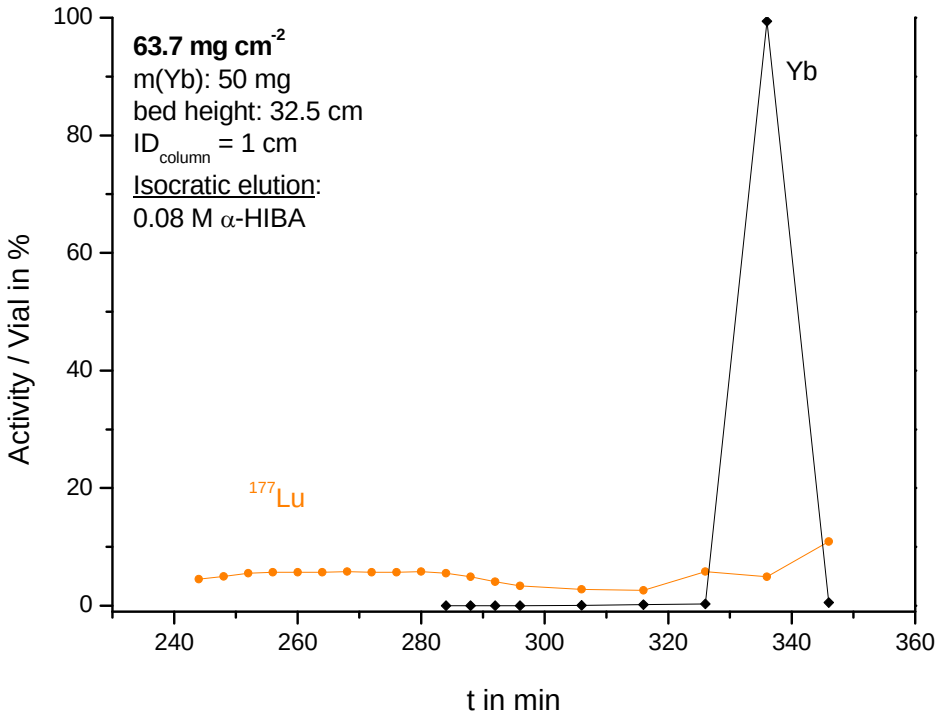

Fig. 37: Separation of ^{177}Lu from Yb, 50 mg target (63.7 mg/cm^2), 25.5 mL bed volume, 30 µm particle size, 32.5 cm bed height, 1 cm column diameter, flow rate 0.7 mL/min (0.89 mL/cm^2/min), isocratic elution (0.08 M α-HIBA)

In order to improve the separation result, a gradient elution was examinated (Table 9). At start, the mixer provided a 0.05 M α-HIBA solution which increased the molarity with a 0.01 M step over a time of 85 min.

Utilisation of HPLC pump as an efficient solvent delivery system (set-up 2) provided high quality steady flow of the eluent.

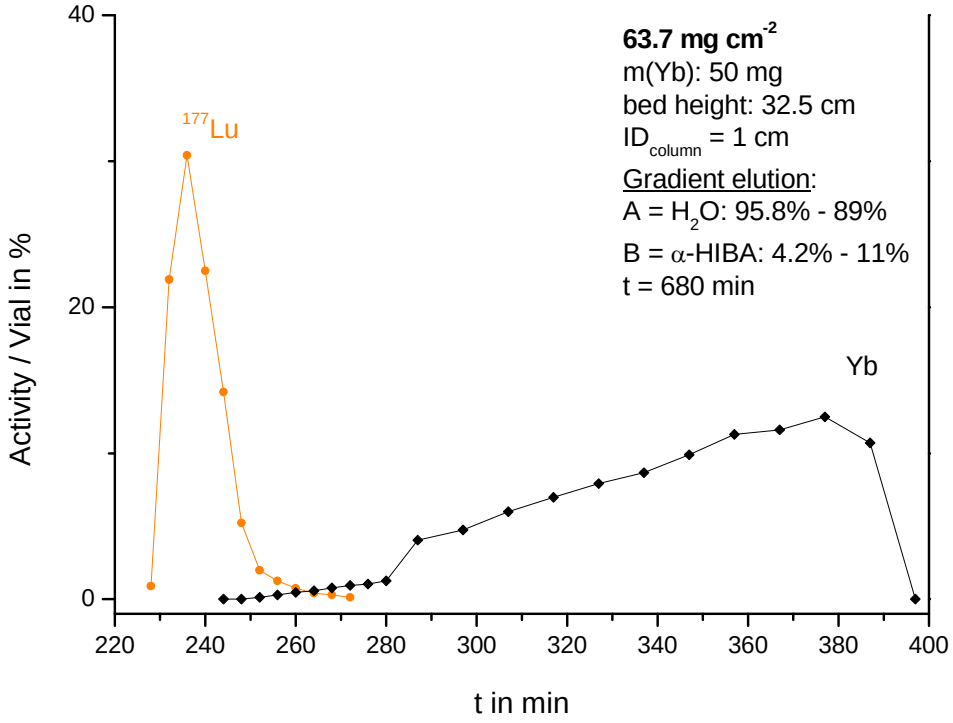

Fig. 38: Separation of ^{177}Lu from Yb, 50 mg target (63.7 mg/cm^2), 25.5 mL bed volume, 30 µm particle size, 32.5 cm bed height, 1 cm column diameter, flow rate 0.7 mL/min (0.89 mL/cm^2/min), gradient elution

A significant improvement in elution profile could be achieved by using the gradient elution by processing of 50 mg Yb-target which corresponds to 63.7 mg/cm^2 mass per column cross section. ^{177}Lu was eluted as a sharp peak while about 75 % of the radionuclide could be obtained with a Yb amount reduced by a factor of $2.73 \cdot 10^5$.

To further improve this advancement and to enhance the yield of separated n.c.a.^{177}Lu, the column length was changed. The column bed-length was extended to 46.2 cm. Fig. 39 shows the result for processing of 50 mg Yb-target, applying the same elution gradient. The elution profile demonstrates improved resolution and more than 90 % of ^{177}Lu could be obtained while Yb mass is reduced by a factor of $9.23 \cdot 10^6$.

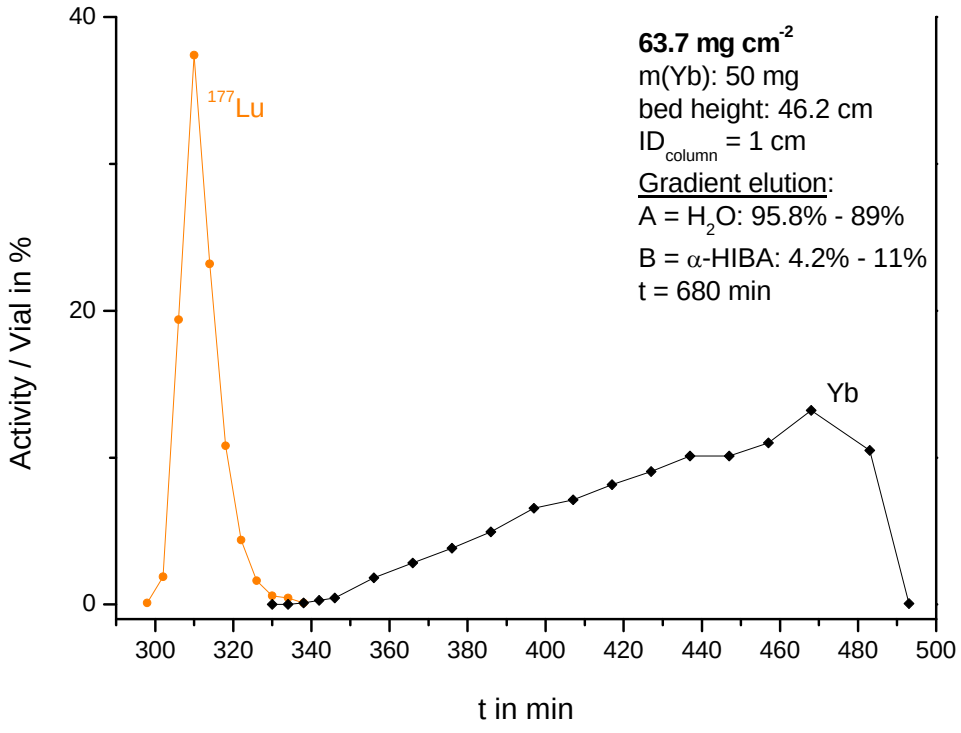

Fig. 39: Separation of ^{177}Lu from Yb, 50 mg target (63.7 mg/cm^2), 36.3 mL bed volume, 30 µm particle size, 46.2 cm bed height, 1 cm column diameter, flow rate 0.7 mL/min (0.89 mL/cm^2/min), gradient elution

As demonstrated by these model-experiments, it is possible to produce high quality n.c.a.^{177}Lu with this system in only a single separation step. With a Yb mass per column cross-section of 63.7 mg/cm^2 target, masses up to 50 mg can be separated under these specific conditions.

Another important point is the overall yield of the produced ^{177}Lu and enriched ^{176}Yb, respectively. Throughout all of the presented separations, the loss of activity and thus loss of final yield was only about 10 - 15% (time corrected).

While up to 50 mg Yb-targets could be effectively processed on a column with 1 x 46.2 cm dimension, further increasing of Yb mass is necessary for large-scale production of ^{177}Lu. In this respect a column of 1.5 x 49 cm dimension was applied for processing of massive Yb-targets (Fig. 40 & Fig. 41).

Gradient elution was applied as well for processing of massive Yb targets. Separation from 90 mg Yb target is shown in Fig. 40. More than 95 % ^{177}Lu could be isolated with a decontamination factor from Yb of $6.42 \cdot 10^6$.

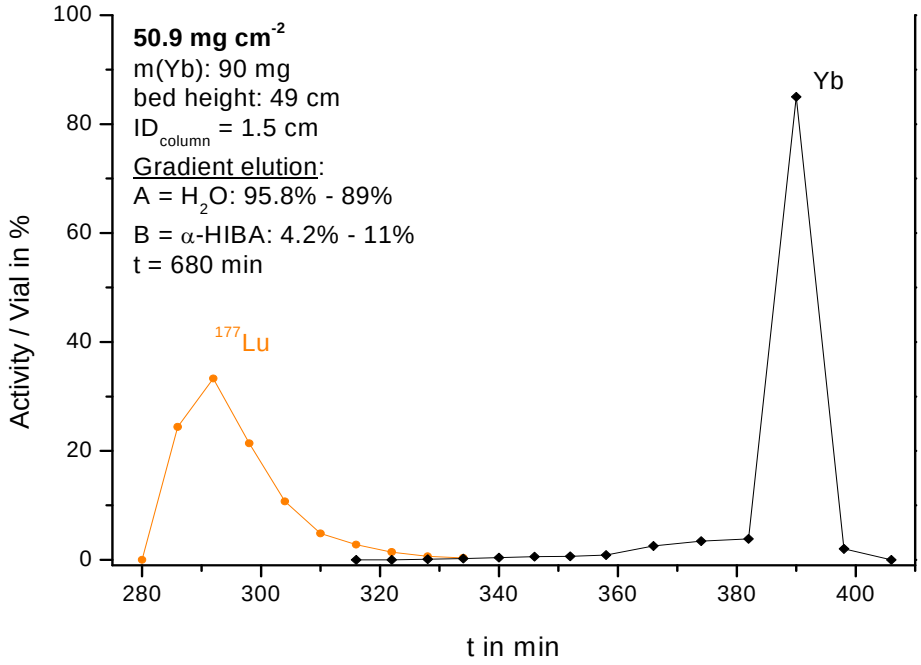

Fig. 40: Separation of ^{177}Lu from Yb, 90 mg target (50.9 mg/cm^2), 86.6 mL bed volume, 30 µm particle size, 49 cm bed height, 1.5 cm column diameter, flow rate 1.7 mL/min (0.96 mL/cm^2/min), gradient elution

Furthermore, an efficient processing of 120 mg target could be performed and not less than 98 % ^{177}Lu with Yb reduced by a factor of $3.26 \cdot 10^6$ was obtained. A mass of 120 mg highly enriched ^{176}Yb target would yield 113 GBq of ^{177}Lu at EOB after 14 d irradiation at KBA 1-1. Considering the small percentage loss owing to the separation process, it is possible to obtain n.c.a.^{177}Lu at a multi-Curie level with the developed system.

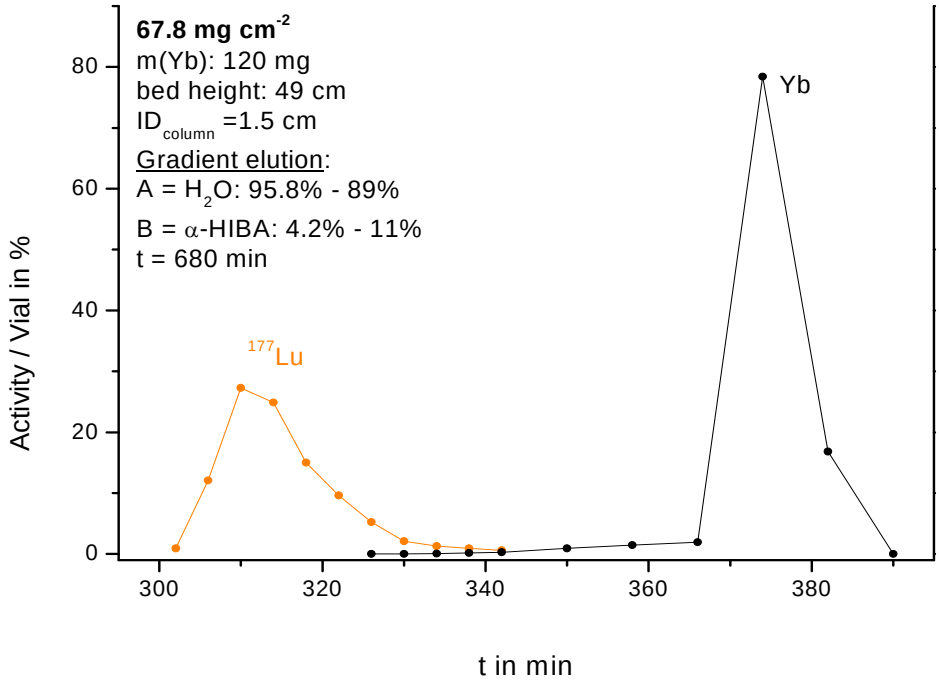

Fig. 41: Separation of ^{177}Lu from Yb, 120 mg target (67.8 mg/cm^2), 86.6 mL bed volume, 30 µm particle size, 49 cm bed height, 1.5 cm column diameter, flow rate 1.7 mL/min (0.96 mL/cm^2/min), gradient elution

6.1.2 Routine production model / proof of concept

As described above (5.6.3.1), according to the performed model experiments, a semi-automated equipment was installed in a shielded glove box (Fig. 42) in order to carry out production of n.c.a. ^{177}Lu obtained after long-term irradiations of highly enriched ^{176}Yb. Up to 150 mg targets were prepared and then irradiated for 14 d at a neutron flux of $1.29 \cdot 10^{14}$ n/cm^2/s. Theoretically, ^{177}Lu yielded 141 GBq at EOB, while the activation of traces of ^{174}Yb resulted in 5.64 GBq ^{175}Yb.

After 2 weeks of irradiation, the sealed glass ampoules were still intact, i.e. although the Yb target was irradiated in its nitrate form, the samples remained stable. In addition, after crushing the ampoule open, the target could effectively be dissolved with the loading solution of 0.05 NH_4Cl. Furthermore, the whole dissolved target could be directly and quantitatively transferred onto the column within only 15 – 30 minutes without any significant activity losses.

Several separations from highly active samples could be performed on the same column. It can be concluded that the resin shows high resistance to radiolytical degradation. Even the loading area on top of the resin bed with the highest activity concentration showed no visual change. After 20 and more separations without change of resin material, the confirmed high quality of the product could be reproduced. No change in the elution profile in respect to elution time or peak form could be observed.

Fig. 42: Glove box in which highly enriched ^{176}Yb targets were processed; for the picture, lead bricks were removed on the left side

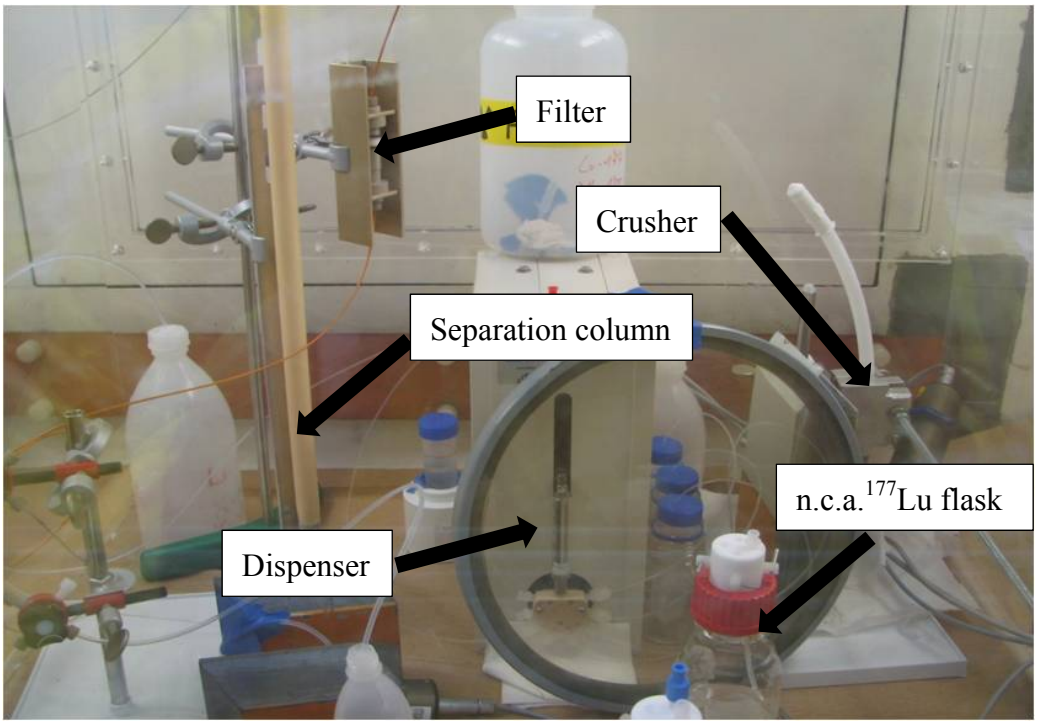

Fig. 43: Built-up inside the glove box

6.1.3 Cl-conversion

The conversion to n.c.a.$^{177}LuCl_3$ is a relatively simple process and no difficulties like large losses of activity or the introduction of impurities could be observed. Yields above 99 % were obtained for each conversion done. The labelling results (Table 11) were excellent and proved the outstanding quality of the product.

Finally, n.c.a.$^{177}LuCl_3$ could be produced with an overall yield of up to 120 GBq, displaying a loss of activity of about 15% throughout the whole production process. This is in good agreement with theoretically expected irradiation yields and the observed separation performance.

6.2 Target recovery

6.2.1 Cation exchange chromatography method

Yb accumulated after the column procedure was released from the α-HIBA chelator, concentrated on the exchange resin, and washed. Thereby, a good separation from α-HIBA and inorganic impurities can easily be achieved.

Another big advantage is the quite feasible scale-up to a gram-level of the recovery material, which is of course an important aspect for future productions when irradiation targets are scaled-up too.

A drawback to this approach is the use of concentrated 4 M nitric acid for eluting Yb from the column. This way of processing demands an evaporation step under highly aggressive acidic conditions before any further steps can be implemented (e.g. precipitation or calcinations). The thereby regained target material could be used in further production processes.

6.2.2 Extraction chromatography method

The processed 220 mg of the target material could be quantitatively recovered. The method allows obtaining the target material in a quality to be reused in further irradiations.

An advantage of this alternative route is the use of diluted acid (0.1 M hydrochloric acid) as a final eluent. Thus, the risk of corrosion of the system is minimised and the maintenance facilitated.

A disadvantage arises from the fact that the resins (DGA, RE) possess a smaller overall capacity in comparison to strong cation exchangers and therefore larger columns and larger volumes of solvents are needed. However, combined with a subsequent precipitation as an oxalate these volumes of diluted acid do not present a problem (Moreno, 2009).

6.2.3 Oxalate method

The experiments conducted with natural Yb at 150 -300 mg have shown that almost a quantitative precipitation of Yb oxalate in 0.5 M α-HIBA occurs without adjusting the pH of the solution. As no further adjustment of the acid concentration is necessary, it is a very simple process which in addition is easy to scale up. Direct separations from the α-HIBA solution are possible due to the insolubility of the oxalate salt in aqueous solutions. The only drawback is the calcination step, which requires high temperatures to convert the oxalate into the oxide. Combined with one of the two methods 5.7.1 or

5.7.2, an even higher degree of purified recycled Yb can be achieved, to be used for further irradiations.

Due to incomplete separation of α-HIBA, oxalic acid or any organic matter, often a brown residue was observed. If that was the case, the solution was wet ashed with concentrated nitric acid to remove those impurities. As a result of the use of the nitric acid instead of oxalates nitrate salts are obtained. Therefore, a lower temperature for calcination of the salt is possible (~ 600°C). The process of wet ashing and calcinating was repeated until a white precipitate is obtained. As with the two methods above, preparation of new target samples according to this method seems feasible (Moreno, 2009).

6.3 Labelling experiments - Utilisation of n.c.a. ^{177}Lu in radiolabelling reactions

6.3.1 n.c.a. ^{177}Lu

The quality of the n.c.a. ^{177}Lu produced was validated in radiolabelling reactions of DOTA-peptide. For this propose the radiolabelling efficiency and achievable SA of ^{177}Lu-DOTA-Tyr3-otreotate as a model compound was systematically investigated.

Fig. 44 and Table 11 show the results of the labelling experiments conducted to evaluate the minimal mass of DOTATATE that can be used to achieve excellent labelling yields with the produced n.c.a.^{177}Lu. It is already possible to achieve excellent labelling results with a molar ratio as low as 1:3 ^{177}Lu:DOTATATE. The highest yield of 99.95 % was obtained with a ratio of 1:4.

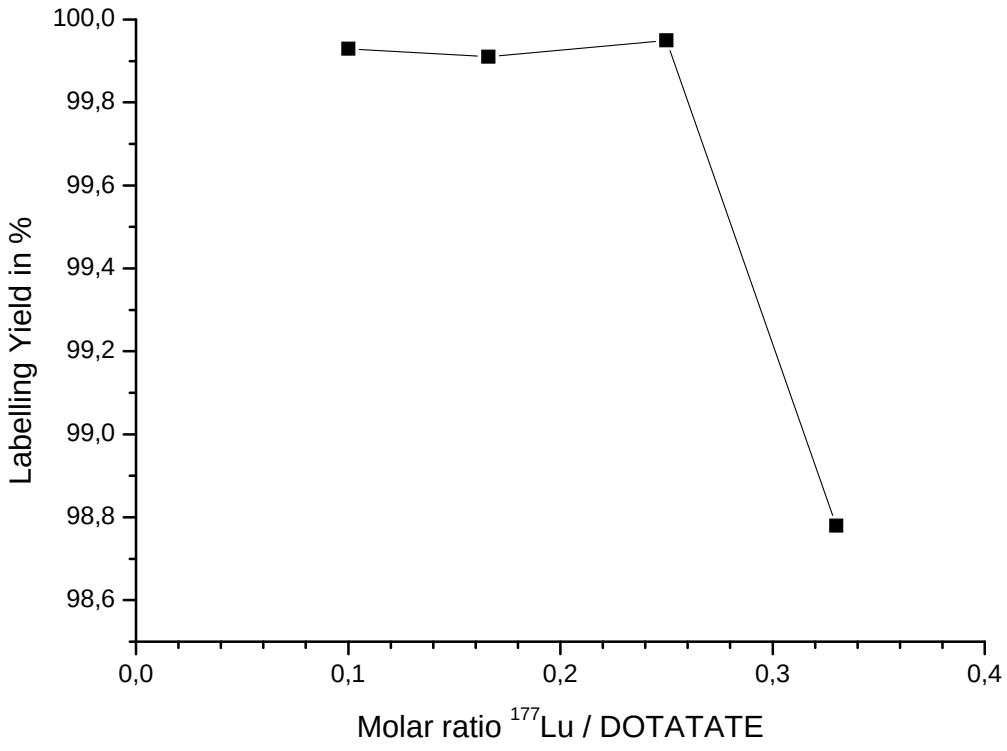

Fig. 44: Formation of n.c.a.^{177}Lu-DOTATATE as a function of peptide amount; A177Lu 500 MBq; pH = 4.5; n(^{177}Lu):n(DOTATATE) 1:3 (2.98 µg DOTATATE); 1:4 (3.97 µg DOTATATE); 1:6 (5.96 µg DOTATATE); 1:10 (9.93 µg DOTATATE)

Table 11: Labelling of n.c.a. ^{177}Lu in dependence of DOTATATE mass

m (DOTATATE) in µg	**2.98**	**3.97**	**5.96**	**9.93**
A (n.c.a.^{177}Lu) in MBq	500	500	500	500
ratio	1:3	1:4	1:6	1:10
Labelling yield in %	99.78	99.95	99.91	99.93

As already mentioned under 4.2, a high SA is mandatory for a successful application of radiopharmaceuticals. Utilisation of ^{177}Lu in radiolabelling reactions provides information about the quality of the produced n.c.a.^{177}Lu as the labelling yield indicates the presence or the absence of competitors for the available labelling positions. For an efficient distribution of ^{177}Lu to the clinics long shelf-life of the preparation is essential as well.

Fig. 45 and Table 12 show the results of the radiolabelling efficiency tests performed to evaluate the quality of n.c.a.^{177}Lu produced over a period of 5, 10, and 15 days after production. High radiolabelling efficiency could still be obtained after 15 days post-production. A labelling yield as high as 98.07% could be realised, which showed once more the theoretically predicted qualities of ^{177}Lu in n.c.a.-form. By eliminating the ^{176}Lu contamination already from the start and reducing the content of ^{175}Yb in the target material to avoid ^{175}Lu, n.c.a.^{177}Lu has a minimal amount of competitors (unavoidable due to the production process) during labelling. Also ^{177}Lu decays to ^{177}Hf, both consequences, the loss of ^{177}Lu and the formation of ^{177}Hf, do not affect the outcome of the labelling procedure as Hafnium is not a competitor in the reaction of ^{177}Lu-DOTA complex formation (Breeman, et al., 2003) and the small amount of Lu present in the target material that originates from the production process of the latter (Table 7) is negligible.

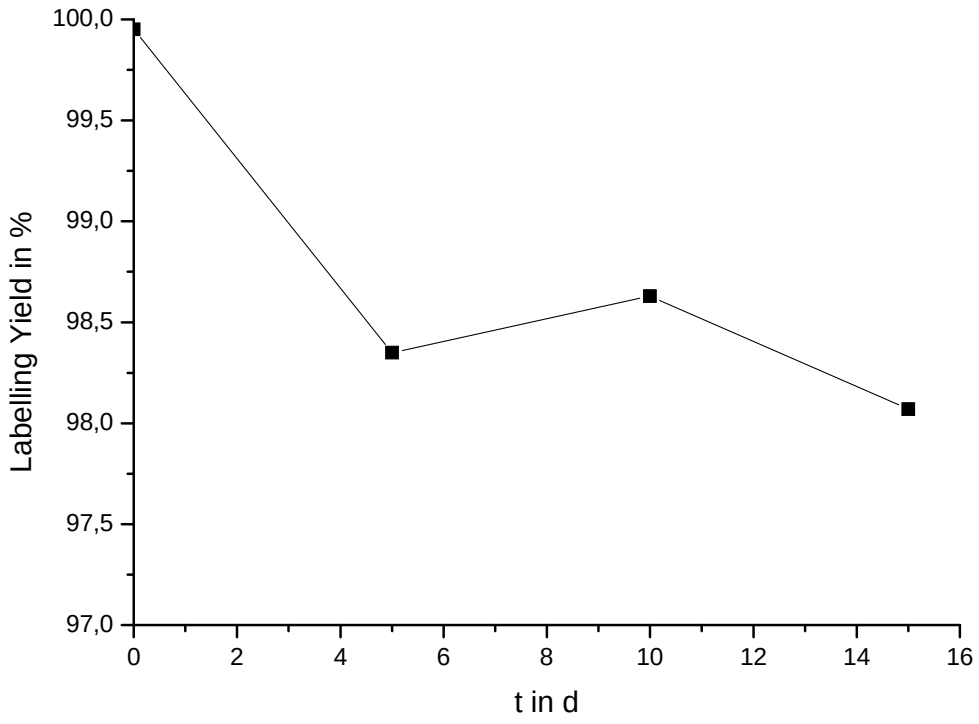

Fig. 45: Formation of n.c.a.^{177}Lu-DOTATATE as a function of time passed after production; A(n.c.a.^{177}Lu) = 500 MBq pro labelling; pH = 4.5; n(n.c.a.^{177}Lu):n(DOTATATE) 1:4 (3.97 µg DOTATATE)

Table 12: Long-time labelling of n.c.a. ^{177}Lu after 0, 5, 10 and 15 days

Time in d	0	5	10	15
m (DOTATATE) in µg	3.97	3.97	3.97	3.97
A (n.c.a.^{177}Lu) in MBq	500	500	500	500
ratio	1:4	1:4	1:4	1:4
Labelling yield in %	99.95	98.35	98.63	98.07

6.3.2 c.a. ^{177}Lu

In order to compare the quality of n.c.a.^{177}Lu to c.a.^{177}Lu, the same experiments were repeated with commercially available c.a.^{177}Lu purchased from IDB Holland. The starting SA activity of the preparation was 756.9 GBq/mg as claimed by the supplier. Due to the significant amount of cold Lutetium in ^{177}Lu only limited radiolabelling efficiency could be achieved (Fig. 46, Table 13). A relatively high molar ratio between DOTATATE and ^{177}Lu is needed (1:10, c.a.^{177}Lu : DOTATATE) in order to achieve quantitative labelling yields. SA of the c.a.^{177}Lu decreases more rapidly with time (Fig. 47).

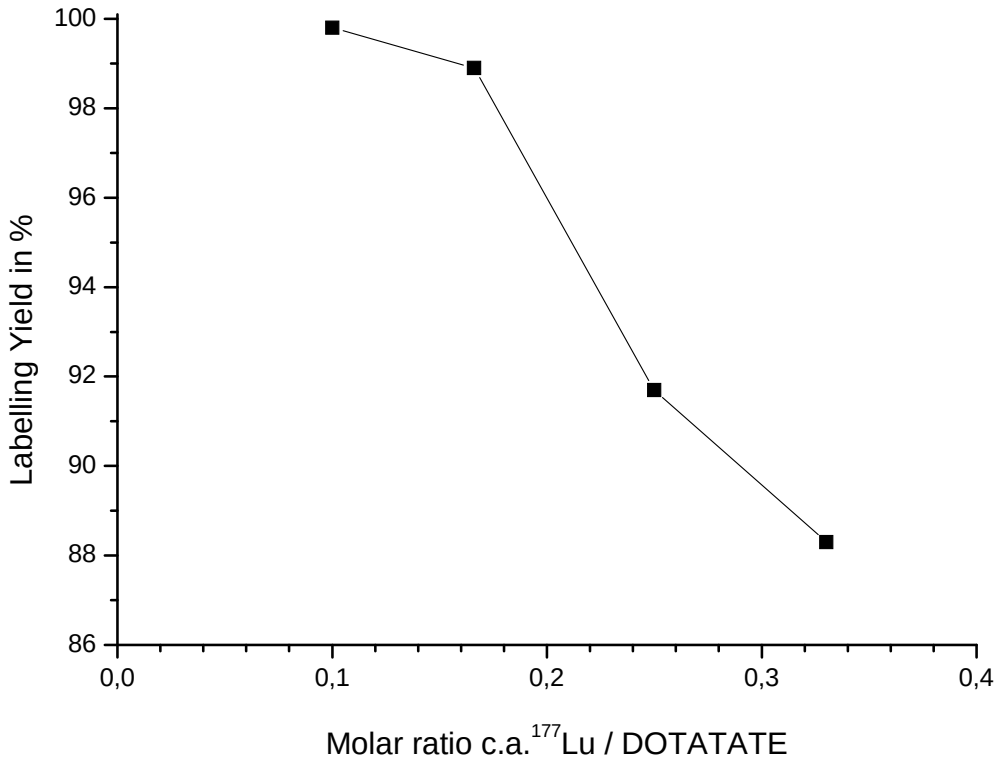

Fig. 46: Formation of c.a.^{177}Lu-DOTATATE as a function of petide amont; A(c.a.^{177}Lu) = 500 MBq; pH = 4.5; n(c.a.^{177}Lu):n(DOTATATE) 1:3 (2.98 µg DOTATATE); 1:4 (3.97 µg DOTATATE); 1:6 (5.96 µg DOTATATE); 1:10 (9.93 µg DOTATATE)

Table 13: Labelling of c.a.^{177}Lu in dependence of DOTATATE mass

m (DOTATATE) in µg	**2.98**	**3.97**	**5.96**	**9.93**
A (c.a.^{177}Lu) in MBq	500	500	500	500
ratio	1:3	1:4	1:6	1:10
Labelling yield in %	88.3	91.7	98.9	99.8

The radiolabelling efficiency as a function of the time of the c.a. ^{177}Lu preparation is presented in Fig. 47 and Table 14. The rapid degradation in the quality was detected after 5 days already. Thus, over 30 % yield is lost after nearly one half-life and after 15 days, a labelling yield of only 9.8 % could be achieved. A further use after a few days post-production, doesn't seem practicable as the shelf-life of c.a.^{177}Lu is very short.

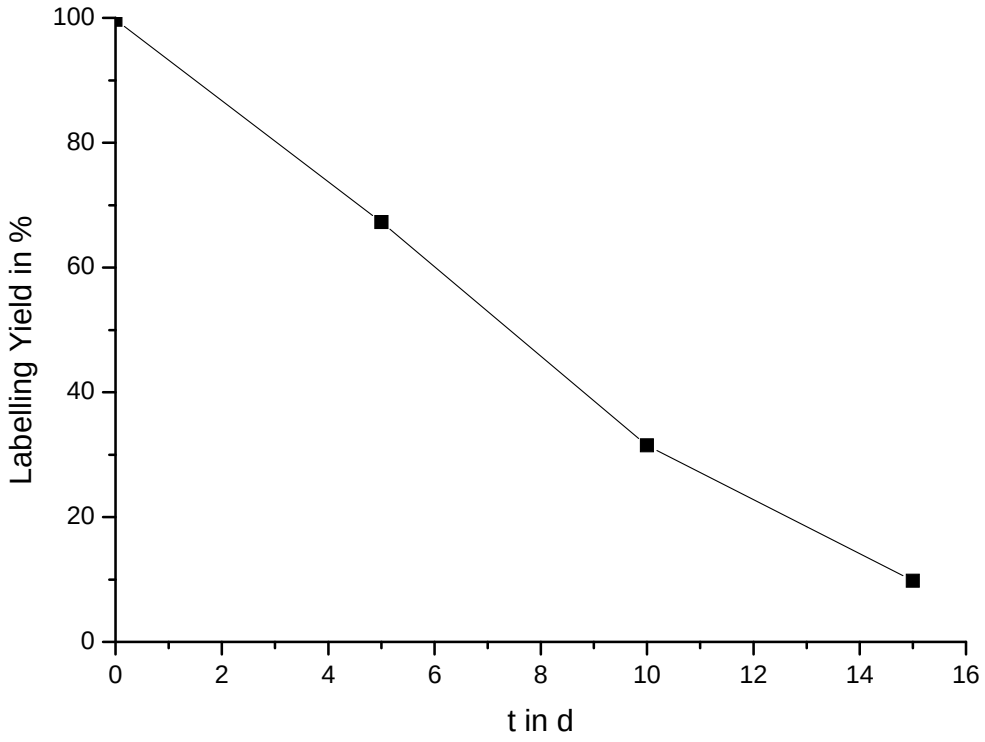

Fig. 47: Formation of c.a.^{177}Lu-DOTATATE as a function of time; A(c.a.^{177}Lu) = 500 MBq pro labelling; pH = 4.5; n(c.a.^{177}Lu):n(DOTATATE) 1:10 (9.93 µg DOTATATE)

Table 14: Long-time labelling of c.a. ^{177}Lu after 0, 5, 10 and 15 days

Time in d	**0**	**5**	**10**	**15**
m (DOTATATE) in µg	9.93	9.93	9.93	9.93
A (c.a.^{177}Lu) in MBq	500	500	500	500
ratio	1:10	1:10	1:10	1:10
Labelling yield in %	99.7	67.3	31.5	9.8

Fig. 48 shows the direct comparison of the labelling results. Not only the quick decline of the labelling yield indicates the exceptional quality of n.c.a.^{177}Lu versus c.a.^{177}Lu but also the applied protein mass. While n.c.a.^{177}Lu displays already excellent labelling results using a molar ratio of 1:4 n.c.a.^{177}Lu : DOTATATE, c.a.^{177}Lu needs a molar ratio of 1:10 c.a.^{177}Lu : DOTATATE in order to achieve good results.

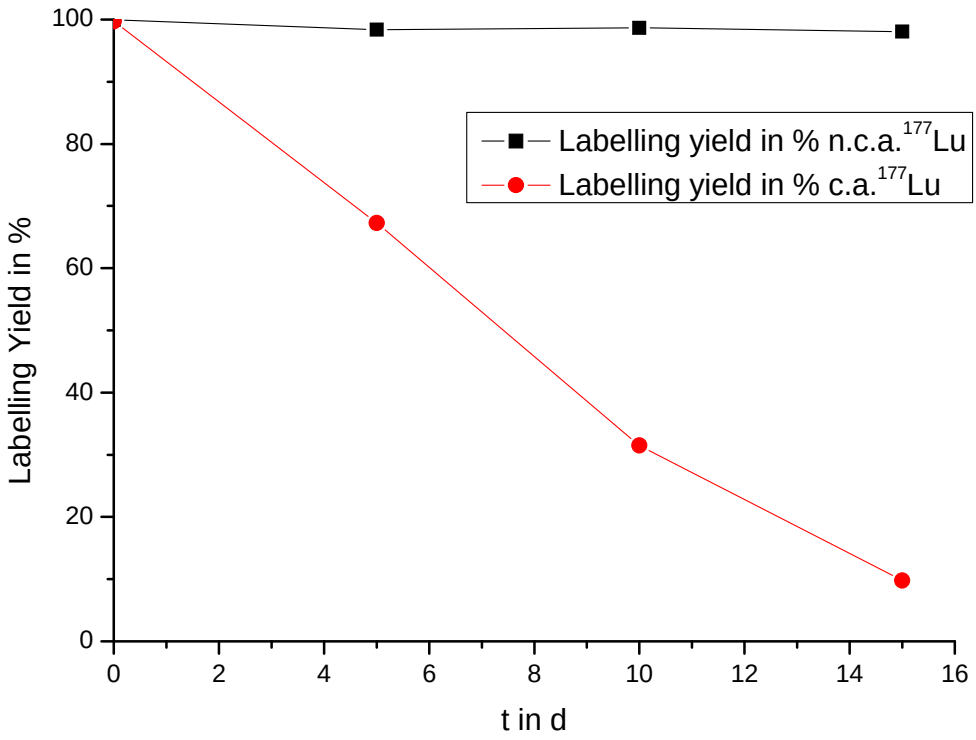

Fig. 48: Comparison of the formation of n.c.a.^{177}Lu- and c.a.^{177}Lu-DOTATATE as a function of time; A(n.c.a.^{177}Lu/c.a.^{177}Lu) = 500 MBq pro labelling; pH = 4.5; n(n.c.a.^{177}Lu):n(DOTATATE) 1:4 (3.97 µg DOTATATE); n(c.a.^{177}Lu):n(DOTATATE) 1:10 (9.93 µg DOTATATE)

7

CONCLUSION & OUTLOOK

7 Conclusion and Outlook

The main goal of the present dissertation was to investigate the feasibility of producing the therapeutic radionuclide ^{177}Lu at a multi-Curie level at the Munich research reactor FRM II in its non-carrier-added form. Generally, two routes are available to obtain ^{177}Lu, either the direct route via ^{176}Lu(n,γ)^{177}Lu or via the indirect route ^{176}Yb(n,γ)^{177}Yb →^{177}Lu. This work exclusively evaluates the second route, as the desired radioisotope should be attained in its n.c.a.-form, which is only achievable through the indirect production process. The n.c.a.-form of nuclides provides high specific activity that is required in targeted receptor therapy in order to avoid saturation of the targeted receptors. Otherwise, the competition for those sites reduces the effectiveness of the applied therapy. Furthermore, highest radionuclide purity of the radionuclide can be achieved as well.

A suitable target material for ^{177}Lu production was evaluated and a reliable method was set up to perform high-quality separations of the ^{177}Lu(micro)/Yb(macro)-system. Labelling procedures were established to verify the high quality and the reproducibility of the separations performed. As no significant target burn-up occurs due to the small cross-section of ^{176}Yb (3.1 b), a recycling procedure for the irradiated target was designed. The recovery of the target material was evaluated for three different processes to regain the deployed material for reuse in further irradiations.

Through considerations, it became evident that natural Yb cannot be used at all as target material. Calculations showed, that even an already high degree of enrichment, 97.2% (target 1), compared to an enrichment grade of 99.72% (target 2) shows a considerable loss in the specific activity. Target 2 reached 95.6% of the max. theoretical value (~ 4.07 TBq/mg) whereas target 1 only 85.7% at most. Due to the relatively high content of ^{174}Yb in the Trace target material (2.23%, target 1) the ingrowth of ^{175}Lu became significant, which could be seen in the early decrease of the specific activity after only about 2 days of irradiation. A thorough selection of available target materials is therefore mandatory in order to maximise the specific activity and thus the quality of the n.c.a. ^{177}Lu.

The process developed in this work used, as described above, ion exchange chromatography. By implementing a factor that takes into consideration the target mass per column cross-section, it was possible to characterise different columns according to their ability to process samples until a certain mass. The achieved results were then transferred to a semi-automated model for routine production, using highly enriched ^{176}Yb targets. All theoretical and experimental considerations made beforehand were confirmed and n.c.a.^{177}Lu could be produced at a multi-Curie level (TBq) just as the goals of this work demanded. Furthermore, through long-time irradiations two important facts could be tested: The stability and consistence of the target on the one hand and the robustness of the resin against high doses of radiation on the other. After an irradiation time of 14 days with a neutron flux of 10^{14} up to 150 mg of the target material proofed stable and showed no chemical degradation in respect to solubility. Likewise was the outcome concerning the resin. Over a period of 20 and more separations, no alteration in the quality of the separation profile as well as in the quality of the final product could be observed.

Three procedures to recover the target material were explored. The simplest way to regain the irradiation material seems to be the recovery via cation exchange. Only the demanding evaporation step of the HNO_3 makes its set-up challenging with respect to the surrounding working environment.

A similar process evaluated, also implementing chromatography, was the Yb-recovery process via extraction chromatography. Again, a good separation of Yb from inorganic impurities and α-HIBA is obtained. Here, the relatively low resin capacity is a drawback that imposes restrictions on the system scale-up that may limit its applicability.

The third method implemented a precipitation of the Yb as $Yb_2(C_2O_4)_3$. This method presents the easiest way to regain the Yb from the collected fraction after the ^{177}Lu separation. Due to the solubility of the complexing agent α-HIBA in water and the insolubility of the oxalate precipitate, Yb can be directly separated from the solution without need of any adjustment beforehand.

All three procedures to recover the Yb target for further irradiations seem feasible. The third method appears to be the best way to regain Yb.

In comparison to the other methods, no large volumes of highly acidic HNO_3 are used and also the need for larger amounts of extraction resin is avoided. Yb is precipitated quantitatively and easily separated from the supernatant solution. The conversion to oxide may require high temperatures but is mandatory for all three methods. This results from the demand for Yb_2O_3 as target material instead of $Yb(NO_3)_3$ if it might be mandatory with increasing target masses in the future. At larger target masses, nitrate might produce too much radiolytic gases, which might lead to the destruction of ampoules during irradiation.

The outstanding quality of the produced n.c.a.^{177}Lu could be demonstrated by the labelling experiments conducted in this work. It still was possible to obtain labelling yields above 99% with a n.c.a.^{177}Lu to DOTATATE particle ratios of 1:3. This cannot be rivalled by c.a.^{177}Lu.
The comparison with c.a.^{177}Lu purchased from IDB Holland showed again the exceptional superiority of n.c.a.^{177}Lu with respect to c.a.^{177}Lu. Not only the particle ratio showed the advantages of the n.c.a. nuclide, but also the long-term comparison over a period of 15 days revealed the inferior character of c.a.^{177}Lu with regard to the high requirements regarding the specific activity set by RIT. The ever-present cold Lu in c.a.^{177}Lu-solutions lowers the quality of the product drastically already after one half-time. A further application seems not to be feasible.

The now established production system for n.c.a.^{177}Lu at a TBq-level is subject to already started experiments to extend the mass of the target processed. As the last results showed, a target mass of 150 mg can easily be handled by the developed set-up and a further augmentation of the Yb mass up to 1000 mg will be possible without any doubt. To realise this increase of target mass slight changes in the set-up are necessary. Two ways are thinkable: either the ID of the column at its length are increased so that the mass per column diameter value meets the predetermined value (0). Alternatively, the irradiated target is split up after it has been dissolved and then transferred to two simultaneously working columns.

The next step will be the production under GMP (Good Manufacturing Practice) conditions in order to sell it as a pharmaceutical product (amendment of the ‘AMG’, Arzneimittelgesetz; §4a, Satz 1, Nr. 3).

Therefore, in close cooperation with the authorities for pharmacy the break point at which the relevant pharmaceutical process starts has to be established. A possible start would be right after the separation and before the conversion to n.c.a.$^{177}LuCl_3$ is started. The final product must then be delivered in autoclaved vials. The whole process would be built up in a hot cell, that itself would be considered an isolator according to pharmaceutical regulations. The so called 'Reinraumklasse' (cleanroom level) for the whole process has to be C. Further analyses have to be implemented such as the determination of the content of endotoxins as well as tests for sterility.

8

REFERENCES

8 Referecenes

Anthony, L. B., et al. 2002. Indium-111-Pentetreotide prolongs survival in gastroenteropancreatic malignancies. *Seminars in Nuclear Medicine.* 2002, Vol. 2, pp. 123 – 132.

Bakker, W. H., et al. 1991. In vivo use of a radioiodinated somatostatin analogue: dynamics, metabolism, and binding to somatostatin receptor-positive tumors in man. *The Journal of Nuclear Medicine.* 1991, Vol. 32, 6, pp. 1184-1189.

Bakker, W. H., et al. 2006. Practical aspects of peptide receptor radionuclide therapy with 177Lu DOTA-Tyr-3-octreotate. *The Quaterly Journal of Nuclear MEdicine and Molecular Imaging.* 2006, Vol. 50, pp. 265-271.

Balasubramanian, P. S. 1994. Separation of carrier-free lutetium-177 from neutron irradiated natural ytterbium target. *Journal of Radioanalytical and Nuclear Chemistry.* 1994, Vol. 185, pp. 305-310.

Becker, D.V. and Sawin, C.T. 1996. Radioiodine and thyroid disease: the beginning. *Seminars in Nuclear Medicine.* 1996, Vol. 26, 3, pp. 155-164.

Behr, T. M., et al. 2000. Therapeutic advantages of Auger electron- over β- -emitting radiometals or radioiodine when conjugated to internalising antibodies. *European Journal of Nuclear Medicine.* 2000, Vol. 27, pp. 753 – 765.

Benali, N., et al. 2000. Somatostatin Receptors. *Digestion.* 2000, Vol. 62, 1, pp. 27-32.

Bernhardt, P., et al. 2001. Dosimetric Comparison of Radionuclides for Therapy of Somatostatin Receptor-Expressing Tumors. *International Journal of Radiation Oncology, Biology, Physics.* 2001, Vol. 51, 2, pp. 514-524.

Bernhardt, P., et al. 2001. Low-energy Electron Emitters for Targeted Radiotherapy of Small Tumours. *Acta Oncologica.* 2001, Vol. 40, 5, pp. 602-608.

Böning, Klaus, Petry, Winfried und Waschkowski, Wolfgang. 2004. Neutronen für die Wissenschaft, Technik und Medizin - Der FRM II geht in Betrieb. München : s.n., 2004.

Breeman, W.A.P., et al. 2003. Optimising conditions for radiolabeling of DOTA-peptides with 90Y, 111In, and 177Lu at high specific activities. *European Journal of Nuclear Medicine and Molecular Imaging.* 2003, 30, pp. 917-920.

Chaves, Silvia, Delgado, Rita und Da Silva, J.J.R. Frausto. 1991. The Stability of the Metal Complexes of Cyclic Tetra-Aza Tetra-Acetic Acids. 1991, Bd. 39, 3.

Clarke, Eric T. and Martell, Arthur E. 1991. Stabilities of trivalent metal ion complexes of the tetraacetate derivates of 12-, 13- and 14-membered tetraazamacrocycles. *Inorganica Chimica Acta.* 1991, 190, pp. 37-46.

—. 1991. Stabilities of the alkaline earth and divalent transition metal complexes of the tetraazamacrocyclic tetraacetic acid ligands. *Inorganica Chimica Acta.* 1991, 190, S. 27-36.

Coakley, A.J. 1998. Drug Therapy Alternatives in the Treatment of Thyroid Cancer. *Drugs.* 1998, Vol. 55, 6, pp. 801-812.

Cooker, E. N. 2000. *Encyclopedia of Separation Science.* New York : Academic Press, 2000.

Cotton, S. 2006. *Lanthanide and Actinide Chemistry.* West Sussex : John Wiley and Sons, 2006.

De Corte, F. and Simonits, A. 2003. Recommended nuclear data for use in the k0 standardization of neutron activation analysis. *Atomic Data and Nuclear Data Tables.* 2003, 85, pp. 47–67.

de Goeij, J. J. and Bonardi, M. L. 2005. How do we define the concepts specific activity, radioactive concentration, carrier, carrier-free and no-carrier-added? *Journal of Radioanalytical and Nuclear Chemistry.* 2005, Vol. 263, 1, pp. 13-18.

Deelstra, H. and Verbeek, F. 1964. The Separation of the Lanthanides and Yttrium by Cation Exchange Elution with Ammonium a-Hydroxyisobutyrate and Lactate. *Journal of Chromatography.* 1964, 17, pp. 558-566.

Delgado, Rita und Da Silva, J.J.R. Fraústo. 1982. Metal Complexes of Cyclic Tetra-Azatetra-Acetic Acids. *Talanta.* 1982, 29, S. 815-822.

Dorfner, K. 1991. *Ion exchangers.* Berlin : Walter de Gryter, 1991.

Druce, M. R., Lewington, V. and Grossman, A. B. 2009. Targeted radionuclide therapy for neuroendocrine tumours: principles and application. *Neuroendocrinology.* 2009. published online.

Dvorakova, Z., et al. 2008. Production of 177Lu at the new research reactor FRM II: Irradiation yield of 176Lu(n,g)177Lu. *Applied Radiation and Isotopes.* 2008, Vol. 66, 2, pp. 147-151.

Dvorakova, Zuzana. 2007. Production and chemical processing of 177Lu for nuclear medicine at the Munich research reactor FRM II. *Dissertation.* Munich : s.n., 2007.

Dyer, A. 2000. *Encyclopedia of Separation Science, chapter Ion Exchange.* New York : Academic Press, 2000.

Eichrom. eichrom - expertise collaboration results. [Online] http://www.eichrom.com/products/info/dga_resin.cfm.

Essen, M., et al. 2007. Peptide receptor radionuclide therapy with 177Lu-octreotate in patients with foregut carcinoid tumours of bronchial, gastric and thymic origin. *European Jorunal of Nuclear Medicine and Molecular Imaging.* 2007, Vol. 34, pp. 1219-1227.

Firestone, B. R., et al. 1996. *Table of Isotopes.* 8. New York : John Wiley & Sons, Inc., 1996.

Forrer, F., et al. 2005. Treatment with 177Lu-DOTATOC of Patients with Relapse of Neuroendocrine Tumors after Treatment with 90Y-DOTATOC. *The Journal of Nuclear Medicine.* 2005, Vol. 46, 8, pp. 1310-1316.

Forsberg, J. H., Marcus, Y. and Moeller, T. 1983. *Gmelin handbook of Inorganic Chemistry: Sc, Y, La-Lu Rare Earth Elements.* Berlin : Springer-Verlag, 1983. Vols. 6, D6.

Forssell-Aronsson, F., et al. 1995. Indium-111 activity concentrations in tissue samples after intravenous injection of Indium-111-DTPA-D-Phe-1-octreotide. *Journal of Nuclear Medicine.* 1995, Vol. 36, pp. 7-12.

FRM-II. [Online] http://FRM2.tum.de.

—. Forschungs-Neutronenquelle Heinz Maier-Leibnitz (FRM II). [Online] http://www.frm2.tum.de/de/technik/kurzbeschreibung/index.html.

Glass, R. A. 1955. Chelating Agents Applied to Ion-exchange Separations of Americium and Curium. *Journal of American Chemical Society.* 1955, Vol. 77, pp. 807-809.

Hashimoto, K., Matsuoka, H. and Uchida, S. 2003. Production of No-Carrier-Added 177Lu via the 176Yb(n,g)177Yb --> 177Lu process. *Journal of Radioanalytical and Nuclear Chemistry.* 2003, Vol. 255, 3, pp. 575-579.

—. 2003. Production of no-carrier-added 177Lu via the 176Yb(n,γ)177Yb --> 177Lu process. *Journal of Radioanalytical and Nuclear Chemistry.* 2003, Vol. 255, pp. 575–579.

Heeg, M. J. and Jurisson, S. 1999. The role of inorganic chemistry in the development of radiometal agents for cancer therapy. *Accounts of Chemical Research.* 1999, Vol. 32, pp. 1053-1060.

Heppeler, A., et al. 2000. Receptor Targeting for Tumor Localisation and Therapy with Radiopeptides. *Current Medicinal Chemistry.* 2000, Vol. 7, 9, pp. 971-994.

Holden, N. E. 1999. Temperature Dependence of the Westcott g-factor for Neutron Reactions in Activation Analysis. (Technical Report). *Pure and Applied.* 1999, 71, S. 2309–2315.

Horwitz, E. P. and Bloomquist, C. A. 1972. The preparation, performance and factors affecting band spreading of high efficiency extraction chromatographic columns for actinide separations. *Journal of Inorganic and Nuclear Medicine.* 1972, Vol. 34, pp. 3851-3871.

Horwitz, E.P., et al. 2005. A Process for the Separation of 177Lu from Neutron Irradiated 176Yb targets. *Applied Radiation and Isotopes.* 2005, Vol. 63, pp. 23-36.

Isotopen Technologie München, AG. Isotopen Technologie München AG. [Online] http://www.itg-garching.de/index.php?option=com_content&view=article&id=49&Itemid=92.

Jurkin, Denis. 2009. Etablierung der FISRE (Free-Ion Selective Radiotracer Extraction)-Technik zur Bestimmung der kinetischen Stabilitäten von Radionuklidkomplexen. *Dissertation.* München : s.n., 2009.

Kassis, A.I. and Adelstein, S.J. 2005. Radiobiologic Principles in Radionuclide Therapy. *The Journal of Nuclear Medicine.* 2005, Vol. 46, 1, pp. 4S-12S.

Knapp, Jr., F. F., et al. 1995. *Nuclear Medicine Program Progress Report for Quarter Ending September 30, 1995.* Technical Report ORNL/TM-13107, Oak Rich National Laboratory. 1995.

Kodama, M., et al. 1991. Thermodynamic and Kinetic Studies of Lanthanide Complexes of 1,4,7,10,13-Pentaazacyclopentadecane-N,N',N'',N''',N''''-pentaacetic Acid and 1,4,7,10,13,16-Hexaazacyclooctadecane-N ,N'N," ,N "'N," "N,' ""hexaacetic Acid. *Inorganic Chemistry.* 1991, Bd. 31, 6, S. 1270-1273.

Köhler, G. and Milstein, C. 1975. Continuous cultures of fused cells secreting antibody of predefined specificity. *Nature.* 1975, Vol. 256, 5517, pp. 447-526.

Kopecky, J. Atlas of Neutron Capture Cross Sections (IAEA). [Online] http://www-nds.iaea.org/ngatlas2/.

Krenning, E. P., Kwekkeboom, D. J. and Bakker, W. H. 1993. Somatostatin receptor scintigraphy with [111-In-DTPA-Phe-1] and [123-In-Tyr-3]-octreotide: The Rotterdam experience with more than 1000 patients. *European Journal of Nuclear Medicine.* 1993, Vol. 20, pp. 716-731.

Kwekkeboom, D. J., et al. 2001. [177Lu-DOTA0, Tyr3]octreotate: comparison with [111In-DTPA0]octreotide in patients. *European Journak of Nuclear Medicine.* 2001, Vol. 28, 9, pp. 1319-1325.

Kwekkeboom, D. J., et al. 2005. Overview of results of peptide receptor radionuclide therapy with 3 radiolabeled somatostatine anlogs. *Journal of Nuclear Medicine.* 2005, 46, pp. 62S-66S.

Kwekkeboom, D., et al. 2003. Treatment of patients with gastro-entro-pancreatic (GEP) tumours with the novel radiolabelled somatostatin analogue [177Lu-DOTA0,Tyr3]octreatate. *European Journal of Nuclear Medicine.* 2003, Vol. 30, pp. 417-422.

Kwekkeboom, D.J., et al. 2008. Treatment with the Radiolabeled Somatostatin Analog [177Lu-DOTA0,Tyr3]octrotate: Toxicity, Efficacy and Survival. *Journal of Clinical Oncology.* 2008, Vol. 26, 13, pp. 2124-2130.

Lahiri, S., et al. 1998. Separation of Carrier Free Lutetium Produced in Proton Activated Ytterbium with HDEHP. *Applied Radiation and Isotopes.* 1998, Vol. 49, 8, pp. 911-913.

Lamberts, S. W. J., Koper, J. W. and Reubi, J. C. 1987. Potenital role of somatostatin analogues in the treatment of cancer. *European Journal of Clinical Investigation.* 1987, Vol. 17, 4, pp. 281-287.

Laue-Langevin, Institut. Institut Laue-Langevin. [Online] http://www.ill.eu.

Lebedev, N. A., et al. 2000. Radiochemical separation of no-carrier-added Lu-177 produced via the Yb-176(n,γ)Yb-177→Lu-177 process. *Applied Radiation and Isotopes.* 2000, Vol. 53, pp. 412 – 425.

Levi, H. 1976. George Hevesy and his concept of radioactive indicators - in retrospect. *European Journal of Nuclear Medicine.* 1976, Vol. 1, pp. 3-10.

Lieser, K. H. 1980. *Einführung in die Kernchemie.* Weinheim : Verlag Chemie, 1980.

Lin, Xilei, et al. 2006. Neutron flux parameters at irradiation positions in the new research reactor FRM II. *Nuclear instruments & methods in physics research A.* 2006, 564, pp. 641-644.

Liu, S. and Edwards, D.S. 2001. Bifunctional chelators for therapeutic lanthanide radiopharmaceuticals. *Bioconjugate Chemistry.* 2001, 12, pp. 7-34.

Maecke, H. R. 2002. Recent advances in the use of radiometals for therapeutic Application. [book auth.] M. Nicolini and U. Mazzi. *Technetium, rhenium and other metals in chemistry and nuclear medicine.* Padua : SGE Editoriali, 2002, Vol. 6, pp. 35-41.

Maecke, H.R. and Good, S. 2003. Radiometals (non-Tc, non-Re) and bifunctional labeling chemistry. [book auth.] A. Vértes, S. Nagy and Z. Klencsár. *Handbook of Nuclear Chemistry.* Amsterdam : s.n., 2003, 8, pp. 279-314.

Magill, J., Pfenning, G. and Galy, J. 2006. Chart of the Nuclides. 7th, 2006.

Marhol, M. 1982. *Ion Exchanger in Analytical Chemistry/ Their Properties and Use in Inorganic Chemistry.* Prague : Academia, 1982.

Markl, P. 1972. Extraktion und Extraktions-Chromatographie in der anorganischen Analytik. [book auth.] R. Kaiser, E. Pungor, W. Simon F. Hecht. *Methoden der Analyse in der Chemie.* Frankfurt/Main : Akadenische Verlagsgesellschaft, 1972, p. [13].

Mayer, S. W. and Freiling, E. C. 1953. Ion Exchange as a Separation Method. VI. Column Studies of the Relative Efficiencies of Various Complexing Agents for the Separation of Lighter Rare Earths. *Journal of American Chemical Society.* 1953, Vol. 75, pp. 5647-5649.

Medvedev, D.G., et al. 2008. Activation of natural Hf and Ta in relation to the production of 177Lu. *Applied Radiation and Isotopes.* 2008, 66, pp. 1300-1306.

Mikolajczak, R., Pawlak, D. and Parus, J. L. 2005. Separation of microgram quantities of 177Lu from milligram amounts of Yb by the extraction chromatography. [book auth.] C. Chemaly, B. J. Allen and H. Bonet. *Proceedings of the 5th International Conference on Isotopes (5ICI).* Brussels, Belgium : s.n., 2005.

Miller, J.M. 1994. *Chromatographische Trennmethoden.* Stuttgart, New York : Georg Thieme Verlag, 1994.

Mirzadeh, S., Mausner, L. F. and Garland, M. A. 2003. Reactor-produced medical radionuclides. [book auth.] F. Roesch. *Handbook of Nuclear Chemistry.* Amsterdam : s.n., 2003, 4, pp. 279-314.

Moreno, Josue. 2009. [personal communication]. 2009.

Nash, K.L. and Jensen, M.P. 2001. Analytical-Scale Separations of the Lanthanides: A Review of Techniques and Fundamentals. London : Taylor & Francis Group, 2001, Vol. 36, pp. 1257-1282.

Nayak, T., et al. 2005. A Comparison of High- Versus Low-Linear Energy Transfer Somatostatin Receptor Targeted Radionuclide Therapy In Vitro. *Cancer Biotherapy & Radiopharmaceuticals.* 2005, Vol. 20, 1, pp. 52-57.

Nijsen, J.F.W., Krijger, G.C. and van het Schip, A.D. 2007. The Bright Future of Radionuclides for Cancer Therapy. *Anti-Cancer Agents in Medicinal Chemistry.* 2007, 7, pp. 271-290.

Nir-El, Y. 2004. Production of 177Lu by neutron activation of 176Lu. *Journal of Radioanalytical and Nuclear Chemistry.* 2004, Vol. 262, 3, pp. 563-567.

Patel, Y.C. 1999. Somatostatin and its Receptor Family. *Frontiers in Neuroendocrinology.* 1999, 20, pp. 157-198.

Pauwels, E. K. and Erba, P. 2007. Radioimmunotherapy of non-Hodgkin's lymphoma: molecular targeting and novel agents. *Drug News & Perspectives.* 2007, Vol. 20, pp. 87-93.

Pawlak, D., et al. 2004. Determination of elemntal and radionuclidic impurities in 177Lu used for labelling of radiopharmaceuticals. *Journal of Radioanalytical and Nuclear Chemistry.* 2004, 261, pp. 469-472.

Pillai, M.R.A., et al. 2003. Production Logistics of 177Lu for radionuclide therapy. *Applied Radiation and Isotopes.* 2003, 59, pp. 109-118.

Pillay, K. K. S. 1986. A review of the radiation stability of ion exchange materials. *Journal of Radioanalytical and Nuclear Chemistry.* 1986, Vol. 102, pp. 247-268.

—. 1986. The effects of ionizing radiations on synthetic organic ion exchangers. *Journal of Radioanalytical and Nuclear Chemistry.* 1986, Vol. 97, pp. 135-210.

Postema, E. J., Boerman, O. C. and Oyen, W. J. 2001. Radioimmunotherapy of B-cell non-hodgkins Lymphoma. *European Journal of Nuclear Medicine.* 2001, Vol. 28, pp. 1725-1735.

PSI. Einführung in die Pharmazie II. [Online] http://zrw.web.psi.ch/lectures/Einf_Pharma/EinfuehrungPharmazieII.pdf.

Raut, N. M., Jaison, P. G. and Aggarwal, S. K. 2002. Comparative evaluation of three alpha-hydroxycyrboxylic acids for the separation of lanthanides by dynamically modified reversed-phase high performance liquid chromatography. *Journal of Chromatography A.* 2002, Vol. 959, pp. 163-172.

Reubi, J. C. 1997. Regulatory peptide receptors as molecular targets for cancer diagnosis and therapy. *The Quaterly Journal of Nuclear Medicine and Molecular Imaging.* 1997, Vol. 41, 2, pp. 63-70.

Robards, K. and Clarke, S. 1988. Advances in the analytical chromatography of the lanthanides. *Analyst.* 1988, Vol. 113, pp. 1757-1779.

Roesch, F. (volume editor), et al. 2003. *Handbook of Nuclear Chemistry: Radiochemistry and Radiopharmaceutical.* Amsterdam : Kluwer Academic Publishers, 2003. Vol. 4.

Roesch, F. and Forssell-Aronsson, E. 2004. Radiolanthanides in Nuclear Medicine. [book auth.] A. Siegel and H. Siegel. *Metal Ions in Biological Systems.* 2004.

Roesch, F. 2003. *Handbook of Nuclear Chemistry: Radiochemistry and Radiopharmaceutical Chemistry in Life Sciences, Volume 4.* Amsterdam : Kluwer Academic Publishers, 2003.

—. 2007. Radiolanthanides in endoradiotherapy: an overview. *Radiochimica Acta.* 2007, 95, pp. 303-311.

Scatchard, G. 1949. The attraction of proteins for small molecules and ions. *Annals of the New York Academy of Science.* 1949, Vol. 51, pp. 660-672.

Schädel, M., Trautmann, T. and Hermann, G. 1977. Fast separation of lanthanides by high pressure liquid chromatography. *Radiochimica Acta.* 1977, Vol. 24, pp. 27–31.

Schmaljohann, J., Beirsack, H. J. and Guhlke, S. 2005. Radiotherapeutika: Herstellung und therapeutische Anwendung von Radiopharmaka. *Pharmazie in unserer Zeit.* 2005, Vol. 34, pp. 498-504.

Schmitt, A., et al. 2004. Radiation Therapy of Small Cell Lung Cancer with 177Lu-DOTA-Tyr3-Octreotate in an Animal Model. *The Journal of Nuclear Medicine.* 2004, Vol. 45, 9, pp. 1542-1548.

Schwedt, G. 1994. *Chromatographische Trennmethoden.* Stuttgart, New York : Georg Thieme Verlag, 1994.

Sisson, D.H., Mode, V.A. and Campell, D.O. 1972. High-Speed Separation of the Rare Earths by Ion Exchange Part II. *Journal of Chromatography.* 1972, Vol. 66, pp. 129-135.

Sivaraman, N., et al. 2002. Separation of lanthanides using ion interaction chromatography with HDEHP coated columns. *Journal of Radioanalytical and Nuclear Chemistry.* 2002, Vol. 252, 3, pp. 491-495.

Smith-Jones, P. M., et al. 1998. Synthesis and characterisation of 90Y-Bz-DTPA-oct: a yttrium-90 labeled octreotide analogue for radiotherapy of somatostatin receptor-positive tumours. *Nuclear Medicine & Biology.* 1998, Vol. 25, pp. 181-188.

Sochacka, R. J. and Siekierski, S. 1964. Reversed-phase partition chromatography with di-(2-ethylhexyl) orthophosphoric acid as the sttionary phase. Part I. Separation of rare earths. *Journal of Chromatography.* 1964, Vol. 16, pp. 376-384.

Stahl, A., et al. 2006. [111In]DOTATOC as a dosimetric substitute for kidney dosimetry during [90Y]DOTATOC therapy: results and evaluation of a combined gamma camera/probe approach. *European Journal of Nuclear Medicine and Molecular Imaging.* 2006, Vol. 33, pp. 1328 - 1336.

Swärd, C., et al. 2008. Comparison of [177Lu-DOTA0.Tyr3]-Octreotate and [177Lu-DOTA0,Tyr3]-Octreotide for Receptor-Mediated Radiation Therapy of the Xenografted Human Midgut Carcinoid Tumor GOT1. *Cancer Biotherapy & Radiopharmaceuticals.* 2008, Vol. 23, 1, pp. 114-120.

Tóth, E. und Brücher, E. 1994. Stability constants of the lanthadie(III)-1,4,7,10-tetraazacyclododecane-N,N',N",N"'-tetraacetate complexes. *Inorganica Chimica Acta.* 1994, 221, S. 165-167.

Uusijärvi, H., et al. 2006. Electron- and Positron-Emitting Radiolanthanides for Therapy: Aspects of Dosimetry and Production. *The Journal of Nuclear Medicine.* 2006, 47, pp. 807-814.

Valkema, R., et al. 2002. Phase I study of peptide receptor radionuclide therapy with [111In-DTPA0]octreotide: the Rotterdam experience. *Seminars in Nuclear Medicine.* 2002, Vol. 2, pp. 110 – 122.

Viola-Villegas, Nerissa and Doyle, Robert P. 2009. The coordination chemistry of 1,4,7,10-tetraazacyclododecane-N,N',N",N"'-tetraacetic acid (H4DOTA): Structural overview and analyses on structure-stbility relationships. *Coordination Chemistry Reviews.* 2009, 253, pp. 1906-1925.

Volkert, W. A. and Hoffmann, T. J. 1999. Therapeutic Radiopharmaceuticals. *Chemical Reviews.* 1999, Vol. 99, pp. 2269-2292.

Waldherr, C., et al. 2002. Tumor response and clinical benefit in neuroendocrine tumors after 7.4 GBq 90Y-DOTATOC. *Journal of Nuclear Medicine.* 2002, 43, pp. 610-616.

Warner, R. P. and O'Doriso, T. M. 2002. Radiolabeled peptides in diagnosis and tumor imaging: Clinical overview. *Seminars in Nuclear Medicine.* 2002, Vol. 32, pp. 79-83.

Weiner, R.E. and Thakur, M.L. 2001. Radiolabeled Peptides in Diagnosis and Therapy. *Seminars in Nuclear Medicine.* 2001, Vol. 31, 4, pp. 296-311.

Wilder, R. B., DeNardo, G. L. and DeNardo, S. J. 1996. Radioimmunotherapy: recent results and future directions. *Journal of Clinical Oncology.* 1996, Vol. 14, pp. 1383-1400.

Williams, C. D. 2000. *Encyclopedia of Separation Science, chapter Zeolites.* New York : Academic Press, 2000.

Wisemann, G. A., White, C. A. and Witzig, T. E. 1999. Radioimmunotherapy of relapsed non-Hodgkin's' lymphoma with zevalin, a 90 Y-Labeled anti CD20 monoclonal antibody,. *Clinical Cancer Research.* 1999, Vol. 5, pp. 3281-3286.

Wish, L., Freiling, E. C. and Bunney, L. R. 1954. Ion Exchange as a Separations Method. VIII. Relative Elution Positions of Lanthanide and Actinide Elements with Lactic Acid Eluant at 87°. 1954, Vol. 76, pp. 3444-3445.

Xilei, L., et al. 2006. Neutron flux parameters at irradiation positions in the new research reactor FRM-II. *Nuclear Instruments and Methods in Physics Research A.* 2006, Vol. 564, pp. 641-644.

Zalutsky, M. R. 2003. Radionuclide Therapy. [book auth.] A., Nagy, S., Klencsár, Z Vértes. *Handbook of Nuclear Chemistry.* Amsterdam : s.n., 2003, pp. 315-350.

Zhernosekov, K. P., et al. 2007. A Nd-140/Pr-140 radionuclide generator based on physico-chemical transitions in Pr-140 complexes after electron capture decay of Nd-140-DOTA. *Radiochimica Acta.* 2007, Vol. 95, pp. 319 – 327.

Zhernosekov, K.P., et al. 2008. Target burn-up corrected specific activity of 177Lu produced via 176Lu(n,g)177Lu nuclear reaction. *Applied Radiation and Isotopes.* 2008, Vol. 66, 9, pp. 1218-1220.

9

ANNEX

9 Annex

9.1 Cross section

The value of the cross section (σ) is dependent on the energy of the incident radiation. That means, the probability of an occurring nuclear reaction is a function of the energy, which is carried by the particle as kinetic energy and transferred as excitation energy onto the compound nucleus. Therefore, the energy dependency of the cross-sections is called excitation function. Examples of such excitation functions are given in Fig. 49, Fig. 50 and Fig. 51. As neutrons do not experience any Coulomb repulsion, the cross sections are rather high in the low energy area. The higher their velocity is the shorter is the retention in the vicinity of the cores which results consequently in low cross sections. Viz. the cross section is reciprocally proportional to the velocity of the neutrons (8.1):

$$\sigma_n \sim \frac{1}{v_n} \tag{8.1}$$

This condition is mostly met in the low energy region. With higher energies maxima appear, so called resonance spots. At these resonance spots the kinetic energy of the neutrons correspond with favorised excitation energies what leads to especially high yields. Fig. 49, Fig. 50 and Fig. 51 show the excitation functions of the ^{176}Lu(n,γ)^{177}Lu, ^{176}Lu(n,γ)^{177m}Lu and ^{176}Yb(n,γ)^{177}Lu reaction, respectively. Qualitatively, the first two functions are similar, however, the formation of ^{177m}Lu is less probable. A distinct resonance can be seen at approximately 0.15 eV. Because of that, the $\frac{1}{v_n}$ – law can not be applied whereas the ^{176}Yb(n,γ)^{177}Lu can be viewed as a $\frac{1}{v_n}$ – conform nuclide.

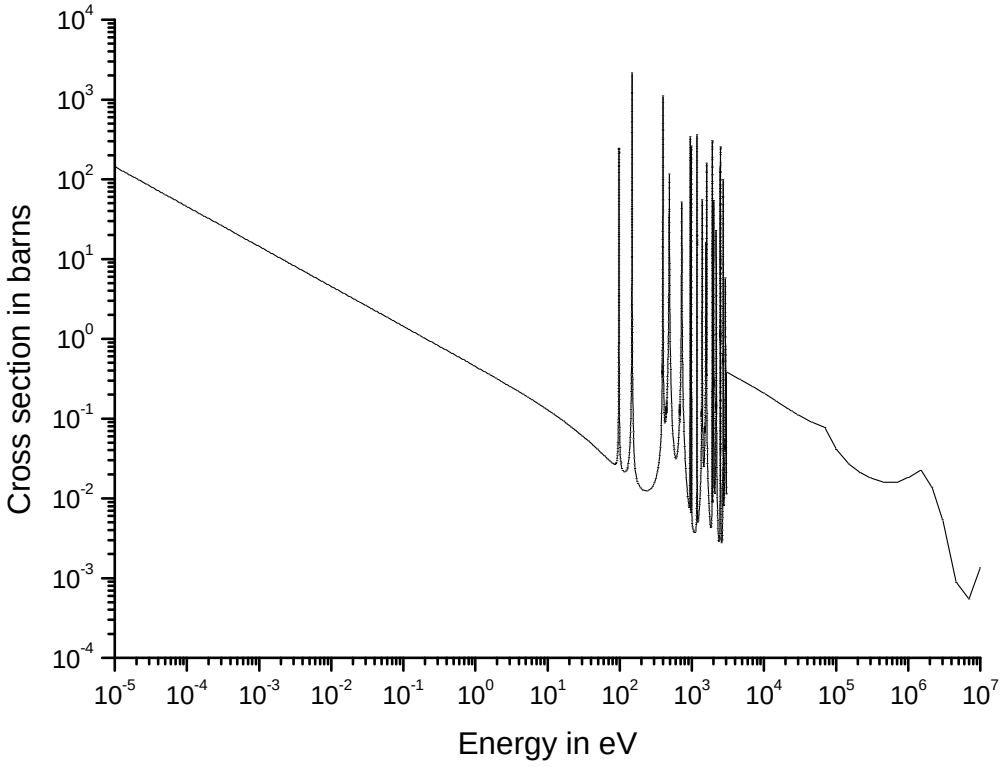

Fig. 49: Excitation function of the ^{176}Yb (n,γ)^{177}Yb reaction. Because the σ(E$_n$) function is in the thermal neutron region linear as $\frac{1}{E_n}$, ^{176}Yb belongs to the $\frac{1}{v_n}$nuclides. Reproduced from (Kopecky).

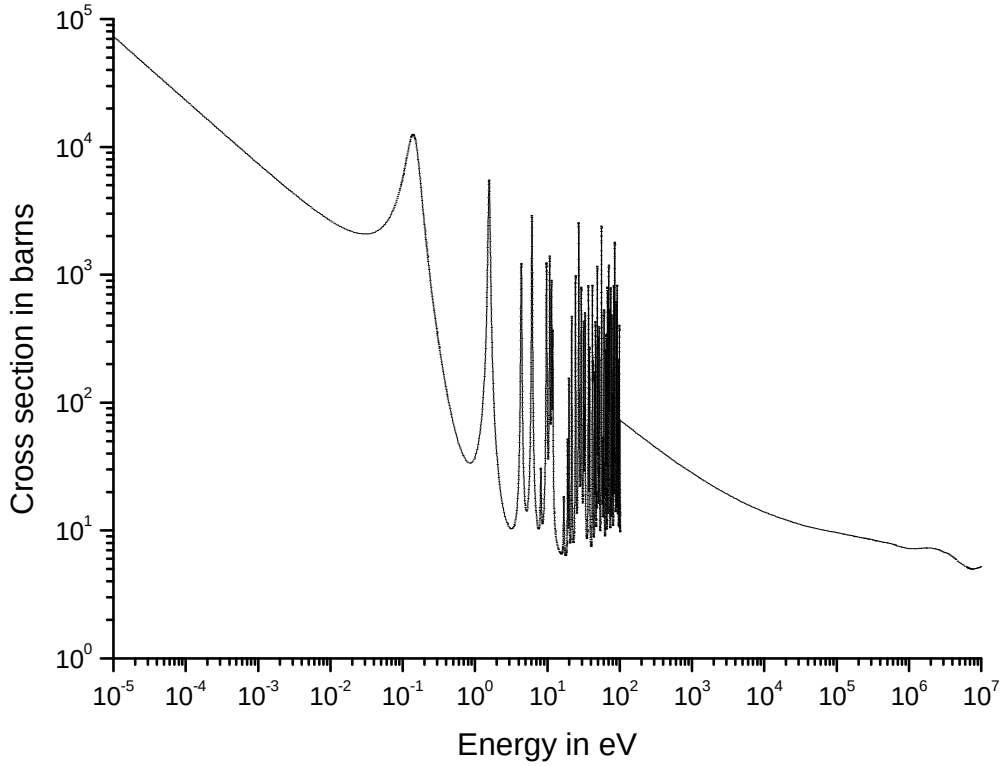

Fig. 50: Excitation function of the ^{176}Lu (n,γ)^{177}Lu reaction. Because the σ(E_n) function is not linear in the thermal neutron region as $\frac{1}{E_n}$, ^{176}Lu belongs to the non - $\frac{1}{v_n}$nuclides. Reproduced from (Kopecky)

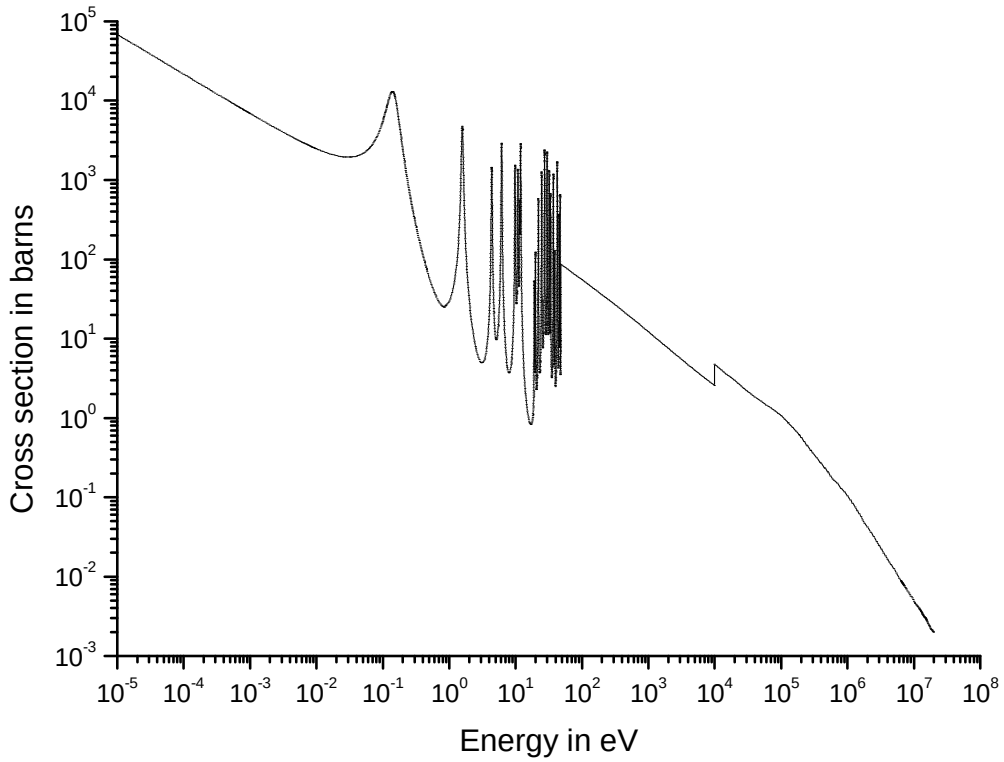

Fig. 51: Excitation function of the ^{176}Lu (n,γ)^{177m}Lu reaction. Because the σ(E_n) function is not linear in the thermal neutron region as $\frac{1}{E_n}$, ^{176}Lu belongs to the non - $\frac{1}{v_n}$nuclides. Reproduced from (Kopecky)

9.2 List of figures

Fig. 1: Design of a receptor mediated radiopharmaceutical; 1: BFC; 2: linker; 3: biomolecule; 4: receptor ___ *21*
Fig. 2: Example for a receptor mediated radiopharmaceutical: [^{111}In]DTPA-octreotide (OctreoScan) ___ *22*
Fig. 3: Tumour to normal tissue mean adsorbed dose rate (TND) as a function of tumour mass and radius; comparison of ^{90}Y and ^{177}Lu (Uusijärvi, et al., 2006) ___ *25*
Fig. 4: Somatostatin-14 ___ *27*
Fig. 5: left: Octreotide; right: Lanerotide ___ *28*
Fig. 6: Vapreotide ___ *28*
Fig. 7: acyclic chelators, 1: EDTA, 2: DTPA, 3: CyEDTA ___ *30*
Fig. 8: macrocyclic chelators, 1: DOTA, 2: TETA, 3: DOTMP ___ *31*
Fig. 9: macrocyclic chelators left: PEPA and right: HEHA ___ *32*
Fig. 10: Types of linker for radiopharmaceuticals; clockwise from above, left: cationic, anionic, cleavable, neutral linker ___ *33*
Fig. 11: Radiolabelling approaches (Liu, et al., 2001) ___ *34*
Fig. 12: Cut-out form chart of the nuclides: red arrows indicate route (1), orange arrow indicates route (2) ___ *35*
Fig. 13: Increase of the masses of ^{177}Hf and ^{177}Lu over irradiation (14 days) and decay time (15 days); Neutron flux = 1.29·10^{14} n/cm^2/s; Target mass = 100 mg; EOB = End Of Bombardment ___ *37*
Fig. 14: Sketch of the irradiation positions at FRM II (Lin, et al., 2006) ___ *38*
Fig. 15: View from above onto the reactor pool at FRM II (FRM-II) ___ *39*
Fig. 16: Thermal neutron flux density in dependence of the distance to the fuel core at half height of the fuel element. The maximum lies approximately at a distance of 12 cm from the core. (FRM-II) ___ *40*
Fig. 17: Number of neutrons emitted during fission process plotted against their kinetic energy (FRM-II) ___ *41*
Fig. 18: Energy of different types of neutron and there specific application. The size of the coloured regions is proportional to the amount of neutrons available. (FRM-II) ___ *43*
Fig. 19: Irradiation yield of ^{177}Lu; 100 mg Yb target (target 1) as a function of irradiation time; neutron flux: 1.29·10^{14}n/cm^2/s; ^{176}Yb(n,γ)^{177}Yb → ^{177}Lu ___ *46*
Fig. 20: Cut-out form chart of the nuclides showing the stable isotopes of natural Yb with their natural abundance and their cross section ___ *47*
Fig. 21: Specific activity of ^{177}Lu of two different Yb-materials: black - grade of enrichment 99.72%; red 97.2%; irradiation time: 14 days; decay time: 15 days; cold Lu: 5 ppm; ___ *50*
Fig. 22: Specific activity of ^{177}Lu two different Yb-materials: black - grade of enrichement 99.72%; red - 97.2%; irradiation time: 14 days; decay time: 15 days; Neutron flux = 1.5·10^{15} n/cm^2/s; Target mass = 100 mg; cold Lu: 5 ppm; ___ *51*
Fig. 23: Theoretical ratio of ^{177m}Lu and ^{177}Lu activities; of highly enriched ^{176}Yb target (Table 8, Table 6), 5 ppm Lu impurities, 14 d irradiation time ___ *52*
Fig. 24: Molecular structure of α-Hydroxisobutyric acid (α-HIBA) ___ *54*

Fig. 25: $Yb(NO_3)_3$ target in sealed glass ampoule for irradiation 60
Fig. 26: Manually assembled separation column 62
Fig. 27: Separation column from G&E Healthcare 62
Fig. 28: Set-up 1 63
Fig. 29: Devise to crack the quartz-ampule containing the irradiation target material. 64
Fig. 30: Set-up 2 65
Fig. 31: Set-up for routine production model 69
Fig. 32: System for conversion of produced n.c.a.^{177}Lu into n.c.a.$^{177}LuCl_3$ 70
Fig. 33: System built-up for Yb-recovery via the cation exchange resin route 72
Fig. 34: Separation of ^{177}Lu from Yb, 10 mg target, 16.53 mL bed volume, 30 μm particle size, 32.5 cm bed height, 1 cm column diameter, flow rate 0.5 mL/min (0.64 mL/cm^2/min), gradient elution 77
Fig. 35: Separation of ^{177}Lu from Yb, 10 mg target, 25.5 mL bed volume, 30 μm particle size, 32.5 cm bed height, 1 cm column diameter, flow rate 0.7 mL/min (0.89 mL/cm^2/min), isocratic elution 78
Fig. 36: Separation of ^{177}Lu from Yb, 30 mg target, 25.5 mL bed volume, 30 μm particle size, 32.5 cm bed height, 1 cm column diameter, flow rate 0.7 mL/min (0.89 mL/cm^2/min), isocratic elution 79
Fig. 37: Separation of ^{177}Lu from Yb, 50 mg target (63.7 mg/cm^2), 25.5 mL bed volume, 30 μm particle size, 32.5 cm bed height, 1 cm column diameter, flow rate 0.7 mL/min (0.89 mL/cm^2/min), isocratic elution (0.08 M α-HIBA) 80
Fig. 38: Separation of ^{177}Lu from Yb, 50 mg target (63.7 mg/cm^2), 25.5 mL bed volume, 30 μm particle size, 32.5 cm bed height, 1 cm column diameter, flow rate 0.7 mL/min (0.89 mL/cm^2/min), gradient elution 81
Fig. 39: Separation of ^{177}Lu from Yb, 50 mg target (63.7 mg/cm^2), 36.3 mL bed volume, 30 μm particle size, 46.2 cm bed height, 1 cm column diameter, flow rate 0.7 mL/min (0.89 mL/cm^2/min), gradient elution 82
Fig. 40: Separation of ^{177}Lu from Yb, 90 mg target (50.9 mg/cm^2), 86.6 mL bed volume, 30 μm particle size, 49 cm bed height, 1.5 cm column diameter, flow rate 1.7 mL/min (0.96 mL/cm^2/min), gradient elution 83
Fig. 41: Separation of ^{177}Lu from Yb, 120 mg target (67.8 mg/cm^2), 86.6 mL bed volume, 30 μm particle size, 49 cm bed height, 1.5 cm column diameter, flow rate 1.7 mL/min (0.96 mL/cm^2/min), gradient elution 84
Fig. 42: Glove box in which highly enriched ^{176}Yb targets were processed; for the picture, lead bricks were removed on the left side 85
Fig. 43: Built-up inside the glove box 86
Fig. 44: Formation of n.c.a.^{177}Lu-DOTATATE as a function of peptide amount; A177Lu 500 MBq; pH = 4.5; n(^{177}Lu):n(DOTATATE) 1:3 (2.98 μg DOTATATE); 1:4 (3.97 μg DOTATATE); 1:6 (5.96 μg DOTATATE); 1:10 (9.93 μg DOTATATE) 89
Fig. 45: Formation of n.c.a.^{177}Lu-DOTATATE as a function of time passed after production; A(n.c.a.^{177}Lu) = 500 MBq pro labelling; pH = 4.5; n(n.c.a.^{177}Lu):n(DOTATATE) 1:4 (3.97 μg DOTATATE) 90
Fig. 46: Formation of c.a.^{177}Lu-DOTATATE as a function of petide amont; A(c.a.^{177}Lu) = 500 MBq; pH = 4.5; n(c.a.^{177}Lu):n(DOTATATE) 1:3 (2.98 μg DOTATATE); 1:4 (3.97 μg DOTATATE); 1:6 (5.96 μg DOTATATE); 1:10 (9.93 μg DOTATATE) 92

Fig. 47: Formation of c.a.^{177}Lu-DOTATATE as a function of time; A(c.a.^{177}Lu) = 500 MBq pro labelling; pH = 4.5; n(c.a.^{177}Lu):n(DOTATATE) 1:10 (9.93 µg DOTATATE) 93

Fig. 48: Comparison of the formation of n.c.a.^{177}Lu- and c.a.^{177}Lu-DOTATATE as a function of time; A(n.c.a.^{177}Lu/c.a.^{177}Lu) = 500 MBq pro labelling; pH = 4.5; n(n.c.a.^{177}Lu):n(DOTATATE) 1:4 (3.97 µg DOTATATE); n(c.a.^{177}Lu):n(DOTATATE) 1:10 (9.93 µg DOTATATE) 94

Fig. 49: Excitation function of the ^{176}Yb (n,γ)^{177}Yb reaction. Because the σ(E_n) function is in the thermal neutron region linear as $\frac{1}{E_n}$, ^{176}Yb belongs to the $\frac{1}{v_n}$nuclides. Reproduced from (Kopecky). 113

Fig. 50: Excitation function of the ^{176}Lu (n,γ)^{177}Lu reaction. Because the σ(E_n) function is not linear in the thermal neutron region as $\frac{1}{E_n}$, ^{176}Lu belongs to the non - $\frac{1}{v_n}$nuclides. Reproduced from (Kopecky) 114

Fig. 51: Excitation function of the ^{176}Lu (n,γ)^{177m}Lu reaction. Because the σ(E_n) function is not linear in the thermal neutron region as $\frac{1}{E_n}$, ^{176}Lu belongs to the non - $\frac{1}{v_n}$nuclides. Reproduced from (Kopecky) 115

9.3 List of tables

Table 1: Targeting vehicles 23

Table 2: relevant therapeutic radiometals 24

Table 3: Stability constants (logK) for metal-DOTA complexes; 1 - 14 (Tóth, et al., 1994); 15 (Chaves, et al., 1991); 16 – 18 (Delgado, et al., 1982) 53

Table 4: Neighbouring lanthanides with separation factors on a Dowex 50 cation-exchanger resin; eluent: α-HIBA (Marhol 1982) 55

Table 5: Isotopic distribution of Trace target material Yb_2O_3 (target 1) 59

Table 6: Chemical impurities of Trace target material Yb_2O_3 (target 1) 59

Table 7: Isotopic distribution of IsoFlex target material Yb_2O_3 (target 2) 59

Table 8: Chemical impurities of IsoFlex target material Yb_2O_3 (target 2) 59

Table 9: Gradient specifications, Flow: 1.7 mL/min 67

Table 10: Irradiation of different target masses of natural Yb; neutron flux: 3.57·10^{13} n/cm^2/s; 76

Table 11: Labelling of n.c.a. ^{177}Lu in dependence of DOTATATE mass 89

Table 12: Long-time labelling of n.c.a. ^{177}Lu after 0, 5, 10 and 15 days 91

Table 13: Labelling of c.a.^{177}Lu in dependence of DOTATATE mass 92

Table 14: Long-time labelling of c.a. ^{177}Lu after 0, 5, 10 and 15 days 93

Abbreviations

Ala	**Alanine**
A_s	Specific Activity
Asn	Asparagine
BFC	Bifunctional chelator
c.a.	Carrier added
Cys	Cysteine
Gly	Glycine
Ig	Immunoglobulin
IgA	Immunoglobulin A
IgD	Immunoglobulin D
IgE	Immunoglobulin E
IgG	Immunoglobulin G
IgM	Immunoglobulin M
Lys	Lysine
mAbs	Monoclonal antibody
n.c.a.	Non carrier added
Phe	Phenylalanine
PTA	Percutanous Transluminal Angioplasty
RIT	Radioimmunotherapy
Ser	Serine
SST	Somatostatin
SSTR 1…5	Somatostatin receptors 1…5
Thr	Threonine
Trp	Tryptophan
Tyr	Tyrosine

Val	Valine
DOTA	1,4,7,10-Tetraazacyclododecane-1,4,7,10-tetraacetic acid
EDTA	Ethylenediaminetetraacetic acid
DTPA	Diethylenetriaminepentaacetic acid
TETA	1,4,8,11-tetraazacyclotetradecane-1,4,8,11-tetraacetic acid
DOTMP	1,4,7,10-tetraazacyclododecane-1,4,7,10-tetramethylenphosphonic acid
PEPA	1,4,7,10,13-pentaazacyclododecane-1,4,7,10,13-pentaacetic acid
HEHA	1,4,7,10,13,16-hexaazacyclododecane-1,4,7,10,13,16-hexaacetic acid
PRRT	peptide receptor radionuclide therapy
LET	Linear energy transfer
DOTATOC	(DOTA-Phe(1)-Tyr(3))octreotide
DOTATATE	DOTA-(Tyr(3))octreotate
FRM II	Forschungsreaktor München II (germ.)
KBA	Kapselbestrahlungsanlage (germ.)
HFRP	Hochfluss Rohrpost (germ.)
ILL	Institute Laue-Langevin
FCV	Free column volume

Hiermit erkläre ich, dass ich diese Dissertation selbständig verfasst und nur mit den angegebenen Hilfsmitteln gearbeitet habe.

_____

Christoph Barkhausen